

**Community ecology of aquatic insects in forested headwater streams
in the southern Appalachians**

Eric R. Sokol

Dissertation submitted to the faculty of the Virginia Polytechnic Institute and State University in
partial fulfillment of the requirements for the degree of

Doctor of Philosophy

In

Biological Sciences

E. Fred Benfield, Chair

Lisa K. Belden

Robert H. Jones

H. Maurice Valett

J. Reese Voshell, Jr.

September 4, 2009

Blacksburg, Virginia

Keywords: community assembly, niche, neutral, disturbance, streams, benthic
macroinvertebrates

Community ecology of aquatic insects in forested headwater streams in the southern Appalachians

Eric R. Sokol

Abstract

Competing paradigms of community assembly emphasize different mechanisms for predicting patterns in biogeography. *Niche assembly* emphasizes the role of environmental gradients as filters that organize a metacommunity by locally selecting colonizers with similar functional traits, whereas *dispersal assembly* emphasizes the importance of source pool characteristics and dispersal limitation in organizing a metacommunity. In this study, I developed a framework that uses spatially explicit patterns in taxonomic and functional measures of community composition as diagnostics for community assembly processes for benthic macroinvertebrates in headwater streams in the southern Appalachians. Distance decay in taxonomic and functional similarity was used to determine the scales at which taxonomic turnover occurred within functional niches. Trait-neutral models of community composition were used as null models to assess which functional traits were the best candidates to explain how community composition was influenced by environmental gradients: an assessment of niche-based community assembly. Regional scale patterns suggested that niche-based community assembly was the dominant mechanism organizing community composition in headwater streams at local scales (<30km). Therefore, I compared how well trait-neutral models identified functional traits as relevant to community sorting against how well observed trait distributions correlated with environmental variation at a local scale, in the Ray Branch catchment (<10km study extent). Functional traits exhibiting non-random distributions within the Ray Branch watershed were most strongly correlated with environmental variation. Lastly, I assessed how the influences of niche and dispersal assembly on benthic macroinvertebrate community composition were affected by disturbance (shelterwood logging). Environmental variables defining the habitat template, and macroinvertebrate community composition, were measured before and after the disturbance; and path analysis was used to quantify the disturbance effect. The relationship between environmental variation and functional composition increased

following logging, indicating disturbance augmented the influence of environmental filters, and consequently, the importance of niche-based community assembly. My dissertation provides the framework for a novel assessment of taxonomic and functional community composition data to infer the types of ecological dynamics that organize communities in the landscape. Additionally, this work provides a theoretical basis for assessing how dominant ecological processes change, in predictable ways, in response to changes in the habitat template.

Grant information

This work was supported by the National Science Foundation Ecosystems Program (DEB0425642), the Coweeta Hydrologic Laboratory LTER (NSF-DEB 9632854), the U.S. Forest Service (04-CA-11330139-164 and 03-CA-11330139-202), the Virginia Academy of Science, the Graduate Research Development Program at Virginia Tech, the President's Award from the North American Benthological Society, and matching funds from the Department of Biological Sciences at Virginia Tech for all grants that were awarded to me, up to \$500.

Author's acknowledgements

This work would not have been possible without the support of my family, friends, and colleagues. I thank my parents, Kenneth and Joanne Sokol, for support and encouragement from afar. I thank my sister, Kristina Araya, and her family; and my brother, Christopher Sokol, for encouraging me along the way. I am especially grateful for the inspiration from my niece, Angelica Araya, who has reminded me why I love scientific inquiry, and how the fun is in always finding a new way to ask “why.”

I thank Fred for being such a supportive and encouraging advisor, as well as an assistant in the field. I am thankful for to my committee (Lisa Belden, Bob Jones, Maury Valett, and Reese Voshell) for support and guidance. I thank my large and growing academic family, the Virginia Tech Stream Team. Jack Webster, Jeb Barrett, and Bobbie Niederlehner have provided valuable mentorship in many aspects of my academic pursuits. I thank Kate Morkeski, Travis Gray, and Nick Jeremiah for their extensive friendship and help in the field; and other past and current Stream Team members, including Chris Burcher, Jack Brookshire, Damon Ely, Erika Kratzer, Beth Cheever, Corrie Maxwell, Jeff Norman, Robert Northington, and Lawrence Lin, and all of the Stream Team graduate students. Many undergraduates, including Crystal Maier, Julie Frank, and Matt O'Rourke provided assistance in this work.

Dave Allan provided valuable mentorship for me in undergraduate research at the University of Michigan, and I credit him with steering me toward a career in freshwater ecology.

I thank Jean Lindahl, for her unwavering support and encouragement, and for everything. Everyone I have acknowledged, in addition to many names I don't have room to list, have contributed significantly to my life, and this achievement, and I thank you all.

Table of Contents

Abstract	ii
Grant information	iv
Author’s acknowledgements	v
Table of Contents	vi
List of Tables	viii
List of Figures	ix
Chapter 1 - Introduction	1
Chapter 2 - The $\alpha\beta\gamma$'s of community sorting: using taxonomic- and trait-based measures of community composition to infer assembly processes	3
Introduction.....	3
Observed community composition data.....	6
Diagnostic 1 (D ₁): Taxonomic and functional trait β -diversity.....	9
Diagnostic 2 (D ₂): Source pool characteristics	15
Conclusions.....	21
Chapter 3 - Multivariate environmental filters determine β-diversity in functional composition of benthic macroinvertebrate communities	23
Introduction.....	23
Methods.....	25
Results.....	32
Discussion.....	48
Chapter 4 - The interaction between community assembly and disturbance: how logging affects benthic macroinvertebrate communities in headwater streams	53
Introduction.....	53
Methods.....	55
Results.....	62
Discussion.....	76
Chapter 5 - Conclusions	81
Literature Cited	84
Appendix A – Taxonomic groups and observed relative abundances	95
Appendix B – Functional trait scores for the southern Blue Ridge	101

Appendix C – Functional trait correlograms	107
Appendix D – Trait-neutral model fits	109
Appendix E – Functional trait scores for Ray Branch sites.....	113
Appendix F – Estimating channel velocity	118
Appendix G – Path analysis of the habitat template	121

List of Tables

Table 2.1. Trait code descriptions.....	8
Table 2.2. Trait sorting summary.....	14
Table 3.1. Trait sorting ranks based on a trait-neutral lottery model.....	35
Table 3.2. Descriptions of reach scale environmental variables.....	36
Table 3.3. Variance partition of β -diversity in Taxonomic and Functional composition.....	38
Table 3.4. Multiple regression models for individual traits.....	39
Table 4.1. Observed environmental and community composition variables.....	62
Table 4.2. ANCOVA of environmental and macroinvertebrate response to logging.....	64
Table 4.3. Trait loading for a PCA of functional composition.	70
Table 4.4. Variance partitioning of raw data matrices of taxonomic and functional trait composition.....	71
Table 4.5. Multiple regression model fits for each functional trait	72

List of Figures

Figure 2.1. Four community assembly hypotheses.....	5
Figure 2.2. Multivariate correlograms	12
Figure 2.3. Values for trait-neutral models.....	19
Figure 3.1. Map of sampling sites.....	25
Figure 3.2. Principal coordinate analysis (PCoA) of sites in taxonomic space	32
Figure 3.3. Principal coordinate analysis (PCoA) of sites in functional trait space	33
Figure 3.4. Distributions of observed and predicted CFT scores	34
Figure 3.5. Principal component analysis of environmental variables	37
Figure 3.6. Relationship between trait ranks and MLR fits.....	43
Figure 3.7. Path models illustrating the relationships among environmental variables and a composite functional composition variable	45
Figure 3.8. Path models for environmental variables and community functional composition	47
Figure 4.1. Site map	56
Figure 4.2. General ANCOVA model	58
Figure 4.3. Path models of the covariance structure of observed environmental variables.....	67
Figure 4.4. The observed distribution of CFT scores	68
Figure 4.5. Path models for Crwl and Hab.Climb	74
Figure 4.6. Path models for principal components of functional trait composition	75

Chapter 1 - Introduction

Competing paradigms of assembly of ecological communities emphasize different mechanisms for generating biogeographic patterns of interacting groups of species in the landscape. A deterministic perspective of community assembly was pioneered by Clements' (1916) work on successional theory, which emphasized how local environmental constraints defined the niches that organized community composition based on the functional attributes of the resident species. Alternatively, the individualistic concept, proposed by Gleason (1939), provided a conceptual foundation for incorporating stochasticity into mechanistic hypotheses of community assembly by way of dispersal and colonization dynamics.

The ideas of Clements and Gleason were the precursors to the antagonistic hypotheses of niche-based (deterministic) (Chase 2003) and dispersal-based (stochastic) community assembly (Hubbell 2001), which have served as alternative models to describe how species are sorted into groups in the landscape to create spatially explicit patterns in community composition within a metacommunity. Niche-based community assembly (Chase and Leibold 2003) is the filtering effect of the local environmental constraints that select certain species to become established while excluding others based on their functional traits, whereas dispersal-based community assembly (Hubbell 2001) emphasizes the importance of source pool characteristics and dispersal limitation in organizing a metacommunity.

The degree to which niche-based and dispersal-based assembly processes describe the underlying mechanisms for species sorting in the landscape is contingent on the characteristics of the study system (Chase 2007), the taxonomic and functional constraints used to define the study community (Hubbell 2001, 2006), and the scale of observation (Nekola and White 1999). The manner in which these factors influence community assembly has been recognized as an important, and largely unaddressed, question (Chase 2005, Bell et al. 2006, Holyoak and Loreau 2006, Hubbell 2006, Leibold and McPeck 2006, McGill et al. 2006).

In this study, I focused on benthic macroinvertebrate communities in headwater streams in the southern Appalachians, but my goal was to contribute to basic ecological understanding of how the perceived relative importance of community assembly processes were influenced by the characteristics of the organisms, landscape, and study design. The three main objectives of this investigation were to (1) develop a framework to infer community assembly processes from

patterns in community composition, (2) test the inferred community assembly processes at a local scale, and (3) determine how disturbance affects the relative influence of different community assembly processes.

Chapter Two, “The $\alpha\beta\gamma$ ’s of community sorting: using taxonomic- and trait-based measures of community composition to infer assembly processes,” describes a framework by which community assembly processes can be diagnosed from spatially explicit patterns in community composition. Taxonomic and functional diversity patterns, together, were used to create two simple diagnostics that indicate the scales at which niche-based and dispersal-based community assembly processes organize the metacommunity. This framework was used to determine the scales at which the different sorting processes were relevant for benthic macroinvertebrate communities in forested headwater streams in the southern Appalachians.

Chapter Three, “Multivariate environmental filters determine β -diversity in functional composition of benthic macroinvertebrate communities,” describes an application and test of the theoretical framework developed in Chapter Two. Patterns in taxonomic and functional community composition described in Chapter Two suggest that niche-based assembly dominates in forested headwater streams at study extents less than 30km, when benthic macroinvertebrate communities are observed at a reach scale (10-100m observational grain size). Chapter Three describes how the correlation between observed environmental gradients and variation in measures of community composition were used to test the dominance of niche-based community assembly at a local scale (<30km) in the Ray Branch catchment in the Nantahala National Forest in western North Carolina, and determine specifically which environmental gradients and functional traits interact to organize the benthic metacommunity.

Chapter Four, “The interaction between community assembly and disturbance: how logging affects benthic macroinvertebrate communities in headwater streams,” is a study of how community assembly processes for benthic macroinvertebrate communities in the Ray Branch catchment are affected by a landscape scale disturbance (logging).

In Chapter Two I derive a new perspective for inferring community assembly processes from simultaneously considering patterns in taxonomic and functional community composition data, and the subsequent two chapters are ecological studies grounded in the theory developed in Chapter Two. Thus, Chapter Five, provides a synthesis and overview of the conclusions derived from this body of work.

Chapter 2 - The $\alpha\beta\gamma$'s of community sorting: using taxonomic- and trait-based measures of community composition to infer assembly processes

Introduction

A long history of empirical and theoretical work in ecology provides an ambiguous story about the processes that drive the assembly of ecological communities. Whittaker (1975) developed metrics for metacommunity diversity, which can be used to test the predictions of different community assembly hypotheses: α -diversity is a measure of community composition (e.g., richness and evenness) of the local assemblage within an observational unit (OU), β -diversity is a quantification of the difference in community composition among OUs, and γ -diversity is a measurement of the composition of the regional community (all OUs pooled). Niche theory and neutral theory (Hubbell 2001) both seek to explain the same patterns in community composition, but they employ opposing mechanisms and assumptions to explain observed α -, β -, and γ -diversity.

Baas Becking (1934) succinctly described the niche theory perspective of community assembly when he stated that “everything is everywhere, but the environment selects.” This cannon of community ecology invokes the process of environmental filtering, which predicts local community composition (α -diversity) is correlated with the characteristics of the local habitat, and among-site differences in community composition (β -diversity) are due to differences in environmental constraints that non-randomly select subsets of organisms based on their functional traits (Hutchinson 1957, Southwood 1977, Poff 1997, Weiher and Keddy 2001, Westoby and Wright 2006). Grime (2006) labeled this community assembly process “convergent sorting” because functionally similar taxa tend to co-occur at the same sites if the same source pool is universally available. Environmental filtering alone is not sufficient to predict taxonomic variation in community composition among sites when different source pools of potential colonizers are available to different sites; however, the prevalence of convergent sorting in the ecological literature suggests that the assumption of a homogenous (non-dispersal limited) source pool is valid at the scales of interest for many different types of communities (Tilman et al. 1982, Finlay 2002, Lamouroux et al. 2004).

Neutral theory refers to a family of hypotheses that predict β -diversity patterns within a landscape based on an interaction between metacommunity dynamics (per capita birth and death rates, immigration and emigration) and stochastic processes (local speciation and extinction), while assuming ecological equivalence among all organisms (Bell 2001, Hubbell 2001, Tuomisto and Ruokolainen 2006). Like their niche theory based counterparts, neutral community models (NCMs) predict non-random variation in community composition. Unlike niche theory, NCMs hypothesize that all individuals in a source pool of potential colonizers have an equal probability of colonizing a site; therefore, there is no expectation for diversity patterns indicative of convergent sorting or a correlation between habitat characteristics and community composition. Instead, NCMs predict decay in among-site similarity in community composition with an increase in geographic distance because of the decreased likelihood for interactions (e.g., emigration/immigration) among communities that are farther apart (Nekola and White 1999, Hubbell 2001).

The interaction between dispersal limited source pools and environmental filters were originally organized into a mechanistic hypothesis in Gleason's (1939) Individualistic Concept (IC). Niche and neutral theory provide opposite ends of a community assembly continuum (Gravel et al. 2006) that has evolved from the IC in two respects: (1) neutral theory assumes ecological equivalence (assumption 1, Figure 2.1), whereas niche theory depends on the interaction between environmental gradients and functional differences among taxa (mechanism 1, Figure 2.1) to predict diversity patterns; and (2) niche theory assumes a uniform source pool for all OUs in a metacommunity (assumption 2, Figure 2.1), whereas neutral theory depends on variation in the source of colonizers among sites (mechanism 2, Figure 2.1) to predict diversity patterns. A factorial combination of these two sets of opposing assumption-mechanism pairs provides a framework of four community assembly hypotheses (Figure 2.1) (Tuomisto et al. 2003, Martiny et al. 2006).

		Ecological equivalence (assumption 1)	Environmental filtering (mechanism 1)
Homogenous source pool (assumption 2)		<p>H₀ (Null)</p> <p>D₁: No β-diversity D₂: $\gamma_0 = \gamma_i = \alpha_i$</p>	<p>H₁ (Niche)</p> <p>D₁: Type I β-diversity D₂: $\gamma_0 = \gamma_i \neq \alpha_i$</p>
	Heterogeneous source pool (mechanism 2)	<p>H₂ (Neutral)</p> <p>D₁: Type II β-diversity D₂: $\gamma_0 \neq \gamma_i = \alpha_i$</p>	<p>H₁₊₂ (Niche/Neutral)</p> <p>D₁: Type I and II β-diversity D₂: $\gamma_0 \neq \gamma_i \neq \alpha_i$</p>

Figure 2.1. Four community assembly hypotheses and predicted diversity patterns that result from the factorial combination of the community sorting assumptions/mechanisms of neutral and niche theory. The two assumption/mechanism pairs are (i) ecological equivalence (assumption 1)/environmental filtering (mechanism 1) and (ii) a homogenous source pool (assumption 2)/heterogeneous source pool of dispersal limited colonizers (mechanism 2). Each combination of assumption/mechanism pairs outlines a different community assembly hypothesis: H₀ (null) – an assemblage is a random sample from a homogenous source pool of ubiquitous taxa and dominance ranks are maintained throughout the metacommunity. H₁ (niche theory) – local environmental filters select for organisms with suitable ecological characteristics from a homogenous source pool. H₂ (neutral theory) – a heterogeneous source pool and limited dispersal result in nonrandom assemblages of ecologically equivalent taxa. H₁₊₂ (niche + neutral theory) – local environmental filters select for organisms with the same ecological characteristics from a heterogeneous source pool. Each hypothesis predicts a unique pattern in β-diversity (diagnostic 1 [D₁]): H₀ predicts no detectable type I or type II β-diversity when the assumptions of source pool homogeneity and ecological equivalency are met. H₁ predicts only type I β-diversity, an indicator of local environmental filters selecting colonizers from a homogenous source pool. H₂ assumes no niche differentiation and predicts only type II β-diversity because any turnover in community composition results from differences in source pools (i.e., provincialism) among OUs. H₁₊₂ predicts type I β-diversity at small spatial lags and type II β-diversity at large spatial lags. This pattern is a consequence of environmental filters selecting colonizers from a heterogeneous source pool of dispersal-limited potential colonizers, which results in a divergence of source pool composition at large spatial

lags. Each hypothesis also predicts a unique relationship among regional diversity (γ_0), the local effective source pool (γ_i), and local community composition (α_i) (diagnostic 2 [D₂], see text).

H₀ (Figure 2.1) can be distinguished from the other three hypotheses because it is the only hypothesis that predicts local measurements of α -diversity are random samples of γ -diversity, and β -diversity is not detectable. Niche and neutral models can both predict the same patterns in the diversity metrics, even when spatial patterns are considered. Therefore, a second type of measurement of community composition is necessary to provide additional information for distinguishing between patterns that are indicative of niche and neutral processes.

Functional trait databases provide such information, and supplement taxonomic identifications in the quantification of community composition (Statzner et al. 2001b, Wright et al. 2004, Poff et al. 2006). This creates the possibility for separating tests for dispersal limitation and environmental filtering, instead of using the same null model to test both hypotheses. My objective is to combine measures of taxonomic and functional trait community composition with diversity metrics to create a set of diagnostics that can be used to infer community assembly processes that apply to patterns of diversity observed at a given scale of observational grain size and study extent.

I apply this analysis to benthic macroinvertebrate data from forested headwater streams in the southern Blue Ridge Physiographic Province to investigate why there is so much inter-site variability (β -diversity) in community composition among streams that are commonly classified as “reference” sites by stream ecologists. Is β -diversity in headwater streams an emergent property of dispersal limitation and metacommunity dynamics in a relatively stochastic study system, or is environmental variability in “reference” sites sufficient to justify invoking environmental filtering?

Observed community composition data

A total of 26 observations of aquatic macroinvertebrate assemblages from forested headwater streams (orders 1-3) within the southern Blue Ridge Physiographic Province were included in the meta-analysis. Observational Units (OUs) include four watersheds that were quantitatively sampled with a Surber sampler (see Chapter 3 methods) in 2005 in the Nantahala National Forest as well as macroinvertebrate density data from forested headwater streams from four additional studies (Harding et al. 1998, Sponseller et al. 2001, Cook 2003, Ely in prep). On

average, the macroinvertebrate community composition data for each OU represents a benthic assemblage from a 115m stream reach. OUs were geospatially referenced either from data obtained from the original publication or from sampling location estimates using 7.5 minute USGS topographic maps.

Only taxonomic groups included in the North American trait database compiled by Poff et al. (2006) were included in the analysis, excluding members of Chironomidae. Taxonomic data had a genus level resolution, unless trait data was only available at a coarser taxonomic resolution in the trait database. The mean α -diversity of an OU was 32.7(5.2 s.d.) taxonomic groups, with a total γ -diversity of 98 taxonomic groups (Appendix A) throughout the study extent.

Community-aggregate functional trait (CFT) scores provide information about the functional nature of an assemblage of organisms. A trait refers to an ecologically relevant characteristic of an organism. Each trait state is referred to as a “trait syndrome” and each syndrome is represented by a trait score. The functional trait niche (FTN) (Poff et al. 2006) of a taxonomic group refers to the set of trait syndromes assigned to that taxonomic group. Therefore, community-aggregate functional trait niche (CFTN) refers to a set of CFT scores that best describe the functional characteristics of an assemblage of multiple taxonomic groups.

The CFTN for a set of observations of assemblages of macroinvertebrates were calculated as

$$CFTN = P \cdot T' \quad (1)$$

where $CFTN$ is an OU by trait matrix in which each cell, CFT_{it} , is the average functional trait syndrome for the entire assemblage for observation i for trait t . P is an OU by taxon matrix of relative abundances and T' is the transpose of a taxon by functional trait syndrome matrix (T) (Legendre and Legendre 1998, McCune and Grace 2002). Relative abundance data in P was $\ln(1000x + 1)$ transformed and then rescaled so that transformed relative abundances for each OU summed to 1. For sites with a density ranging from 100 to 1000 no./m², this transformation is similar to the $\log(x+1)$ transformation used on density data before converting it to relative abundances in other trait based studies (Lamouroux et al. 2004, Doledec et al. 2006). T is an n_{taxa} by n_{trait} matrix, where n_{trait} ($n_{trait} = 29$) is the number of traits that were scored for each of n_{taxa} ($n_{taxa} = 98$) taxonomic groups.

For this study, *T* (Appendix B) was modified from the list of taxon specific trait scores provided by Poff et al. (2006), in which traits were grouped into trait classes: ecology, life history, mobility, and morphology (Table 2.1). I rescaled all trait scoring to have a minimum of 0 and a maximum of 1, and non-ordinal traits (e.g., Functional Feeding Group and Habit) were scored as a set of binary variables for each category (see Table 2.1, and Table 1 in Poff et al. 2006 for original trait descriptions; see Appendix B for taxon specific trait scoring). In this analysis, a community level trait score of an OU for a categorical trait represents the relative abundance of organisms in the OU with that trait syndrome. For ordinal traits, a community level trait score represents the average trait syndrome for the assemblage of macroinvertebrates of an OU.

Table 2.1. Trait code descriptions (see Poff et al. 2006 for more details).

Trait Class	Trait	Trait Code
ECOLOGY	Functional Feeding Group, Collector-filterer (proportion collector filterers)	FFG.CF
	Functional Feeding Group, Collector-gatherer (proportion collector gatherers)	FFG.CG
	Functional Feeding Group, Predator (proportion predators)	FFG.Pred
	Functional Feeding Group, Scraper or herbivore (proportion scrapers or herbivores)	FFG.SC
	Functional Feeding Group, Shredder (proportion shredders)	FFG.SH
	Habit, Burrow (proportion burrowers)	Hab.Burrow
	Habit, Climb (proportion climbers)	Hab.Climb
	Habit, Cling (proportion clingers)	Hab.Cling
	Habit, Skate (proportion skaters)	Hab.Skate
	Habit, Sprawl (proportion sprawlers)	Hab.Sprawl
	Habit, Swim (proportion swimmers)	Hab.Swim
	Rheophily (correlates with preferences for running water)	Rheo
	Thermal preference (correlates with thermal tolerance)	Ther
	LIFE HISTORY	Desiccation resistance (correlates with resistance to dessication)
Development time (0 indicates fast seasonal, 1 indicates slow/nonseasonal)		Devl

Trait Class	Trait	Trait Code
	Adult ability to exit (correlates with ability/affinity to exit water)	Exit
	Adult life span (correlates with life span length)	Life
	Synchronized emergence (0 indicates poor synchronization, 1 indicates highly synchronized emergence)	Sync
	Voltinism (generations/year, 0 indicates semivoltine, 1 indicates multivoltine)	Volt
MOBILITY	Crawl ability (correlates with crawling ability)	Crwl
	Dispersal of females before oviposition (0 indicates < 1km, 1 indicates greater than 1 km)	Disp
	Drift Occurrence (correlates with occurrence in drift)	Drft
	Adult flight ability (correlates with flight ability)	Flgt
	Swimming ability (correlates with swimming ability)	Swim
MORPHOLOGY	Armoring (0 indicates membranous, 1 indicates highly sclerotized)	Armr
	Attachment (correlates with affinity to attach to substrate)	Atch
	Respiration (0 indicates preference for high DO habitats, 1 indicates tolerance of hypoxia)	Resp
	Shape (0 indicates fusiform, 1 indicates high drag)	Shpe
	Size (correlates with size as an adult)	Size

Diagnostic 1 (D1): Taxonomic and functional trait β -diversity

Interpreting diagnostic patterns in β -diversity

The first diagnostic (D_1 , Figure 2.1) is a prediction of the expected type of β -diversity that should result from each community assembly hypothesis. When he defined β -diversity, Whittaker described two types of patterns of variation among OUs (Whittaker 1975, Ackerly and Cornwell 2007): type I β -diversity is taxonomic turnover along an environmental gradient, type II β -diversity is taxonomic turnover within a niche.

Type I β -diversity is a pattern of community structure that results from convergent sorting in the landscape (Grime 2006), where functionally similar taxa co-occur due to a set of environmental filters selecting for similar physiological constraints (Poff 1997, Weiher et al. 1998, Weiher and Keddy 2001). Therefore, assuming a homogenous source pool for all OUs,

type I β -diversity should result in a positive correlation between the taxonomic composition and the functional composition among all OUs.

Type II β -diversity can result from a negative correlation between taxonomic and functional composition, as in Diamond's (1975) checkerboard pattern. This pattern occurs when the same source pool of colonizers is available throughout the entire extent of the observed metacommunity, but biotic interactions result in localized competitive exclusion (Diamond 1975, Pacala and Tilman 1994) so that functionally similar taxa tend not to co-occur at the same site (overdispersion).

Type II β -diversity can also result from a divergence in source pool composition, referred to as provincialism (Martiny et al. 2006), where sites that are geographically far apart have different taxonomic groups available to occupy a given functional niche. Provincialism results in type I β -diversity locally, and type II β -diversity among sites located in different provinces.

I used a distance based approach to analyze both taxonomic and functional trait β -diversity patterns at different spatial lags using the *ecodist* package (Goslee and Urban 2007b) for R (R Development Core Team 2007). OU by OU geographic (D_{geo} – Euclidean), taxonomic (D_{taxa} – Bray-Curtis), and functional trait (D_{trait} – Bray-Curtis) distance matrices were calculated from geospatial data, relative abundance data (P), and CFT data, respectively.

The *pmgram* function was used to plot multivariate correlograms to show how OU by OU similarity measurements in multivariate community composition space change with an increase in geographic distance between each OU by OU comparison. Multivariate correlograms use the mantel coefficient (r_m), which is analogous to Pearson's r , and indicates how similarly a set of OUs are organized with respect to two different sets of distance measures (Legendre and Legendre 1998). I used this method to visualize the relationship taxonomic-geographic and trait-geographic pairings of distance matrices ($r_m[D_{taxa}, D_{geo}]$ and $r_m[D_{trait}, D_{geo}]$ respectively). OU by OU trait syndrome difference matrices ($D_{trait,t}$) were calculated for each trait t and used to plot correlograms of CFT scores for each trait so that I could detect which traits exhibited patterns indicative of spatially dependent environmental gradients.

The correlation between taxonomic and functional community composition provides an index of whether macroinvertebrate community sorting is convergent or divergent (Ackerly and Cornwell 2007). OU by OU pairwise comparisons were divided into six spatial lag classes based on their geographic separation, and r_m was calculated for each subset of comparisons and used to

plot multivariate correlograms. Type I β -diversity is indicated by a positive correlation between co-occurrence and trait state and type II β -diversity is indicated by a negative correlation. Partial multivariate correlograms were used to plot r_m for each subset of comparisons between the functional trait and taxonomic distance matrices ($r_m[D_{taxa}, D_{trait} | D_{geo}]$, a comparison of overall functional turnover and taxonomic turnover), and for CFT score differences and taxonomic distance matrices ($r_m[D_{taxa}, D_{trait,t} | D_{geo}]$, for $t = 1 \dots n_{traits}$, a comparison of functional turnover for a particular trait and taxonomic turnover) for each trait t . Partial multivariate correlograms were plotted using the *ecodist* package for R (Goslee and Urban 2007b). r_m statistics were calculated at each spatial lag using 10000 iterations, and a two tail p-value of 0.05 was used to indicate statistical significance for all multivariate and partial multivariate correlograms.

For the purposes of diagnosis, I considered there to be a decay in similarity if the r_m statistics of at least one of the two smallest spatial lag classes was significantly positive and one of the two largest spatial lag classes was significantly negative, and other r_m statistics fit a pattern of spatial decay reasonably well. I considered there to be a spatially independent regional correlation if r_m values for all six spatial lags were consistently one sign (positive or negative) and one of the two smallest and largest classes had a significant p-value. A decay in similarity for $r_m(D_{trait}, D_{geo})$ is sufficient to refute H_0 , but not distinguish between type I or type II β -diversity; therefore, partial multivariate correlograms were used to diagnose β -diversity type. A consistent positive $r_m(D_{trait}, D_{taxa} | D_{geo})$ value indicates type I β -diversity, a consistent negative $r_m(D_{trait}, D_{taxa} | D_{geo})$ indicates type II β -diversity, and distance decay in $r_m(D_{trait}, D_{taxa} | D_{geo})$ indicates provincialism. These diagnostic criteria were also applied to correlograms for individual traits.

Observed diagnostic patterns in β -diversity

Multivariate correlograms showed a distance decay of both taxonomic and CFT similarity among OUs (Figure 2.2, A and B), indicating a spatially dependent pattern in β -diversity. Sites included in the smallest spatial lag (mean = 32km) were positively correlated in both taxonomic and CFT composition, intermediate distances showed no significant relationship, and sites in the 221km spatial lag class showed significant divergence in both community composition measures. $r_m(D_{trait}, D_{taxa} | D_{geo})$ is consistently positive at all spatial lags (Figure 2.2C) despite divergence in functional composition with spatial lag, indicating the presence of type I β -diversity and convergent sorting throughout the southern Blue Ridge.

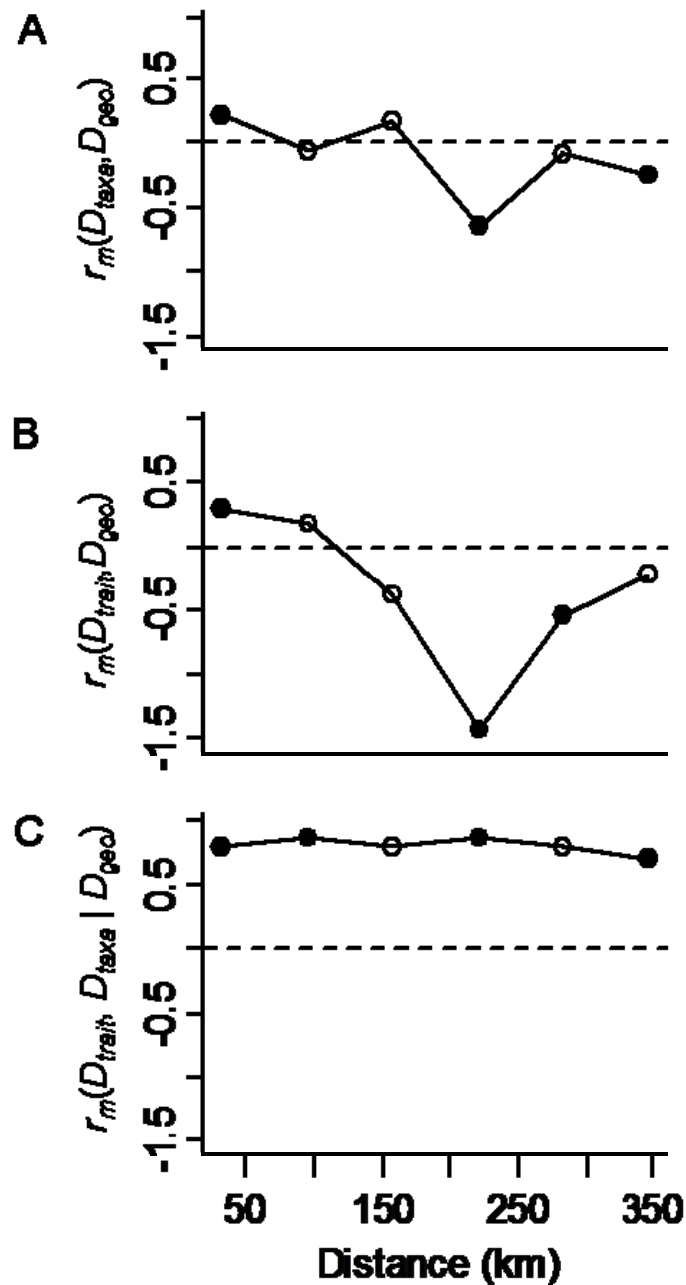


Figure 2.2. Multivariate correlograms of benthic macroinvertebrate community composition in the southern Blue Ridge. The x-axis is spatial lag measured as Euclidean distances in 2 dimensional geographic space. (A) $r_m(D_{taxa}, D_{geo})$ is a mantel statistic that indicates taxonomic similarity at each spatial lag and is estimated from D_{taxa} , an OU by OU Bray-Curtis distance matrix calculated from transformed relative abundances. (B) $r_m(D_{trait}, D_{geo})$ indicates functional similarity and is the mantel correlation at each spatial lag estimated from D_{trait} (Bray-Curtis distance matrix calculated from CFT scores for all traits). (C) $r_m(D_{taxa}, D_{trait} | D_{geo})$ is the mantel correlation between D_{trait} and D_{taxa} for a subset of pairwise comparisons that indicates whether similar

taxa occupy similar functional niches (a positive r_m indicates a correlation between taxonomic and functional community composition) at each spatial lag.

Correlograms for individual traits (Appendix C) showed distance decay of $r_m(D_{trait,t}, D_{geo})$ for nine of 29 traits, including traits from all trait classes. Seven traits, from the ecology, life history, and morphology trait classes, exhibited a positive $r_m(D_{trait,t}, D_{taxa} | D_{geo})$ at all spatial lags indicating type I β -diversity (Table 2.2). No mobility traits showed patterns indicative of type I β -diversity at the regional scale; instead, three mobility traits and one morphology trait (size) showed a decay in $r_m(D_{trait,t}, D_{taxa} | D_{geo})$ indicative of provincialism (Table 2.2).

Inferences from D1

D_1 is a distance based analysis of β -diversity (see Legendre et al. 2005, Tuomisto and Ruokolainen 2006, and Laliberte 2008 for a discussion on the application of this method), and requires three distance matrices: D_{taxa} , D_{geo} , and D_{trait} . Unlike Tuomisto and Ruokolainen (2006), I am not attempting to partition the variation in taxonomic composition among two different predictor distance matrices. Instead, I am using D_{geo} to divide D_{taxa} and D_{trait} pairwise comparisons into groups based on distance, to determine whether there is a positive r_m for each distance class. This method does not provide an estimation of the proportion of taxonomic variance predicted by environment (or in this case functional group) and/or geographic space, but it can provide a general indication of the scale at which taxonomic turnover occurs within a functional group.

D_1 showed decay in similarity for both taxonomic and functional composition (Figure 2.2A). Decay in taxonomic similarity over a spatial lag refutes H_0 ; however, both neutral and niche theory can predict spatially autocorrelated patterns in taxonomic composition. The irregular decay pattern can result either from a community dominated by ubiquitous taxa following neutral metacommunity dynamics, or from spatially autocorrelated environmental gradients acting as filters (Laliberte 2008).

Spatial decay in functional composition (Figure 2.2B) coupled with a consistent positive correlation between functional and taxonomic composition (Figure 2.2C) indicates regular convergent sorting in the community at all spatial lags (type I β -diversity) and that taxonomic turnover follows functional turnover in the landscape. If the regional source pool is not homogenous, the change in the source pool correlates with functional turnover, and presumably

an environmental gradient. Therefore, D_1 provides support for niche theory (H_1 , Figure 2.1) and suggests environmental gradients organize the benthic macroinvertebrate community within the southern Blue Ridge Physiographic Province through convergent sorting, when observations are made at the reach scale.

When I analyzed individual traits instead of overall functional composition, I did see taxonomic turnover within functional groups for *mobility* traits and one *morphology* trait (Size, which is related to mobility) (Table 2.2). This dataset suggests turnover within these traits occurs between 150 and 220 km, a threshold which could be estimated more precisely with more data points. The distance based analysis does not indicate whether there is taxonomic turnover within the “good disperser”, “intermediate disperser”, or “poor disperser” functional groups, but it does indicate that the taxonomic identity of the organisms filling one of those niches must change.

Table 2.2. Trait sorting summary. D_1 : β -diversity patterns for each functional trait (see Appendix C for correlograms). Trait β -diversity is indicated as 1, 2, or 1→2 (type I locally and type II at larger spatial lags, indicating provincialism). D_2 : $P\{CFT_t\}$ are goodness of fit values for each trait t for predicted CFT scores for $f(P_{obs}, D_{geo}, m = 0)$ and $f(P_{obs}, D_{geo}, m \neq 0)$. Sorting ranks are higher for traits with poor fit (low $P\{CFT_t\}$ values).

Trait class	Trait code	β -diversity type	$m = 0$		$m \neq 0$		mean rank
			$P\{CFT_t\}$	rank	$P\{CFT_t\}$	rank	
ECOLOGY	FFG.CG		0.15	6	0.11	4	5
	FFG.CF	1	0.13	4	0.08	1	2.5
	FFG.SC		0.18	11	0.13	5	8
	FFG.Pred		0.08	2	0.09	2	2
	FFG.SH	1	0.28	27	0.25	26	26.5
	Hab.Burrow		0.25	25	0.22	20	22.5
	Hab.Climb		0.05	1	0.19	16	8.5
	Hab.Sprawl	1	0.24	23	0.19	13	18
	Hab.Cling	1	0.22	19	0.16	9	14
	Hab.Swim		0.23	22	0.21	19	20.5
	Hab.Skate		0.46	29	0.44	29	29
	Rheo	1	0.29	28	0.19	14	21

Trait class	Trait code	β -diversity		$m = 0$		$m \neq 0$		mean
		type	$P\{CFT_i\}$	rank	$P\{CFT_i\}$	rank	rank	
	Ther		0.16	8	0.20	17	12.5	
LIFE HISTORY	Desi		0.16	9	0.18	11	10	
	Devl		0.10	3	0.09	3	3	
	Exit		0.27	26	0.22	21	23.5	
	Life		0.15	7	0.14	7	7	
	Sync		0.16	10	0.17	10	10	
	Volt	1	0.20	16	0.27	28	22	
MOBILITY	Crwl	1→2	0.18	12	0.20	18	15	
	Disp	1→2	0.24	24	0.25	27	25.5	
	Drft		0.22	20	0.23	23	21.5	
	Flgt		0.21	18	0.24	24	21	
	Swim	1→2	0.19	14	0.16	8	11	
MORPHOLOGY	Armr		0.22	21	0.23	22	21.5	
	Atch		0.18	13	0.19	15	14	
	Resp		0.13	5	0.14	6	5.5	
	Shpe	1	0.20	17	0.24	25	21	
	Size	1→2	0.20	15	0.18	12	13.5	

Diagnostic 2 (D₂): Source pool characteristics

Using a trait-neutral model to evaluate $\gamma_0 = \gamma_i = \alpha_i$

The second diagnostic (D₂) is a test of the relationship between regional (γ) diversity and local (α) diversity. Hubbell (2001) suggested that without dispersal limitation and perfect connectivity with the source pool, the expected relative abundance for each taxon k at each OU _{i} is the relative abundance of each taxon k in the regional metacommunity, which serves as a source pool. Let α_i be a vector of observed relative abundances (p_{ik}) of the colonizers that establish at OU _{i} , and P_{obs} be an n_{sites} (number of observational units in the study) by n_{taxa} (number of observed taxonomic groups in the study) matrix of observed relative abundances, where each row i is a vector of relative abundances that describes α_i . Then the column means of P_{obs} is a

vector (γ_0) of n_{taxa} relative abundances and provides an estimate of γ -diversity for the region. Therefore, with no dispersal limitation, I expect

$$\gamma_0 = \gamma_i = \alpha_i \quad (2)$$

for all OUs ($i = 1 \dots n_{sites}$), where γ_i is the “effective source pool,” a vector of relative abundances (\hat{p}_{ik}) of the potential colonizers that have access to OU_{*i*}. In equation 2, γ_i is analogous to the “seed-bank” in Gleason’s (Gleason 1939) Individualistic Concept. Equivalence in relative abundances among γ_0 , γ_i , and α_i is expected given the assumptions listed for H₀, (Figure 2.1).

If environmental filters select for taxa with specific combinations of functional traits from a homogenous source pool (i.e., no dispersal limitation or provincialism), then I expect $\gamma_0 = \gamma_i \neq \alpha_i$. Under H₁, neither γ_0 nor γ_i predict α_i , but γ_i should be the same for all OU_{*i*}s and equivalent to γ_0 (i.e., each OU_{*i*} has the same propagule rain, but local environmental constraints select for different individuals at each site).

If dispersal limits the connectivity between each OU_{*i*} and the metacommunity, but the assumption of ecological equivalence holds, then I expect $\gamma_0 \neq \gamma_i = \alpha_i$. Under H₂, γ_0 no longer predicts the α_i of each local assemblage, but the relative abundance of each taxon (\hat{p}_{ik}) in the pool of potential colonizers that actually reach OU_{*i*} (γ_i) should predict its probability of establishment, and ultimately its relative abundance (p_{ik}).

Lastly, niche assembly mechanisms are sorting from different source pools at different points in the landscape, then I expect $\gamma_0 \neq \gamma_i \neq \alpha_i$. The inequalities among the regional pool, effective source pool, and local community for each OU_{*i*} indicate that environmental filters are selecting individuals to establish at the site from a source pool that is different than the one predicted by γ_0 . This pattern indicates either nested environmental filters that function at different spatial and temporal scales (Tonn et al. 1990b, Poff 1997) or environmental filters acting locally in the context of larger scale biogeographic processes (Gravel et al. 2006, Martiny et al. 2006, Thompson and Townsend 2006).

The first step in determining the relationships between γ_0 , γ_i , and α_i is to calculate an estimate of the effective source pool (γ_i) with and without dispersal limitation. I used a trait-neutral lottery model to calculate an n_{sites} by n_{taxa} matrix, \hat{P} , of expected relative abundances, \hat{p}_{ik} ,

for each taxon k at each OU $_i$. Each row i of \hat{P} is an estimate of γ_i for OU $_i$. $f(P_{obs}, D_{geo}, m)$ is a function that estimates each \hat{p}_{ik} in \hat{P} given a set of observed relative abundances (P_{obs}), an n_{sites} by n_{sites} matrix of geographic distances between sites (D_{geo}), and a parameter for dispersal limitation (m).

$f(P_{obs}, D_{geo}, m)$ is based on a simplified version of Hanski's (1994, 1999) metacommunity model that describes colonization probability from a permanent mainland population as a function of dispersal limitation:

$$C_{ij} = \exp(-md_{ij}) \quad (3)$$

where C_{ij} is the probability that a potential colonizer from a source pool j (the mainland in Hanski's model) will successfully disperse distance d_{ij} to the sink site (OU $_i$). m is a measure of dispersal limitation ranging from 0 to infinity, where 0 indicates no dispersal limitation and infinity indicates no connectivity with the metacommunity.

I applied C_{ij} in $f(P_{obs}, D_{geo}, m)$ so that

$$\hat{p}_{ik} = b_i \sum_{j \neq i} C_{ij} p_{jk} \quad (4)$$

where C_{ij} represents the contribution of OU $_j$ to the local source pool (γ_i) for OU $_i$ as a proportion of the nearest neighbor OU, p_{jk} (for $k = 1 \dots n_{taxa}$, and $j \neq i$) are elements of P_{obs} for all neighboring OUs, and b_i is a scaling factor. Each \hat{p}_{ik} for taxon k at site i is estimated as a weighted mean of the relative abundances of taxon k at all other OUs, with closer sites having a greater weight. Then all \hat{p}_{ik} values at OU $_i$ are rescaled to sum to 1 using the scaling factor (b_i).

Substituting equation 3 for C_{ij} results in

$$\hat{p}_{ik} = b_i \sum_{j \neq i} \exp(-md_{ij}) p_{jk} \quad (5)$$

When $m = 0$, \hat{p}_{ik} is simply calculated as the mean of the relative abundances of all neighboring sites, and for large sample sizes the estimates of γ_i for all OUs converge on the regional γ_0 relative abundance values.

Following Hubbell's (2001) logic, because $f(P_{obs}, D_{geo}, m)$ provides an estimate of the structure of the source pool of potential colonizers that is unique to each OU $_i$, it also serves as a prediction of the expected relative abundances for each OU $_i$ under the assumption of ecological equivalence. Therefore, if $\hat{P} = P_{obs}$, then $\gamma_i = \alpha_i$, and if the best estimate of m is 0, then $\gamma_0 = \gamma_i$. I

calculated estimates of m for the entire dataset, P_{obs} , for a subset including only taxonomic groups in the 50th percentile (q_{50}) of regional relative abundances, and a subset only including groups from the 90th percentile (q_{90}). The *optimize* function, available in the *stats v2.6.2* package for R (R Development Core Team 2007), was used to estimate the parameter m iteratively by minimizing the residual sum of squares (RSS) when comparing \hat{P} against P_{obs} . I then estimated \hat{P} for $f(P_{obs}, D_{geo}, m \neq 0)$ and $f(P_{obs}, D_{geo}, m = 0)$ for each dataset.

$P\{\gamma_i = \alpha_i\}$ was calculated for each γ_i estimate for both trait neutral models [$f(P_{obs}, D_{geo}, m \neq 0)$ and $f(P_{obs}, D_{geo}, m = 0)$] as the probability that the expected value of the absolute value of the differences between observed and predicted relative abundances for each OU_i is 0. If d_i , the expected difference between p_{ik} and \hat{p}_{ik} , is a normally distributed random variable for each OU_i where the mean can be estimated as

$$\bar{d}_i = \frac{1}{n_{taxa}} \sum_{k=1}^{n_{max}} |p_{ik} - \hat{p}_{ik}| \quad (6)$$

and the standard deviation is estimated by

$$s_{d_i} = \sqrt{\frac{\sum_{k=1}^{n_{max}} (|p_{ik} - \hat{p}_{ik}| - \bar{d}_i)^2}{n_{taxa} - 1}}, \quad (7)$$

$$\text{then } X_i^2 = \left(\frac{d_i - \bar{d}_i}{s_{d_i}} \right)^2 \quad (8)$$

where X_i^2 follows a chi-squared distribution with one degree of freedom. Therefore, if $d_i = 0$, then

$$X_i^2 = \left(\frac{\bar{d}_i}{s_{d_i}} \right)^2 \quad (9)$$

is a chi-squared statistic that yields a p-value ($P\{\gamma_i = \alpha_i\}$) for the null hypothesis $\bar{d}_i = 0$ (there is no difference between predicted and observed community composition at site i). $P\{\gamma_i = \alpha_i\}$ values for taxonomic community composition estimates for OUs by the two trait-neutral models were compared with a t-test to determine if there was a difference in how well the models predicted local relative abundances.

CFT scores were calculated from \hat{P} for each trait-neutral model. The goodness of fit statistic described above was used to compare the rows and columns of predicted CFT score matrices against the observed CFT matrix. A comparison of rows provides estimates of $P\{\gamma_i = \alpha_i\}$ for functional composition, a measure of how well each model predicts the CFTN of each OU_i (Q route analysis) (McCune and Grace 2002). The p-values from a comparison of columns provides an estimate of $P\{CFT_t\}$, which is a measure of how well each model predicts the distribution of trait syndromes among sites for each trait t , (R route analysis) (McCune and Grace 2002). Traits were then ranked by fit, where traits with the lowest fit ranked as the most likely candidates to be subject to sorting by an environmental filter.

Trait-neutral prediction of the source pool

Change in C_{ij} with distance, when modeled as a function of m (equation 3), resulted in similar curves for all abundance data and when rare taxa were excluded (Figure 2.3A). Estimates of the distances beyond which neighboring OUs contribute 0.95, 0.50, and 0.05 times as much to γ_i as the nearest neighboring site (Figure 2.3B, labeled d_{95} , d_{50} , and d_{05} , respectively) did not change when rare taxa were excluded. Assuming the metacommunity dynamics that cause variation in community composition among OUs with a grain size of $\sim 100m$ function at a scale larger than 5.4 km (the mean nearest neighbor distance), sites greater than 36km away contributed less than half as much as nearest neighbor sites to γ_i .

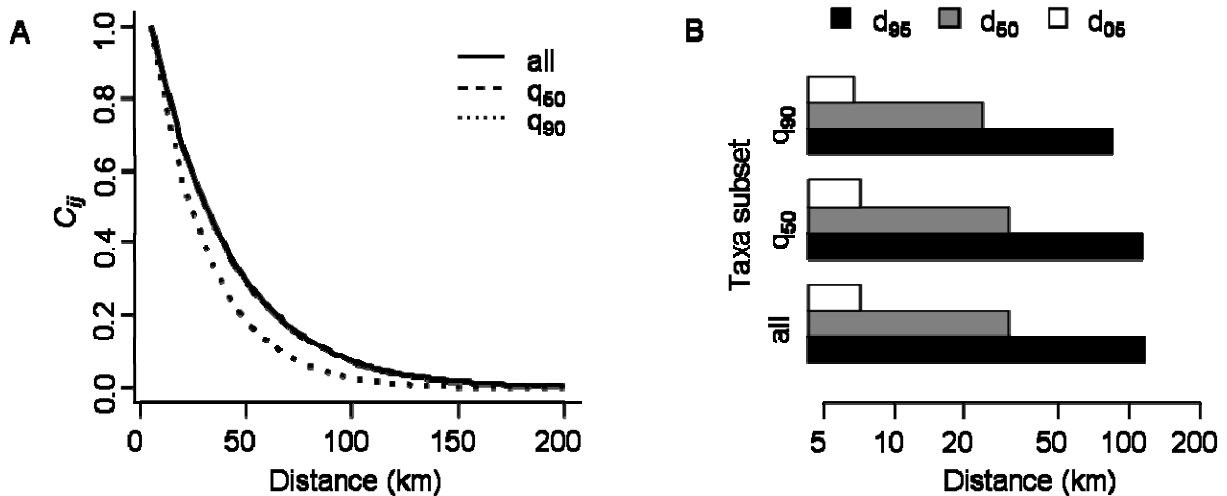


Figure 2.3. Values for models where m was fit with all observed taxa (all), 50th percentile taxa (q_{50}), and 90th percentile taxa (q_{90}). Percentiles were calculated from mean regional observed relative abundances. (A) Fitted distance decay curves for C_{ij} , where C_{ij} is a measure of connectivity between OUs i and j . (B) Distances at which C_{ij} is 0.95 (d_{95}), 0.50 (d_{50}), and 0.05 (d_{05}).

Mean $P\{\gamma_i = \alpha_i\}$ values for taxonomic composition were consistently above 0.05 (both excluding and including rare taxa in the calculation), and near 0.40 when rare taxa were included in the analysis, indicating that both models provide a reasonable estimate of relative abundances (see Appendix D for figures illustrating model fit). $P\{\gamma_i = \alpha_i\}$ values are slightly higher for $f(P_{obs}, D_{geo}, m \neq 0)$ ($p = 0.05$) when all taxonomic groups or the 50th percentile taxonomic groups were used in the analysis. Mean $P\{\gamma_i = \alpha_i\}$ values (± 1 s.d.) for functional trait composition were between 0.20 and 0.40 for both models and for estimates calculated either with or without rare taxa.

$P\{CFT_i\}$ values, estimates of goodness of fit for how well trait scores were predicted to vary among OUs, averaged near 0.20 for both $f(P_{obs}, D_{geo}, m \neq 0)$ and $f(P_{obs}, D_{geo}, m = 0)$, and no trait had a $P\{CFT_i\}$ value less than 0.05. Trait ranks (Table 2.2) for potential as candidates for community sorting based on $P\{CFT_i\}$ from the two models were roughly similar and positively correlated ($r = 0.71$, $p < 0.001$). Functional feeding group (excluding FFG.SH) and life history traits had the highest average rank.

Inferences from D_2

Niche and neutral theory both make predictions about the relationship between the regional source pool (γ_0) and local community composition (α_i) at site i (OU_i). If a source pool of ubiquitous colonizers is available, the effective source pool at any site i (γ_i) should be a random sample of γ_0 . Therefore the assumption of ecological equivalence in combination with a homogenous source pool results in the prediction in equation 2 (all three metrics are equal). Distinguishing between niche and neutral community assembly means distinguishing which metrics are unequal. A difference between γ_i and α_i indicates a difference in composition between the effective source pool and the observed local community composition. Disparity between γ_0 and γ_i indicates a divergence in available source pools among OUs.

The trait-neutral models used here are both null model predictions of α_i under the assumption of ecological equivalence (assumption 1, Figure 2.1), and predict $\gamma_i = \alpha_i$. Both models will be rejected if local environmental filters are selecting colonizers based on their functional traits. Both trait neutral models use the function $f(P_{obs}, D_{geo}, m)$, which estimates the relative contribution of neighboring OUs to γ_i as a prediction of the effective source pool for OU_i ; however, $f(P_{obs}, D_{geo}, m \neq 0)$ provides a dispersal limited estimate of γ_i , and $f(P_{obs}, D_{geo}, m =$

0) assumes $\gamma_0 = \gamma_i$. For the observational grain size used in this study, OUs up to 35km away contributed approximately half as much to γ_i as the nearest neighboring OU in the dispersal limited model.

The results do not provide sufficient evidence to reject the assumption $\gamma_0 = \gamma_i$, because both models had a mean goodness of fit ($P\{\gamma_i = \alpha_i\}$) between 0.30 and 0.40 for each OU. The dispersal limited model provided a slightly better estimate of the γ_i than the homogenous source pool model (t-test comparison of $P\{\gamma_i = \alpha_i\}$ values for the two models, $p = 0.05$) when rare taxa are included, but both models performed the same ($p = 0.46$) when the ten most ubiquitous taxa were included in the analysis (see Appendix D). These ambiguous results suggest there is some detectable dispersal limitation in the regional source pool for less dominant taxa, but the regional source pool is a reasonable estimate of the effective source pool.

The two models described above provide two different trait neutral predictions of γ_i that can be compared against α_i to test the assumption of ecological equivalence, and the prediction $\gamma_i = \alpha_i$. I used the predicted community composition, \hat{P} , to calculate an expected CFT score for each trait t . Comparisons of observed against predicted CFT scores for each trait t provide a measure of how strongly each trait is being sorted at the scale of the OU. If community composition is a result of convergent environmental filtering, observed CFT scores should be more extreme than expected, but the mean CFT score among OUs should not differ from the expected mean CFT score. Therefore, I used a null hypothesis that the absolute differences between predicted and observed CFT scores for OUs were predicted by a random variable with a mean of zero to create a test for environmental filtering, where a low $P\{CFT_t\}$ indicates environmental filtering with respect to trait t . Trait ranks based on $P\{CFT_t\}$ (Table 2.2) show functional feeding group and life history traits are the best candidates for sorting.

Conclusions

I implemented a study design in which I expected a bias for detecting neutral processes because habitats were similar (forested headwater streams) and there was little variation among the CFTNs calculated for OUs within the study (Appendix B). While the community composition data did exhibit spatial decay in similarity (Figure 2.2A), it corresponded with functional turnover (Figure 2.2C), providing support for the environmental filtering mechanisms of community assembly hypothesized by niche theory (H_1).

The two diagnostics described here are complimentary analyses of diversity that provide testable predictions for niche and neutral theory. D_1 (spatially explicit patterns in β -diversity) yields two important pieces of information: (1) a measure of the scale at which there is a decay in compositional similarity among communities, and (2) the spatial lags at which there is disparity between taxonomic and functional composition. D_2 indicates whether the different functional guilds for a respective trait are underdispersed ($P\{\gamma_i = \alpha_i\} < 0.05$), regardless of whether the functionally homogenous group is taxonomically homogenous. Together, these two diagnostics indicate which functional traits are the best candidates to describe how environmental filters influence community assembly, and the spatial lag at which source pool composition begins to diverge.

The results of this study are likely influenced by the lack of resolution in taxonomic identifications and the coarse level at which functional groups are identified. I used genus level taxonomic resolution, which would miss turnover within a niche among congeneric species. Recent developments in barcoding techniques for indentifying macroinvertebrates (Janzen et al. 2009) show promise for a high throughput technique that may result in high resolution phylogenetic data that I expect would show greater source pool heterogeneity (i.e., provincialism) and a greater role for dispersal limitation in community assembly. Similar applications of barcoding in microbiology have alluded to a more important role for biogeography as a determinant of community composition (Lachance 2004) than the cannon (Baas Becking 1934) suggests.

Patterns in the data available for benthic macroinvertebrates in forested headwater streams in the southern Blue Ridge suggest “everything is everywhere, but the environment selects.” The lack of evidence for turnover within functional groups leads me to suspect that turnover within functional groups, if it does occur, occurs among congeneric species. This conclusion suggests that if turnover within a niche occurs, it results from a race between range expansion and genetic drift. Thus, the dynamics extensively described in Hubbell’s (2001) unified neutral theory and the manner in which a community is defined for an investigation in patterns in biodiversity may become increasingly important as high resolution taxonomic data becomes more readily available.

Chapter 3 - Multivariate environmental filters determine β -diversity in functional composition of benthic macroinvertebrate communities

Introduction

Niche and neutral theory provide two ends of a continuum of community assembly processes (Hubbell 2001, Gravel et al. 2006) that predict patterns of β -diversity in metacommunities (Leibold et al. 2004). At the niche theory end of the continuum, the interaction between the habitat template (Southwood 1977) and organisms' functional traits determines community composition at a site (Poff et al. 2006, Westoby and Wright 2006); whereas metacommunity dynamics (e.g., dispersal, local extinctions, speciation) (Martiny et al. 2006) organize community composition at the neutral theory end of the community assembly continuum. Therefore, the proportion of β -diversity described by environmental variation and spatial structure (independent of spatially structured environmental gradients) indicates the relative influence of niche and neutral community assembly processes, respectively (Legendre et al. 2005, 2008).

The niche theory based mechanism of environmental filtering (Keddy 1992, Weiher et al. 1998) has long been invoked as the primary mechanism for determining among site variation in benthic macroinvertebrate community composition (β -diversity) (Tonn et al. 1990a, Poff 1997). With the development of functional trait databases (Usseglio-Polatera et al. 2000, Poff et al. 2006), researchers have demonstrated that ecologically significant relationships exist between variation in the habitat template and the functional composition of communities (e.g., Charvet et al. 1998, Bady et al. 2005, Statzner et al. 2005, Diaz et al. 2008). However, different functional-trait/environmental-constraint interactions have been shown to organize benthic community composition at different scales of observation (Lamouroux et al. 2004) because lotic habitat templates are defined by nested, hierarchical environmental gradients (Frissell et al. 1986, Poff 1997).

Recent studies (Thompson and Townsend 2006) have also shown neutral community assembly processes may play a role in determining benthic macroinvertebrate community

composition, especially at recently disturbed sites. However, the relative influence of neutral theory is likely influenced by observational grain size and study extent (Nekola and White 1999), and neutral community models are likely not appropriate for explaining β -diversity at local (intra-basin) scales (Heino and Mykra 2008).

If environmental filters are organizing communities by traits, then organisms that are functionally similar with respect to the traits that are being sorted are more likely to co-occur, resulting in a non-random distribution of the trait types (modalities) for the sorted traits among sites (Grime 2006). Therefore, neutral community models can be used as null models to predict β -diversity in functional community composition, which can be used to evaluate the different components of observed functional β -diversity and identify the functional traits that are most strongly influenced by environmental filters.

In this study, I seek to identify whether niche theory processes alone are sufficient to determine variation in benthic macroinvertebrate community composition (β -diversity) among reaches located along an environmental gradient influenced by a logging disturbance within the Ray Branch basin, and to determine the direct and indirect relationships by which different aspects of the habitat template influence β -diversity. The results of this study are not meant to draw conclusions about watershed scale logging practices as a disturbance. Instead, I took advantage of the among-reach environmental variation to address the influence of reach scale variation in the habitat template on benthic macroinvertebrate community composition observed at the reach scale. Specifically, my objectives were to (1) determine the relative influence of spatial and environmental variation on community composition (i.e., β -diversity), (2) determine which functional traits are distributed among sites in a manner that indicates they are influenced by an environmental filter, (3) validate the traits identified as relevant to community sorting in objective 2 with actual correlations between functional composition and observed variation in environmental variables, and (4) resolve the habitat characteristics that interact to create environmental gradients that act as filters to organize the benthic macroinvertebrate community.

Methods

Study site and design

All sampling reaches were located in headwater tributaries of Ray Branch (Figure 3.1) in the Nantahala National Forest, North Carolina. Sites were located between elevations of 800 and 1100 m, in watersheds with 20-30% slope and similar geology (biotite gneiss with locally abundant quartz and aluminum silicates). Shelterwood cut timber harvest occurred in 6.5 – 9.7 ha sections (13-28% of the basin area) in two watersheds (L1 and L2, Figure 3.1) in 2005, while two reference watersheds (R1 and R2) remained forested with secondary growth, montane oak-hickory forests. Streams had perennial flow, with median discharge of 6 - 10 L/s at upstream sites and 14 - 25 L/s at downstream sites during the study period.

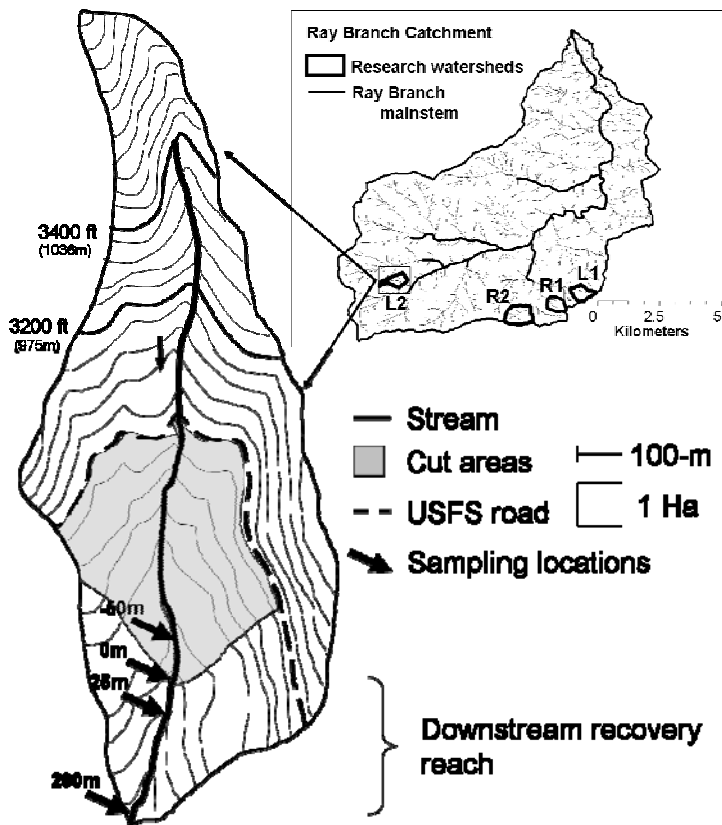


Figure 3.1. Map of sampling sites. Four sampling reaches were located in headwater subwatersheds that were logged (L1 and L2) and two reference subwatersheds (R1 and R2) in the Ray Branch watershed in the Nantahala National Forest, North Carolina. 10 m sampling reaches were spaced longitudinally along streams at -50 m (50 m upstream of the cut boundary), 0 m (at the but boundary), 25 m and 200 m in logged watersheds, and spaced similarly in reference watersheds.

The primary goal of this study was to explore the relationship between environmental variables that define the habitat template and the β -diversity of benthic community functional composition. Therefore, sites were distributed longitudinally in sub-watersheds, which were subject to different logging treatments to ensure that study sites spanned a detectable environmental gradient. Habitat characteristics and benthic macroinvertebrate community composition sampling schemes were designed to be representative of a 10 m reach observational unit. Four sampling reaches were located longitudinally along a stream at -50 m, 0 m, 25 m, and 200 m, with the 0 m site located at the downstream cut boundary (or arbitrarily at a similar position in the watershed in the reference streams), for a total of 16 reach scale observational units. Samples were collected in April 2006 and the location of the upstream end of each sampling reach was estimated using a handheld GPS unit.

Macroinvertebrate community composition

Reach scale observations of macroinvertebrate densities were estimated from five Surber samples within a 10 m reach of stream. Benthic Surber samples were collected from each reach in April, 2006, and samples were preserved in 80% ethanol and sorted in the lab. All insects were identified to genus (Wiggins 1977, Stewart et al. 1993, Merritt and Cummins 1996), or the highest taxonomic resolution available in the trait database compiled by Poff et al. (2006). Other macroinvertebrates not included in the database and members of Chironomidae were excluded from the analysis.

Community-aggregate functional trait (CFT) scores provide information about the functional nature of an assemblage of organisms. A trait refers to an ecologically relevant characteristic of an organism. Each trait state is referred to as a “trait syndrome” and each syndrome is represented by a trait score. The functional trait niche (FTN) (Poff et al. 2006) of a taxonomic group (e.g., *Baetis*) refers to the set of trait modalities assigned to that taxonomic group (e.g., the trait modalities for *Baetis* in Appendix E describe its FTN). Therefore, a community-aggregate functional trait niche (CFTN) refers to a set of community-aggregate functional trait (CFT) scores that best describe the functional characteristics of an assemblage of multiple taxonomic groups (e.g., the macroinvertebrates that make up a benthic assemblage in a watershed).

CFT scores for a set of observations of assemblages of macroinvertebrates was calculated as

$$C = P \cdot T' \quad (1)$$

where C is a sampling reach by trait matrix in which each cell, $C_{i,t}$, is the average functional trait modality (CFT score) for the entire assemblage for observation i for trait t . P is a reach by taxon matrix of relative abundances and T' is the transpose of a taxon by functional trait syndrome matrix (T) (Legendre and Legendre 1998, McCune and Grace 2002). Relative abundance data in P was calculated from Hellinger transformed (Legendre and Gallagher 2001) densities that were rescaled so that transformed densities for each reach summed to 1. T is an n_{taxa} by n_{trait} matrix, where n_{trait} ($n_{\text{trait}} = 29$) is the number of traits that were scored for each of the observed taxonomic groups.

For this study, T was modified, from the list of taxon specific trait scores provided by Poff et al. (2006), in which traits were grouped into trait classes: ecology, life history, mobility, and morphology (Table 2.1). Trait scores for Tipulidae were expanded to a genus level resolution, and trait scores for Peltoperlidae were added using information available in Merritt and Cummins (1996) and Stewart et al. (1993). I rescaled all trait scores as described in Chapter 2 (see Table 2.1 or Table 1 in Poff et al. 2006 for trait descriptions; see Appendix E for taxon specific trait scoring).

Testing CFT distributions

I used a bootstrapping procedure to create a trait-neutral null model of the distribution of CFT scores among sites to calculate probabilities for the observed CFT scores using R statistical software (R Development Core Team 2007). The model assumes no dispersal limitation, a homogenous source pool, and ecological equivalence among all taxonomic groups. The procedure calculates a site by taxa matrix of abundances (A_{boot}), where each row, i , is a simulated reach scale sample, α_i , of n_i individuals from the regional source pool, γ_0 . Each n_i was randomly set to one of the observed reach scale total densities (no./m² summed across all taxonomic groups). γ_0 is a vector of mean relative abundances of all observed sampling reaches. Individuals are randomly sampled from the source pool and their probability of being selected in each sampling event is equivalent to their relative abundance in γ_0 .

CFT scores were calculated from the Hellinger transformed abundances from each simulated α_i . Percentiles were calculated for each observed CFT score, $p\{C_{i,t}\}$ for each trait t at site i and used to estimate the probability of the observed distribution of CFT scores for each trait t , $P\{C_t\}$, given the null model. $P\{C_t\}$ was estimated as

$$P\{C_t\} = \frac{1}{n_{sites}} \sum_{i=1}^{n_{sites}} 1 - 2|p\{C_{i,t}\} - 0.5| \quad (2)$$

where distributions of CFT scores that are more extreme (either high or low) given the null distribution will have $P\{C_t\}$ scores closer to 0. I used the $P\{C_t\}$ to rank traits as candidates for sorting, where traits with the lowest $P\{C_t\}$ scores were expected to be the most likely to correlate with environmental gradients (a rank of 1 = most likely to be sorted).

Environmental variables

Two to three Thermochron iButton (Maxim Integrated Products, Inc., Sunnyvale, CA) temperature data loggers were installed at each reach in polyethylene centrifuge tubes and anchored in areas in the reach with perennial flow and recorded ambient water temperature every 4 hours from 19 February 2006 to 19 May 2006. Temperature readings from each data logger in a reach were averaged to represent reach temperature for each time period. Degree days were calculated for each reach for the time period that the data loggers were deployed as the sum of mean (across all data loggers in a reach) temperature reading per time interval (1/6 day) multiplied by the number of days of observations.

Streams were surveyed with a Topcon total station GTS 300. I surveyed 300 m of stream thalweg in each watershed (Gordon et al. 1992). At least two cross sections were measured within reach each reach. Cross section depth profiles were measured using a meter tape and meter stick (Gordon et al. 1992), with leveling correction from the survey data. Gradient was calculated as the slope (%grade, where 100% = a 45° angle) over the 10 m sampling reach.

HOBO U20-001 water level loggers from the Onset Computer Corporation were placed in stilling wells near the 0 m mark in each stream and used to record stage height in each watershed between 8 February 2006 and 19 May 2006. Stream discharge (Q) was estimated on select dates at up and downstream sites using the slug dilution method (Gordon et al. 1992). Observed estimates of Q , channel cross sectional shape, thalweg gradient, and the stream stage time series data were used to fit a value for Manning's n (a roughness coefficient) and a time

series of channel velocity for each reach (see Appendix F). Summary statistics were calculated from velocity data for each reach and I used overall median velocity (V_{med}) as an environmental variable to describe differences in reach velocity.

Pebble counts along a zigzag transect, using a heel-to-toe walk, were used to sample 100 observations of bed particle size for each reach, and size classes were determined using a gravelometer (Bunte and Abt 2001). The the 26th, 50th, and 84th percentile b-axis lengths (D26, D50, and D84 respectively) were estimated by interpolation from the b-axis lengths of the nearest observed quantiles (Bunte and Abt 2001).

For each 10 m reach, I laid out a 30 m meter tape, zigzag transect, and recorded the diameter of all pieces of wood greater than 1 cm in diameter. I estimated the proportion of large wood habitat per area active channel as the ratio of wood surface area to transect length (Benke et al. 1984).

Biofilm standing crops were sampled from three sets of three randomly selected cobbles from each sampling reach (Hauer and Lamberti 2006). Samples were homogenized, subsampled, and filtered through GF/F filters (effective 0.7 μ m pore size, Whatman Inc., Piscataway, NJ) for chlorophyll *a* and ash free dry mass (AFDM) analysis. Chlorophyll *a* concentrations in subsamples were determined using a spectrophotometric analysis following hot ethanol extraction (APHA et al. 1998). Biofilm AFDM samples were combusted at 550 °C, AFDM was calculated as the proportion mass lost in combustion, and used to calculate biofilm AFDM standing crop.

Coarse benthic organic matter (CBOM) and fine benthic organic matter (FBOM) were sampled using a steel sampling corer (Hauer and Lamberti 2006). CBOM (>1 mm) samples that were composed primarily of wood and leaves were placed in bags and dried for AFDM analysis. Stream bed sediment was disturbed up to a 5 cm depth, contents in the corer homogenized, and a 250 ml subsample was collected to estimate the FBOM concentration. Five water depths in the corer were recorded to estimate the volume of water that was subsampled for FBOM concentrations.

CBOM samples were dried at 60 °C, ground, subsampled, and combusted at 550 °C to determine CBOM AFDM. FBOM samples were passed through a 1 mm sieve and a GF/F filter using gravimetric filtering. The fraction on the GF/F filter (i.e., 0.7 μ m – 1 mm), was combusted

at 550 °C to determine the AFDM. CBOM and FBOM AFDM were standardized to benthic area sampled and reported as g/m².

Particulate sediment and organic matter (OM) in transport was collected with a 500 µm mesh size drift net, placed in the stream for a 24 h period. Particulate transport samples were collected on two separate dates from each reach in April and May of 2006. Flow velocities into the nets and water depths were measured before and after net deployment and used to estimate the volume of water that had passed through the net. Samples were dried at 60 °C for at least 24 h and weighed. Concentrations of sediment and organic matter in transport were calculated as dry weight per volume of water (g/L).

Each environmental variable was tested for normality with Shapiro test and log or arcsine-root transformed when necessary. All variables were then centered around the mean and scaled to standard deviation. Principal component analysis (PCA) on transformed and scaled data was used to ordinate sites in environmental space. Environmental variables that appeared to be redundant and were suspect of multicollinearity were excluded from the analysis (see Table 3.2 for an environmental variable list).

Evaluating β-diversity

Variance partitioning of raw data matrices was used to determine the relative contribution of environmental and spatial variation as organizers of community composition (Borcard et al. 1992, Legendre et al. 2005). I used the function *varpart* in the *ecodist* package (Goslee and Urban 2007b) for R to conduct a redundancy analysis (RDA) to assess the relationship $Y = X_{env} + X_{space}$. Y is either A (site by taxa community composition matrix of Hellinger transformed densities) or C (site by functional trait matrix of CFT scores), X_{env} is a site by environmental variable matrix, and X_{space} is a matrix describing the spatial structure of the sites (e.g., x and y coordinates or principal coordinates from a principal coordinate of neighbor matrices analysis (PCNM) (Borcard and Legendre 2002)). RDA is analogous to a multiple regression, but the response and predictor variables are multivariate. In this study, the main role of variance partitioning was to show environmental gradients were driving community composition rather than distance decay patterns that function independent of observed environmental gradients.

I used a two-way, stepwise selection process (*stepAIC*, available in the MASS package for R) (Venables and Ripley 2002) to determine the best fit linear models that explained the

relationship between environmental variation and the variation in the distribution of CFT scores among sites for individual traits. The adjusted coefficients of determination for the best model for each trait were used as an index of the overall strength of the influence of the environmental gradient on that trait.

PCoA served to reduce the dimensionality of CFT space and I used the principal coordinate scores from relevant axes as composite variables to describe the variation for a suite of related, multicollinear functional traits (e.g., predators tend to be good dispersers). I then used *stepAIC* to perform two-way stepwise selection for the best linear, multiple regression model describing the relationship between community functional composition and relevant environmental variables.

Environmental variables selected using the *stepAIC* function were then used to construct path models which provide a method for describing and testing the relationships among predictor variables, causal relationships between predictor and response variables, and indirect relationships involving multiple predictor variables. I used AMOS 16.0.1 (Arbuckle 2007) to conduct a specification search on the multiple regression models from the variable selection process. This process allowed me to restrict non-significant relationships to 0, providing degrees of freedom to calculate a model goodness of fit statistic. I constructed and tested path models describing causal relationships among predictor variables using the information from the specification search and my general knowledge about freshwater ecosystems (e.g., LWD may influence FBOM concentrations at a site, but the reverse causal relationship is not likely to be the case).

Results

Macroinvertebrate community composition

A total of 53 taxonomic groups were included in the analysis. Average macroinvertebrate density was 870.2 (± 91.9 SE) individuals/m², and an average of 32 (± 0.8 SE) taxonomic groups were observed among the five Surber samples pooled to represent each reach. The first three axes of the PCoA ordination represent 61.7% of the variance in community composition among reaches (Figure 3.2) and show which taxa tend to co-occur and which sites have similar taxonomic composition.

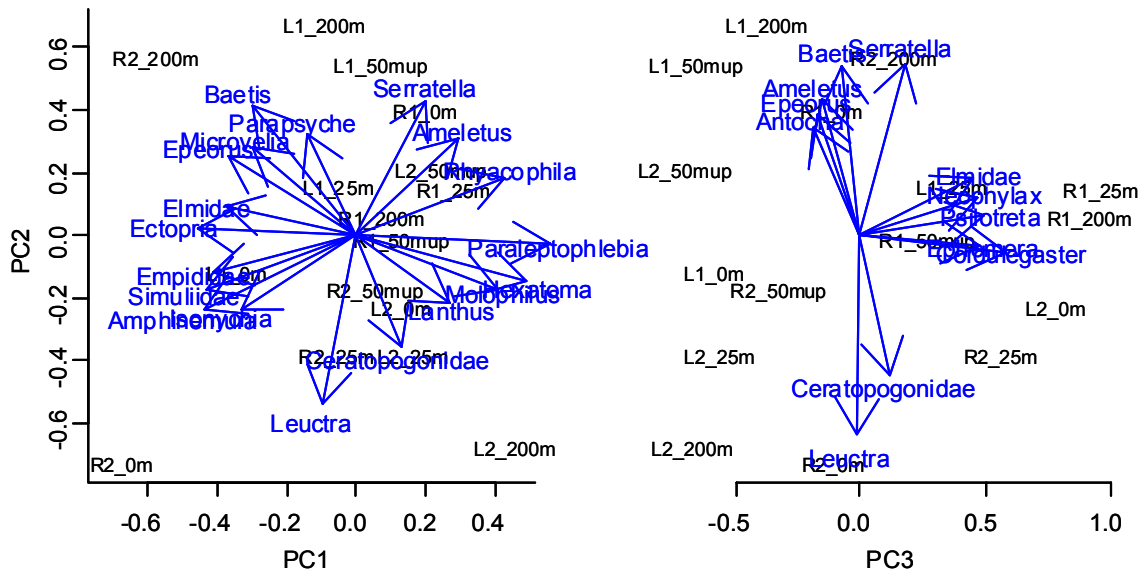


Figure 3.2. Principal coordinate analysis (PCoA) of sites in taxonomic space. The first 3 axes explain 33.7%, 18.4%, and 9.6% (total = 61.7%) of the variation in the data, respectively. Vectors indicating loading of taxa onto PC axes were estimated with the function *vf* available in the R package *ecodist* (Goslee and Urban 2007a), and were only shown if significant ($p < 0.05$).

Variation in CFT scores indicates differences in among reach functional composition (Figure 3.3). The first three axes of a PCoA explain 84.5% of the variation in CFT scores. The ordinations in CFT space indicate which sites have functionally similar communities of macroinvertebrates, and which functional traits co-vary among reaches. Axis 1 (CFT_PC1) is positively correlated with swimming ability (Swim), fusiform shape (Shpe), larger body size (Size), a preference for high DO habitats (Resp), and negatively correlated with synchrony in emergence patterns (Sync), and presence of collector-filtering (FFG.CF) and shredding

(FFG.SH) functional feeding groups. Axis 2 (CFT_PC2) is positively correlated with body size, dispersal ability (Disp, Flgt), crawling (Crwl), burrowing (Hab.Burrow), and predation (FFG.Pred). Axis 3 (CFT_PC3) is positively correlated with voltinism (more generations per year) and negatively correlated with thermal tolerance, development time, life history, armoring, and the scraping functional feeding group.

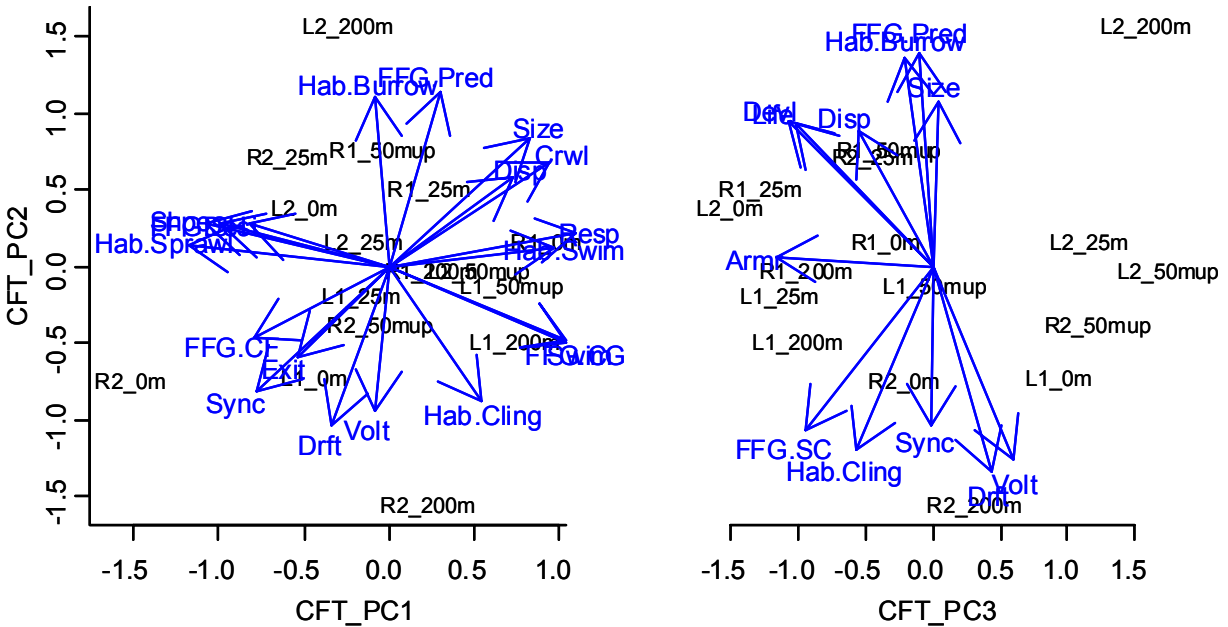


Figure 3.3. Principal coordinate analysis (PCoA) of sites in functional trait space. The first 3 axes explain 40.1%, 30.1%, and 14.2% (total = 84.5%) of the variation in the data, respectively. Vectors indicating loading of traits onto PC axes were estimated, and were only shown if significant ($p < 0.05$).

A comparison of observed CFT distributions against CFT distributions predicted by the trait-neutral null model (Figure 3.4) show a large proportion of traits following a pattern of random sampling from a common source pool. Seven traits (Drift, Disp, Life, Sync, Hab.Swim, Hab.Burrow, and Shpe) have a $P\{C_i\} < 0.05$ (Table 3.1), indicating the observed distribution of CFT scores for those traits tend to be outliers when compared against predicted trait-neutral distributions of CFT scores.

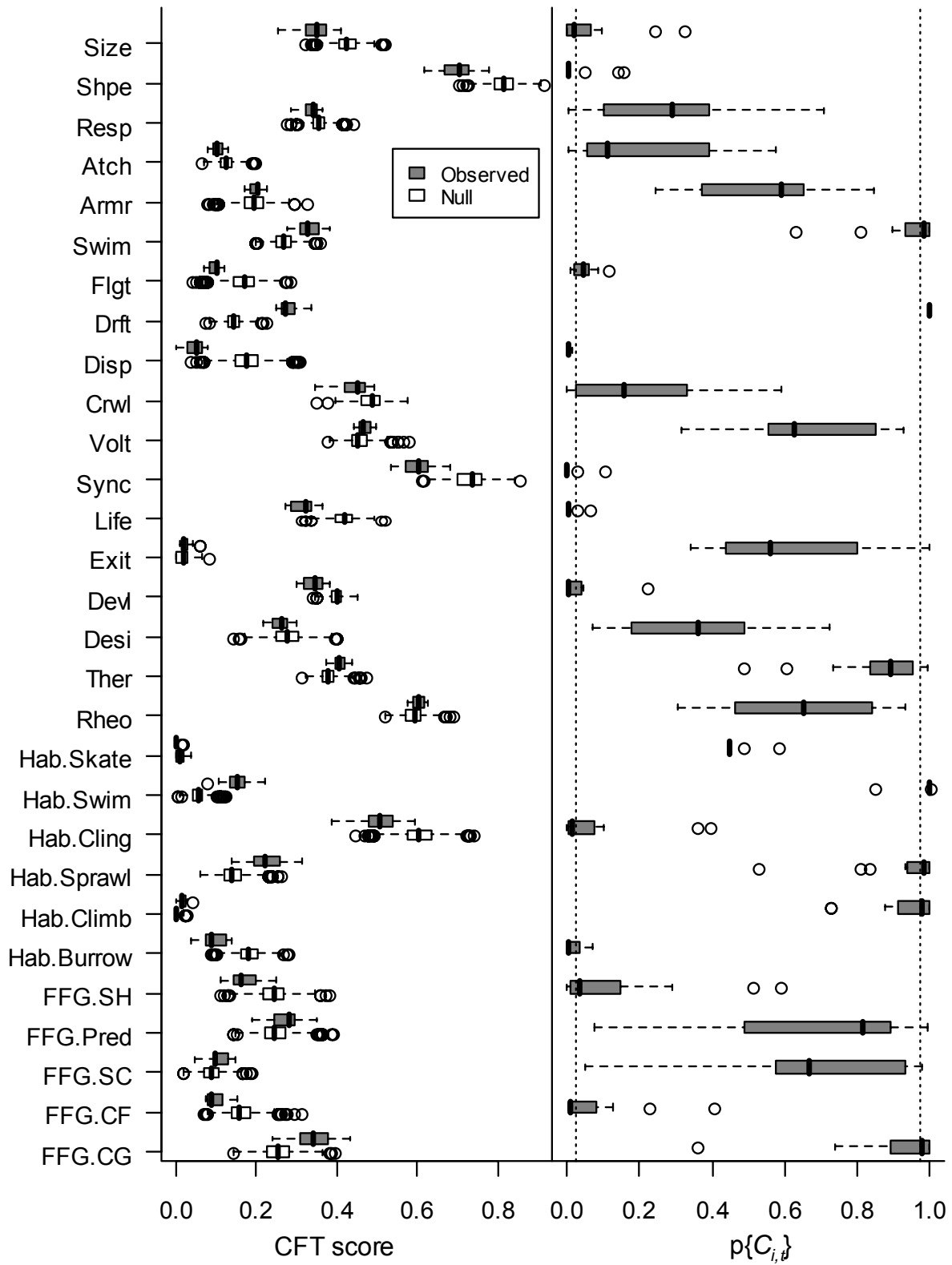


Figure 3.4. Distributions of observed and predicted CFT scores for each trait (t). Boxplots for CFT scores indicate quartiles and median for the observed distribution of CFT scores among sites for each trait, and the

distribution of CFT scores predicted for each trait by the trait-neutral model. $p\{C_{i,t}\}$ is the percentile for the CFT score for trait t at site i when compared to the trait-neutral null distribution of CFT scores for trait t . Boxplots for $p\{C_{i,t}\}$ are distributions of percentiles. Points outside of the vertical dotted lines are outside of the 95% confidence interval of the expected CFT score predicted by the trait-neutral lottery model.

Table 3.1. Trait sorting ranks based on a trait-neutral lottery model. Traits with a $P\{C_t\} < 0.05$, indicating significant sorting, are in bold.

Trait Code	$P\{C_t\}$	Rank	Trait Code	$P\{C_t\}$	Rank
Drft	0.000	1	FFG.CG	0.179	16
Disp	0.006	2	FFG.SH	0.250	17
Life	0.015	3	Ther	0.287	18
Sync	0.017	4	Crwl	0.393	19
Hab.Swim	0.020	5	Atch	0.411	20
Hab.Burrow	0.039	6	Resp	0.585	21
Shpe	0.044	7	FFG.SC	0.610	22
Devl	0.053	8	Volt	0.650	23
Flgt	0.088	9	FFG.Pred	0.668	24
Size	0.116	10	Desi	0.679	25
Swim	0.116	11	Rheo	0.708	26
Hab.Climb	0.130	12	Exit	0.759	27
FFG.CF	0.130	13	Hab.Skate	0.919	28
Hab.Cling	0.135	14	Armr	0.920	29
Hab.Sprawl	0.138	15			

These traits were ranked as the most likely candidates for interacting with an environmental filter, and to correlate with an environmental gradient.

Environmental gradients

The first four axes of a principal component analysis (PCA) capture 81.3% of the among-site environmental variation (Figure 3.5). The ordinations indicate which environmental variables (Table 3.2) covary and which relationships are positive and negative. The environmental gradient along axis 1 is positively correlated with channel velocity (V.med and

V.range) and FBOM and negatively correlated with the amount of large wood habitat (LWD), temperature (Temp_DegDays). Axis 2 shows a gradient positively correlated with biofilm standing crop (BioAFDM) and substrate size (D84 and D26) and negatively with temperature range (Temp_range). Axis 3 is positively correlated with D26 size class and FBOM, and negatively correlated with velocity (V.med and V.range) and material in transport (SedTot). Lastly, axis 4 is negatively correlated with gradient (Gradient) and velocity (V.med, V.range), and positively correlated with material in transport.

Table 3.2. Descriptions of reach scale environmental variables.

Variable ID	Variable description	Mean (SE)
Temp_DegDays (°C day)	Degree days above 0 °C between 19 Feb and 19 May 2006	905.5 (8.8)
Gradient	Gradient over a 10 m stream reach	0.13 (0.01)
V_med (m/s)	Median channel velocity between 8 Feb 2006 and 31 May 2006	0.051 (0.006)
D26 (mm)	26 th percentile of stream bed particle-size (b-axis) distribution	11.1 (1.6)
D84 (mm)	84 th percentile of stream bed particle-size (b-axis) distribution	102.2 (7.9)
LWD	Large wood surface area as a proportion of the active channel surface area	0.039 (0.010)
BioAFDM (mg/cm ²)	Ash free dry mass of biofilm standing crop on cobbles	0.17 (0.02)
Chl_a (mg/cm ²)	Chlorophyll <i>a</i> standing crop on cobbles	0.10 (0.01)
CBOM (g/m ²)	Coarse benthic organic matter (ash free dry mass)	82.6 (22.1)
FBOM (g/m ²)	Fine benthic organic matter (ash free dry mass)	45.0 (10.8)
SedTot (mg/L)	Particulate sediment and OM in transport (dry mass)	7.0 (3.8)

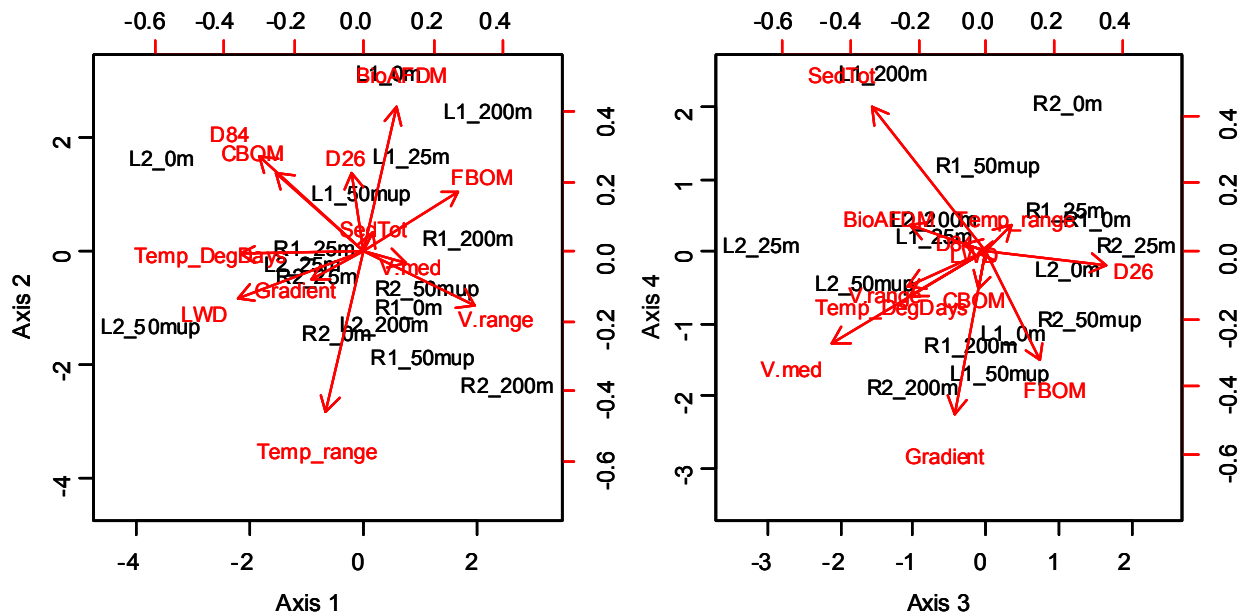


Figure 3.5. Principal component analysis of environmental variables. Biplots show sites plotted in environmental space. The first four principal components explain 29.6%, 21.4%, 17.6%, and 12.7% (total = 81.3%) of the variation in the data, respectively.

Evaluating β -diversity

The adjusted coefficients of determination (R^2) calculated from variance partitioning with RDA (Table 3.3) showed 39.6% ($p = 0.005$) of the variation in taxonomic composition and 57.2% ($p = 0.006$) of the variation in functional composition (CFT scores) was explained by among reach environmental variation. Adjusted R^2 values were not significant for either raw xy coordinates or principal coordinates from a PCNM analysis, used to model non-linear spatial structure, as explanatory variables. These results indicate environmental variation is the main organizer of community composition at the 10m reach observational grain size, and environmental variation is a better predictor of community functional composition than taxonomic composition.

Stepwise linear regression of CFT scores for each trait against environmental variables produced significant ($p < 0.05$) linear models for 17 of the 29 environmental variables (Table 3.4). Gradient, V_med, and LWD were the environmental factors most commonly included as statistically significant predictor variables for CFT variation (included in models for 10, 10, and 9 of the 29 traits, respectively). Chla and SedTot were moderately, statistically significant, predictor variables (included in models for 5 and 4 traits, respectively). The adjusted coefficients

of determination for the best fit model for each trait were predicted moderately well by trait ranks determined by the trait-neutral null model (Figure 3.6, $R^2 = 0.28$, $p = 0.01$).

Table 3.3. Variance partition of β -diversity in Taxonomic and Functional composition.

Predictor variables		Taxonomic comp.		Functional comp.	
		Adj. R^2	p-val*	Adj. R^2	p-val*
[a+b] = X1	Environment	0.40	0.01	0.57	0.01
[a] = X1 X2	Env Sp.St.	0.44	0.02	0.70	0.01
[b+c] = X2	Spatial Structure	0.06	0.09	-0.01	0.49
[c] = X2 X1	Sp.St. Env	0.10	0.31	0.12	0.27
[a+b+c] = X1+X2	Env + Sp.St.	0.50		0.69	
[d] = Residuals	Error	0.50		0.31	

*p-values estimated from 10000 permutations

Table 3.4. Multiple regression models for individual traits. Regression coefficients and p-values are reported for environmental variables that were selected in stepwise selection to describe the variation in CFT scores for each trait. Whole model adjusted coefficients of determination and p-values indicate the model fit for each trait.

Trait	Adj. R ²	p-val	BioAFDM		CBOM		Chla		D26		D84		FBOM	
			coef	p-val	coef	p-val	coef	p-val	coef	p-val	coef	p-val	coef	p-val
Drft	0.47	0.02					-0.174	0.114	0.021	0.110	-0.031	0.144		
Disp	0.76	0.00												
Life	0.66	0.00					0.348	0.002						
Sync														
Hab.Swim	0.75	0.00			0.029	0.001								
Hab.Burrow	0.36	0.06			-0.014	0.057								
Shpe	0.80	0.00	0.061	0.017	-0.015	0.009	0.379	0.019						
Devl	0.61	0.01					0.244	0.015	-0.013	0.210				
Flgt	0.73	0.00							0.007	0.219	0.020	0.129		
Size	0.21	0.17											-0.031	0.059
Swim	0.50	0.01												
Hab.Climb														
FFG.CF	0.19	0.05							0.023	0.050				
Hab.Cling	0.16	0.07												
Hab.Sprawl	0.60	0.01							0.045	0.020	-0.079	0.034		

Table 3.4 (Continued). Multiple regression models for individual traits.

Trait	Adj. R2	p-val	BioAFDM		CBOM		Chla		D26		D84		FBOM		
			coef	p-val	coef	p-val	coef	p-val	coef	p-val	coef	p-val	coef	p-val	
FFG.CG	0.63	0.00												-0.027	0.055
FFG.SH	0.52	0.02							0.034	0.073	-0.103	0.011			
Ther															
Crwl															
Atch	0.64	0.00	0.032	0.001											
Resp															
FFG.SC	0.16	0.07													
Volt	0.52	0.01	0.013	0.169			-0.194	0.007							
FFG.Pred															
Desi	0.65	0.01			-0.008	0.031								0.021	0.004
Rheo	0.19	0.10	0.021	0.056											
Exit	0.36	0.04	-0.018	0.057											
Hab.Skate	0.29	0.04													
Armr	0.15	0.08													

Table 3.4 (Continued). Multiple regression models for individual traits.

Trait	Adj. R ²	p-val	Gradient		LWD		SedTot		Temp_DegDays		V_med	
			coef	p-val	coef	p-val	coef	p-val	coef	p-val	coef	p-val
Drft	0.47	0.02									0.780	0.008
Disp	0.76	0.00			-1.241	0.000			0.000	0.007	-0.486	0.003
Life	0.66	0.00					-0.006	0.118			-0.856	0.001
Sync												
Hab.Swim	0.75	0.00	0.036	0.000			0.018	0.008			-0.029	0.008
Hab.Burrow	0.36	0.06			-0.810	0.125			0.001	0.017	-1.014	0.011
Shpe	0.80	0.00	-0.854	0.000	2.707	0.000	-0.033	0.000				
Devl	0.61	0.01					-0.008	0.031			-0.730	0.003
Flgt	0.73	0.00	-0.183	0.009			-0.004	0.024	0.000	0.071		
Size	0.21	0.17	0.538	0.111	-2.011	0.018					-0.542	0.244
Swim	0.50	0.01	0.564	0.003	-0.861	0.008	0.006	0.133				
Hab.Climb												

Table 3.4 (Continued). Multiple regression models for individual traits.

Trait	Adj. R ²	p-val	Gradient		LWD		SedTot		Temp_DegDays		V_med	
			coef	p-val	coef	p-val	coef	p-val	coef	p-val	coef	p-val
FFG.CG	0.63	0.00	1.290	0.000	-2.328	0.002						
FFG.SH	0.52	0.02	-0.581	0.027	1.911	0.002					0.531	0.202
Ther												
Crwl												
Atch	0.64	0.00	-0.243	0.002	0.522	0.002	-0.006	0.008				
Resp												
FFG.SC	0.16	0.07	-0.309	0.068								
Volt	0.52	0.01									0.416	0.008
FFG.Pred												
Desi	0.65	0.01	-0.315	0.021	1.192	0.002			0.000	0.141		
Rheo	0.19	0.10									-0.259	0.126
Exit	0.36	0.04	-0.224	0.015							0.344	0.030
Hab.Skate	0.29	0.04							0.000	0.064	0.094	0.036
Armr	0.15	0.08									-0.309	0.078

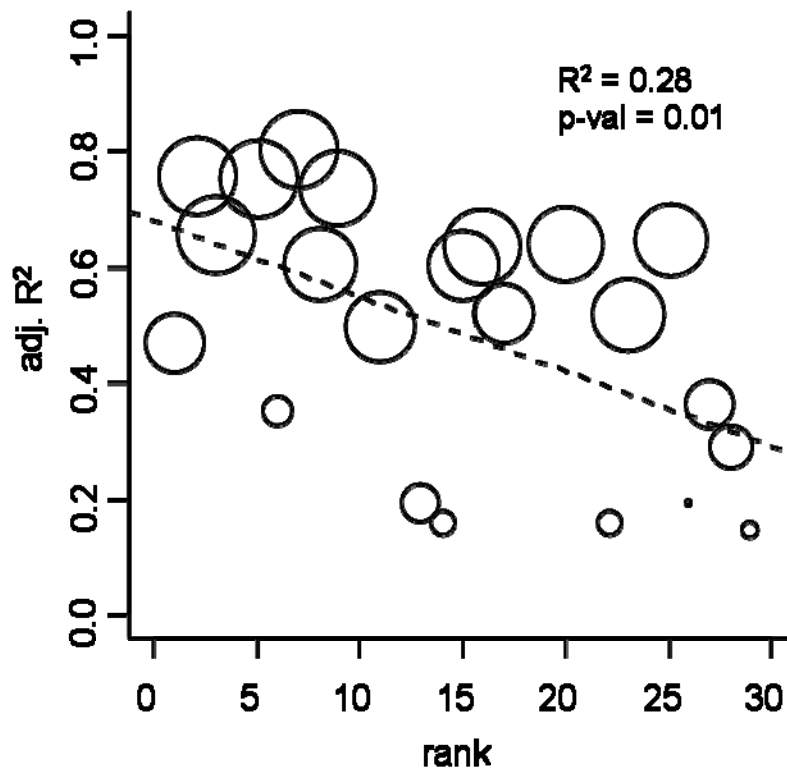


Figure 3.6. Relationship between variation in CFT scores and environmental variation plotted against ranks. Each point represents a functional trait, the x-axis represents trait ranks based on the trait-neutral lottery model, and the y-axis is the adjusted coefficient of determination (adj. R^2) for the best fit linear model describing the observed relationship between among-site CFT score variation and among-site environmental variation for trait t . Point sizes are inversely proportional to p-values from the linear models.

Stepwise linear regression of PCoA axes on individual environmental variables provided a more detailed model of the relationship between functional composition and environmental gradients. Only significant explanatory variables with variance inflation factors less than 5 (McCune and Grace 2002) were included in regression models. Multiple regression models explained between 43% and 61% (adjusted R^2) of the variation in the composite functional community composition variables (PCoA axes), and all models were significant ($p < 0.05$).

Path models of the relationships between environmental variation and functional composition were constructed from the best fit multiple regression model for each CFT composite variable using the procedure outlined in Figure 3.7, using CFT_PC3 as an example. A specification search on the multiple regression model (model A) indicated which causal and correlation pathways could be fixed at 0 (pathways removed from the model), and provided

degrees of freedom to test model goodness of fit (model B). Correlations among predictor variables were redrawn as causal pathways if such a relationship made sense ecologically (model C). Otherwise correlations were left to indicate covariation was due to an unobserved, common causal parent.

The binary variable (Treatment) was added to indicate whether sites were in logged or reference watersheds (model D) to determine which environmental gradients covaried with watershed type. The purpose of adding this variable was to test Treatment as a possible unobserved causal parent. In the example in Figure 3.8, a specification search on model D produced model E, indicating SedTot and Chla were weakly correlated, and it is likely a causal relationship independent of watershed Treatment. The final path models for CFT_PC1 (Figure 3.8A) and CFT_PC2 (Figure 3.8B) showed LWD and Gradient in model A and Treatment and Temp_DegDays and LWD in model B covaried independently of Treatment, respectively, whereas CBOM and Temp_DegDays likely share Treatment as a causal parent (Figure 3.8B).

The path model for the first principal coordinate of functional composition (Figure 3.8A, CFT_PC1 - larger, swimming macroinvertebrates that prefer high DO environments vs. small, poor swimmers tolerant of low DO [relative to headwater streams]) showed a high overall goodness of fit ($p = 0.989$). The model also indicated FBOM, Gradient, and LWD were stronger predictors of CFT_PC1 ($p < 0.05$) than D84 ($p < 0.10$). This path model only indicates a weak indirect relationship between Treatment and CFT_PC1, and variation in functional composition related to CFT_PC1 is likely due to environmental gradients organized independently of the logging/reference dichotomy.

All four predictor variables from the best fit multiple regression model had a significant (path coefficients statistically significant, $p < 0.05$) direct causal influence on variation in CFT_PC2 (large, good-dispersing, predators vs. small, poor dispersing non-predators) (Figure 3.8B). The model explained a large proportion of the variance in CFT_PC2 ($R^2 = 0.79$) but only had a fair goodness of fit ($p = 0.227$).

The two environmental variables, Chla and V_med, were stronger predictors ($p < 0.05$) of CFT_PC3 (multivoltine, short lived, fast developing vs. warm water, longer lived, slow development, uni- or semivoltine scrapers) than the quantity of material in transport (SedTot, $p < 0.10$) (Figure 3.8C). The path model explained a large proportion of the variation in CFT_PC3 ($R^2 = 0.62$) and had the best goodness of fit ($p = 0.756$) of the three path models.

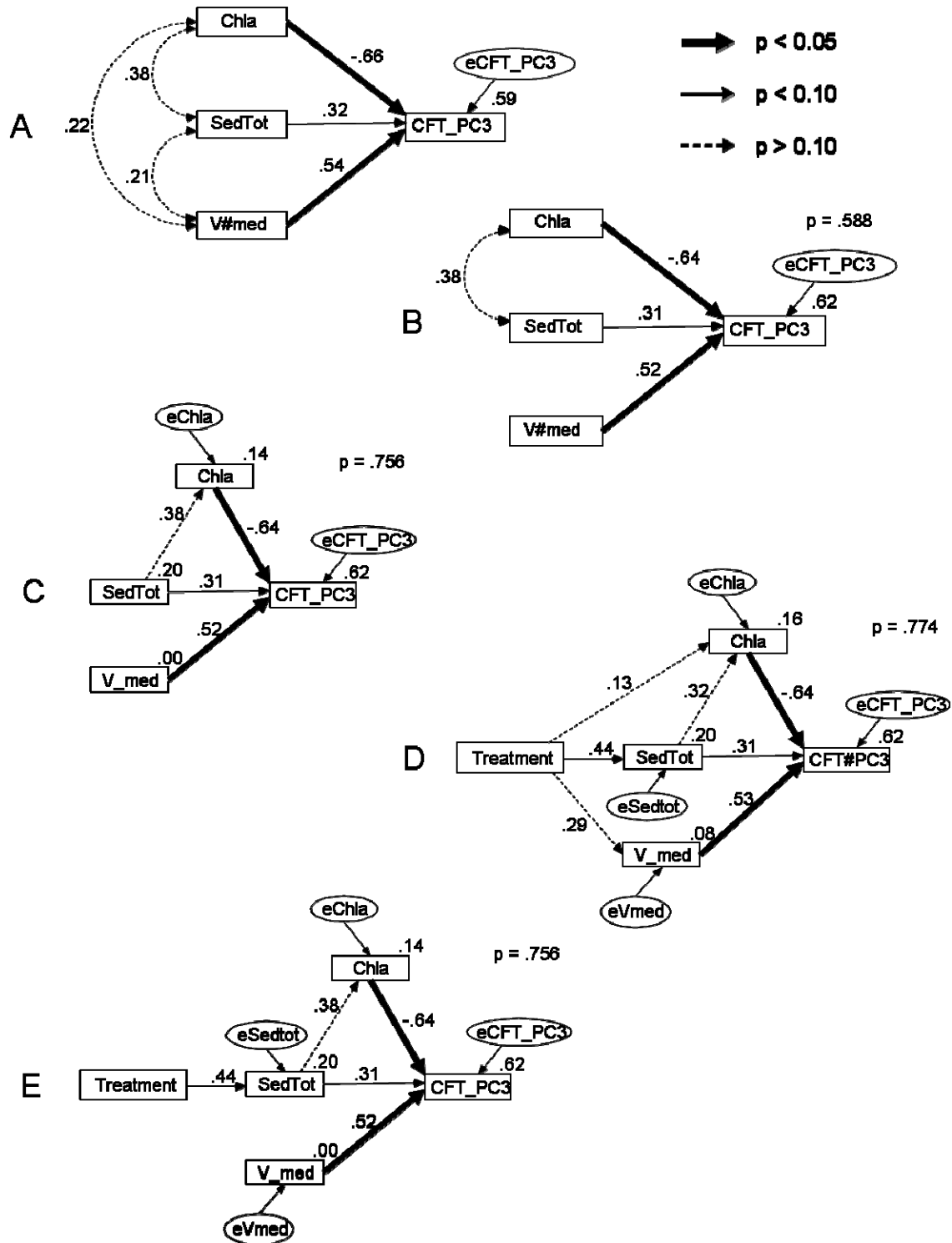


Figure 3.7. Path models illustrating the relationships among environmental variables and a composite functional composition variable (CFT_PC3 is the third axis from the PCoA ordination of functional trait composition). Single headed arrows indicate direct causal relationships and double headed arrows indicate covariance. Paths selected using a specification search were included in the model, standardized path

coefficients are shown, p-values for path coefficients are indicated by arrow thickness, and coefficients of determination for endogenous and response variables are shown. Variables drawn as boxes are observed variables. Variables drawn as ovals represent unexplained error of endogenous, observed variables. See text for description of the different models.

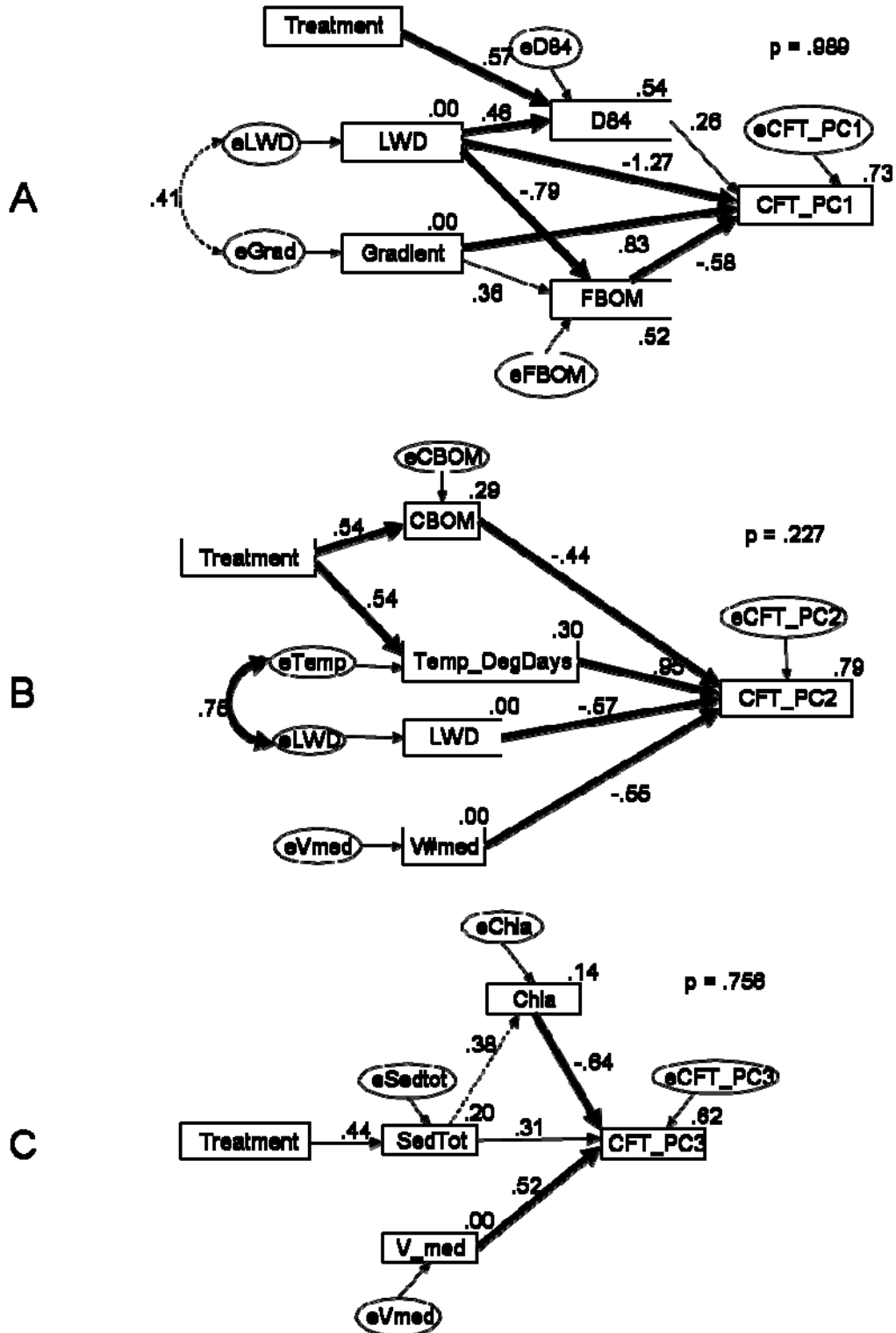


Figure 3.8. Path models describing the relationship between environmental variables and community functional composition. The first three axes from a principal coordinate analysis of sites in trait space are (A) CFT_PC1, (B) CFT_PC2, and (C) CFT_PC3, which serve as composite variables of community composition, and response variables for the models. See Figure 3.7 for details on elements of the path models.

Discussion

What organizes benthic macroinvertebrate community composition?

The perceived organizing factors of patterns of β -diversity (among-site variation in community composition within a metacommunity) for a given study depend on the scale of the observational grain size and the study extent (Nekola and White 1999). Larger observational grain sizes integrate habitat complexity and obscure the influence of local environmental gradients on β -diversity, while emphasizing the influence of broader environmental gradients (Tonn et al. 1990a, Poff 1997), legacy effects (Harding et al. 1998), and biogeographic processes (e.g., dispersal limitation, extinction, speciation – See Chapter Two).

I focused on the reach scale observational grain size because benthic communities seem to respond to changes in the landscape at a sub-watershed scale that is large enough to integrate microhabitat variation (e.g., different bedform structures) (Richards et al. 1997, Sponseller et al. 2001), and I restricted the study extent to avoid the confounding influence of large scale biogeographic patterns. I was able to measure a number of aspects of reach scale environmental variability at a resolution that allowed me to interpret its influence on the functional composition of the benthic macroinvertebrate community in an ecologically meaningful way.

Variance partitioning (Borcard et al. 1992) on raw data matrices (Legendre et al. 2005) revealed that variation in community composition among reaches was organized by environmental variation and not spatial structure (Table 3.3). Environmental gradients were better predictors of β -diversity when it was quantified as variation of functional ($\text{adj } R^2 = 0.57$, $p < 0.05$) rather than taxonomic ($\text{adj } R^2 = 0.40$, $p < 0.05$) composition. Consequently, I focused on functional composition as a response variable because differences in community composition defined by functional traits are easier to interpret ecologically (Doledec et al. 1999), and the results are less likely to be compromised by sampling effort and researcher error (Bady et al. 2005).

The trait ranks (Table 3.1) derived from comparing the difference in the distributions of observed CFT scores compared to those predicted from a trait-neutral null model (Figure 3.4) revealed seven non-neutral traits. Adjusted coefficients of determination for the best fit multiple linear regression models (MLRs) describing the relationship between environmental variables and CFT scores for each trait indicate the relative strength with which environmental filters interact with functional community composition. Traits with lower ranks (more likely to interact

with an environmental filter) based on comparisons against the trait-neutral model had a greater proportion of variation in distribution of CFT scores among sites explained by environmental variation (Figure 3.6). The significant relationship suggests that trait-neutral null models may be useful for distilling a set of candidate traits that are likely to respond to environmental variation, in more focused analyses, by weeding out traits that are not subject to sorting in the landscape by environmental filters.

The rather high variance in the relationship between trait ranks and MLR fits is likely due to a combination of small sample size, imprecise estimates of community functional composition and environmental variation, and a relatively weak environmental gradient. All four watersheds had similar land use, until logging began the year prior to this study. Sites with greater differences in land use histories (e.g., historically agricultural vs. historically forested) would likely produce a more pronounced signal in variation in both environmental and functional composition (Harding and Winterbourn 1995, Harding et al. 1998). Regardless, the general agreement between trait ranks and coefficients of determination from regressions against observed environmental variation provide some validation for the ranking scheme.

Functional traits have been shown to covary (Poff et al. 2006) because trait categories do not necessarily describe phylogenetically independent physiological or ecological characteristics. Additionally, variation among environmental constraints that act as filters on different functional traits may covary in the landscape. Consequently, variation in the distribution of trait types for any one trait can not be assumed to be independent of other traits because variation in functional composition will necessarily be constrained by taxonomic composition. Because of the complicated, multicollinear nature of functional composition, I believe composite variables that describe variation in multiple functional traits simultaneously (e.g., principal coordinates, Figure 3.3) serve as a more appropriate response variable to assess variation in functional composition than individual functional traits. Therefore, I used the first three principal coordinates from a PCoA ordination of the functional composition of the benthic communities of the sample reaches as composite variables to model among-reach variation in related sets of functional traits.

Resolving environmental influences on community composition

Path models (Figure 3.8) illustrate how different variables used to define the stream habitat interact to create gradients that act as environmental filters to organize the macroinvertebrate community in the landscape. The first gradient (Figure 3.8A) is partially a

habitat complexity gradient because it correlates with large wood availability (LWD) and a higher D84 (i.e., more large rocks providing stable substrate). The correlation between large wood habitat and functional composition (CFT_PC1) indicates a positive relationship between large wood and the presence of clinging insects (Hab.Cling), and a negative relationship with sprawling (Hab.Sprawl) insects. Habitat complexity (LWD) also affects FBOM standing crop which correlates with collector filterer dominance (FFG.CF loads negatively on CFT_PC1). This shows that large wood affects community composition directly as habitat (Benke et al. 1984) and indirectly by affecting resource availability for select feeding groups .

The second environmental gradient (Figure 3.8B) organizes the distribution of large (Size) burrowing (Hab.Burrow) predators (FFG.Pred) that are good dispersers (Crwl, Disp). These functional attributes characterize communities at warmer (Temp_DegDays) sites with lower CBOM standing stocks, less large wood habitat (LWD), and lower channel velocity (V_med). Sites on the other end of the gradient with higher V_med and LWD represent reaches with constricted channel morphology, deeper water, and more large wood. This combination of intra-reach habitat characteristics results in the co-occurrence of areas of supercritical flow where collector filterers dominate along with backwater depositional pools. Similar to streams in the western U.S. where riffle-pool sequences had a shorter turnover length in lotic systems with more large wood (Buffington et al. 2003, Allan and Castillo 2007). Consequently, skating (Hab.Skate) and clinging (Hab.Cling) insects and collector-filterer (FFG.CF) insects were similarly distributed along the same reach scale environmental gradient, when they would not necessarily be expected to co-occur in the same microhabitats.

The third gradient (Figure 3.8C) is partially organized by the fluvial process described by Lane's Law (Lane 1955, Gordon et al. 1992, Allan and Castillo 2007), which suggests that the amount of bedmaterial transported downstream is a function of stream power (gradient * discharge). Both V_med (calculated from discharge, gradient, and channel shape) and SedTot are positively correlated with the community functional composition (CFT_PC3), suggesting this fluvial process influences the organization of the habitat template among the study sites. The lack of a statistically significant direct causal path between V_med and SedTot may be a result from among-reach variation in the other parameters used to calculate V_med (e.g., channel cross-sectional shape, Manning's n). Overall, this model suggests communities that average a longer life span (Life), longer development times (Devl), more armoring (Armr), and a larger

proportion of scrapers (FFG.SC) occur at the sites with higher chlorophyll *a*, and insects with faster life cycles and less sclerotization occupy sites with higher stream power and more particulate material in transport.

In the two logged watersheds, the upstream sites were located in the logged area, and downstream sites were only affected by environmental factors that could be translated into a downstream effect in some way (e.g., bedload, temperature, hydrology). This was supported by the path models, which indicated Treatment correlated with stream bed particle size distribution (D84, Figure 3.8A), CBOM standing crop (Figure 3.8B), temperature regime (Figure 3.8B), and material in transport (SedTot, Figure 3.8A). Treatment did not correlate with large wood in the active channel (LWD), which is not likely to be an environmental factor that could easily be transported downstream in the year since timber harvest in the upstream portion of the Treatment watersheds.

The observed “treatment effect” on environmental variables in this study only indicates that the 8 reaches in the two logged watersheds are more similar with respect to that variable than they are to reaches in the reference sites, but it does not necessarily indicate that these sites are more similar because of logging. The Treatment variable is useful for indicating whether habitat characteristics vary similarly among the same sites. For example, in model B (Figure 3.8) covariation between CBOM standing crop and the temperature regime was explained by Treatment, indicating reaches in the two logged watersheds had similar CBOM standing crops and temperature regimes. Alternatively, temperature regime and available large wood habitat also covaried, but independent of Treatment, implying a different unobserved causal parent is driving that relationship between temperature and large wood habitat.

Conclusions

Currently, many studies of variation in the composition of ecological communities have focused on the relative influences of niche and neutral community assembly processes on β -diversity (Gravel et al. 2006, Leibold and McPeck 2006, Tuomisto and Ruokolainen 2006, Laliberte et al. 2009). Therefore, my first step in the statistical analysis of community composition was to conduct variance partitioning between environmental and spatial structure (Borcard et al. 1992, Legendre et al. 2005), which showed β -diversity in this system was organized by among-site variation in the habitat template. From this result, I concluded that if functional traits and the trait modalities assigned to different taxa are ecologically meaningful,

then they should be non-neutrally sorted among sites. Further, the distribution of functional types for a trait will have a greater deviation from the distribution predicted by the null model the more strongly that trait is linked to an organizing environmental gradient. The correlation between trait rank and the proportion of variance in CFT scores for traits explained by environmental variables (Figure 3.6) supports my conclusion; however, the variance in this relationship indicates that the broad categories used to define trait modalities need to be refined.

After establishing that the among-reach β -diversity is organized by the variation in the habitat template, I was free to focus on the relationship between the environmental variables that defined the habitat template and community composition. Path models identified three multivariate environmental gradients and their effects on reach scale community functional composition. Overall, I found factors that organize physical habitat structure (gradient, channel velocity, large wood) play the dominant role in organizing community composition in these headwater streams, and were able to link these factors to most of the traits identified as candidates for sorting by environmental filters.

The environmental gradients described in the path models are important for understanding β -diversity patterns at the local scale; however at larger study extents, these reach scale interactions become harder to detect because of the interaction of nested hierarchical environmental filters (Tonn et al. 1990a, Poff 1997). The procedures outlined here can be adapted for different combinations of observational grain size and study extent to detect the scales at which spatial structure becomes important, which can then be included in path or structural equation models (Grace 2006). A change in observational grain size and study extent will alter the functional traits and environmental gradients perceived to organize β -diversity (Lamouroux et al. 2004), and studies that identify the relevant habitat characteristics and functional traits will play an important role in understanding the relationship among the nested hierarchy of environmental filters and other processes that organize ecological communities.

Chapter 4 - The interaction between community assembly and disturbance: how logging affects benthic macroinvertebrate communities in headwater streams

Introduction

Among-site variation in the composition of assemblages of organisms in a metacommunity (β -diversity) has been suggested to be an emergent property of the interaction between niche-based and dispersal-based assembly processes (Hubbell 2001, Gravel et al. 2006, Zhou and Zhang 2008). *Niche assembly* (Chase 2003) emphasizes the role of environmental gradients as filters that organize a metacommunity by locally selecting colonizers with similar functional traits, whereas *dispersal assembly* (Hubbell 2001) emphasizes the role of source pool characteristics and dispersal limitation in organizing a metacommunity.

Recent studies have successfully implemented both dispersal and niche based mechanisms to explain among-site variation in community composition (Thompson and Townsend 2006, Driscoll and Lindenmayer 2009, Linares-Palomino and Kessler 2009). The balance between the relative dominance of dispersal and niche processes are influenced by the prevalence of disturbance (Chu et al. 2007, Lepori and Malmqvist 2009) and the intensity of the environmental constraints that function as filters to organize the metacommunity in the landscape (Chase 2007).

The environmental filtering concept has served as a useful framework for describing how variation in benthic macroinvertebrate community composition in lotic ecosystems relates to land use characteristics of the associated watershed (Poff 1997, Allan and Castillo 2007). Variation in the characteristics that define the local habitat template (Southwood 1977), which best predict benthic macroinvertebrate composition (Sponseller et al. 2001), tend to be nested within a hierarchy of environmental gradients that define the landscape (Frissell et al. 1986). Consequently, landscape scale disturbances affect benthic fauna indirectly by altering aspects of the local habitat template at the reach scale, such as temperature, sediment load, hydrology, and resource availability (Gurtz and Wallace 1984, Stone and Wallace 1998, Kiffney et al. 2003, 2004).

Applications of dispersal assembly to describe variation in benthic macroinvertebrate communities have indicated that the relevance of dispersal assembly mechanisms in structuring communities is contingent on the strength of environmental gradients that may act as filters (Chase 2007) and the degree to which dispersal capabilities that are inherent in the types of organisms that make up the study community limit inter-community migration (Thompson and Townsend 2006).

The availability of functional trait datasets provides an alternative method for describing community composition. Using available functional trait scoring systems to quantify patterns in variation in functional composition has been shown to provide an ecologically meaningful measure of community response to environmental gradients (Statzner et al. 1997, Statzner et al. 2001a, Bady et al. 2005, Poff et al. 2006). Functional traits available for North American benthic macroinvertebrates are classified into general groups pertaining to ecology, life history, mobility, or morphology (Poff et al. 2006). Traits describing ecological function relate to structural environmental variables (e.g., the relationship between functional feeding group dominance and resource type and availability), which describe aspects of functional composition most likely to respond to niche assembly mechanisms; whereas, traits relating to life history (fecundity, life cycle speed) and mobility are precisely the attributes that define the parameters in dispersal assembly models (Zhou and Zhang 2008).

The purpose of this study was to synthesize a comprehensive description of the response of the lotic habitat template and benthic macroinvertebrate community to small scale logging practices in headwater streams in the southern Appalachians, and to characterize the degree to which the influence of niche and dispersal assembly processes were altered. I evaluated the suitability of the niche and dispersal frameworks in lotic systems by testing two predictions inferred from the pair of hypotheses: (*prediction 1*) If dispersal assembly is more prevalent following a disturbance (Chu et al. 2007), then macroinvertebrate community functional composition should become decoupled from environmental variables that define functional niches, and instead variation in functional composition relating to dispersal and life history traits should correlate with treatment (logged vs. reference). However, shifts in macroinvertebrate community composition following logging have been shown to correlate with changes in resource type and availability which are mediated by microhabitat heterogeneity and geomorphology. Thus, (*prediction 2*) a landscape scale disturbance, such as logging, may

increase the intensity of the filtering effect, and relative importance of environmental variables that were not necessarily involved in organizing β -diversity prior to the disturbance (Chase 2007, Lepori and Malmqvist 2009). My goals for this study were to develop descriptive models that illustrate the multivariate response of the habitat template to logging and use measures of change in community functional composition to provide an ecologically interpretable description of community response to disturbance.

Methods

Study sites and design

All sampling reaches were located in headwater tributaries of Ray Branch (Figure 4.1) in the Nantahala National Forest, North Carolina (see Chapter 3 for a detailed site description). Shelterwood timber harvest occurred in three watersheds (L1,L2 and L3, Figure 4.1; L3 served as a reference site for the analysis in Chapter 3, but was logged following the spring 2006 field season) starting in December 2005 and ending in 2006, and the reference watershed (R1) remained forested with secondary growth forests.

Habitat characteristics and benthic macroinvertebrate community composition sampling schemes were designed to be representative of a 10 m reach observational unit. Four sampling reaches were located longitudinally along a stream at -50 m, 0 m, 25 m, and 200 m, with the 0 m site located at the downstream cut boundary (or arbitrarily at a similar position in the watershed in the reference stream), for a total of 16 reach scale observational units. Pre-disturbance samples and environmental data were collected in spring (unless otherwise noted) 2005. Post-disturbance samples and environmental data were collected in spring 2007, using the same sampling locations as in 2005.

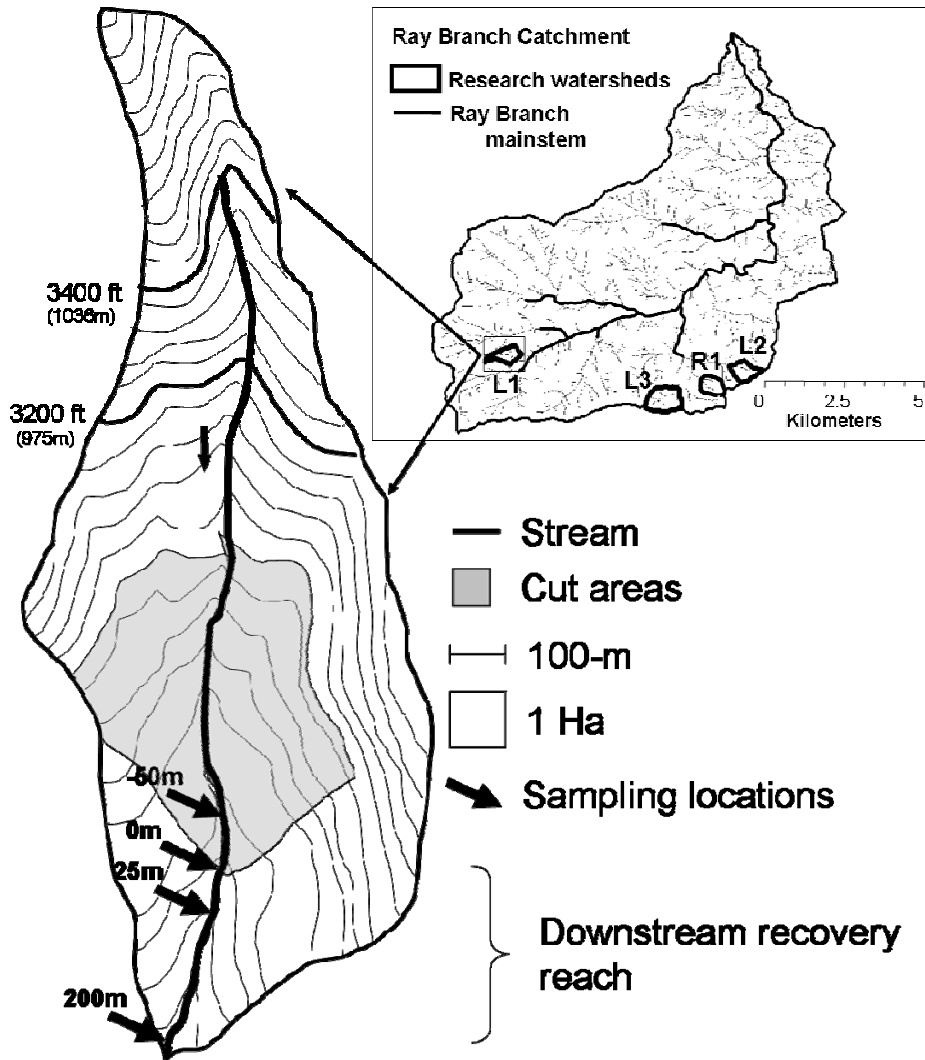


Figure 4.1. Site map. All sampling reaches are located in the Ray Branch watershed in western North Carolina. Distances for sampling locations indicate distance downstream from the lower boundary of the disturbed area.

Habitat template

Reach scale environmental variables were measured in spring (unless noted otherwise) 2005 and 2007 to characterize the local habitat template for each site before and after disturbance (Table 4.1, see Chapter 3 methods for details). Stream temperature was recorded from 1 Sept to 13 Dec in both 2005 and 2007 and temperature summary statistics were calculated for each site for each year. At least two cross sections were measured in each sampling reach. Bank-full hydraulic radius (bank-full wetted perimeter/cross-sectional area) (Gordon et al. 1992) was

calculated from survey data (see Chapter 3) as a metric to summarize channel width, depth, and complexity at each cross section. Longitudinal gradient of the thalweg was only measured in 2005. Samples of particulate sediment and organic matter in transport were collected on 2-4 separate dates from each reach in April and May of 2005 and 2007.

Each environmental variable was tested for normality with Shapiro test and log or arcsine-root (for ratios) transformed when necessary. All variables were then centered around the mean and scaled to standard deviation. Principal component analysis (PCA) on transformed and scaled data was used to ordinate sites in environmental space (data not shown). Environmental variables that appeared to be redundant and were suspect of multicollinearity were excluded from further analysis. All statistical analyses were conducted with R statistical software (R Development Core Team 2009) unless otherwise noted.

Macroinvertebrate community composition

Reach scale observations of macroinvertebrate densities were estimated from five Surber samples for each sampling reach in spring 2005 and 2007 (see Chapter 3 for methods). Community-aggregate functional trait (CFT) scores provide estimates of the community level functional composition with respect to each trait. CFT scores were calculated for the 2005 and 2007 datasets for each reach from estimates of macroinvertebrate densities and taxon specific functional trait data (see Chapter 3 for methods, Table 2.1 for trait descriptions, and Appendix E for taxon specific trait scores).

A mantel test was used to compare how similarly sites were organized in taxonomic and functional trait space. I used a principal component analysis (PCA) to ordinate sites in functional trait space. CFT scores were centered to 0 and standardized to unit variance prior to analysis. Pre- and post-disturbance community composition datasets were combined in a single ordination so that principal component scores could be used to compare pre- and post-disturbance community composition among sites.

Disturbance effect

I used path analysis to evaluate an analysis of covariance (ANCOVA) model (Figure 4.2) of the combined effect of distance downstream, time, and treatment (logging) on variation of each of the response variables described above (Arbuckle 2007). Response variables in this analysis refer to both environmental characteristics that define the habitat template and

measurements of macroinvertebrate community functional-trait composition, both of which may respond to the disturbance. The path model includes four observed variables: (X1) distance downstream from the cut boundary, (X2) treatment, (0 = reference watershed, 1 = logged watershed), (Y1) 2005 values of the response variable, and (Y2) 2007 values of the response variable; and two variables to represent unexplained error (e1 and e2) associated with the two endogenous variables, Y1 and Y2. X1 and X2 are exogenous variables that serve as predictors for the response variables Y1 and Y2. The causal relationships indicated by paths A and B represent the influence of the longitudinal position of a site in the watershed (X1) on the response variable in 2005 (Y1) and 2007 (Y2), respectively. Pathway C represents the expectation that the values of observed variable Y2 in 2007 (post-disturbance) are predicted by the values of Y1 in 2005 (pre-disturbance). Pathway D represents a measure of covariance (two-way arrow) between X2 and Y1, instead of a causal path (one-way arrow), because this provides a measure of whether the sites in the reference watershed were different than the those in the treatment watershed prior to disturbance; consequently, D is not a causal relationship, but is a coincidental relationship that needs to be accounted for in the model. Pathway E represents the causal relationship between X2 (logging) and the values of the response variable in 2007 (Y2).

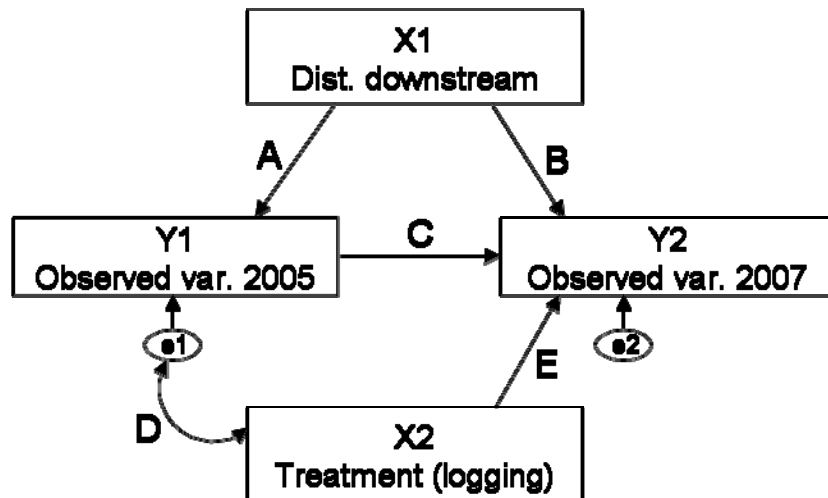


Figure 4.2. General ANCOVA model. This path model represents the ANCOVA used to analyze the treatment and distance downstream effect on each response variable (environmental variables and community composition variables) by testing how the response variable in 2005 (Y1) covaried with the response variable in 2007 (Y2) with respect to distance downstream (X1) and treatment (X2).

The objective of this model is to determine whether Y1 and Y2 are covariates with respect to X1 and X2. If longitudinal position in the watershed affects the response variable regardless of disturbance or year, then the main path of influence of X1 on Y2 should be through Y1 (indirect pathway AC); whereas, if longitudinal position in the watershed only becomes important in 2007, then the only significant pathway will be the direct relationship quantified by pathway B. Similarly, if the treatment watersheds are inherently different than the reference watershed with respect to the response variable, then pathway D will be significant, and the correlation between X2 and Y2 will be accounted for in the indirect pathway through D and C. Otherwise, if there is a treatment effect that results in the treatment sites becoming different than the reference sites following logging, then pathway E will account for the correlation between X2 and Y2.

The model in Figure 4.2 was evaluated for all environmental variables, CFT scores, and composite variables (principal components) summarizing functional community composition using AMOS 16.0.1 (Arbuckle 2007). I used a two-way specification search (similar to a two-way stepwise selection in multiple regression) to determine which paths to include in the best fit model for each response variable, where model fits were compared using an AIC_C statistic. The combination of statistically significant pathways (path coefficients with p-values < 0.05) included in a best-fit model (as described above) indicates whether the treatment sites change relative to the reference sites with respect to the response variable.

The habitat template and community composition

Environmental variables were selected in a two-way stepwise regression (*stepAIC* in R) (Venables and Ripley 2002) to create multiple regression models for each individual trait and each principal component (composite variable of functional composition). Environmental variables that artificially inflated the coefficient of determination (variance inflation factor > 5) (McCune and Grace 2002) were excluded from the model. Environmental variables that were included in at least one multiple regression model were included in path models used to describe the habitat template.

Variance partitioning on raw data matrices using redundancy analysis (RDA) was used to determine the relative influence of environmental variation (X1) and spatial variation (X2) on community composition (Borcard et al. 1992, Legendre and Legendre 1998, Legendre et al. 2005, Peres-Neto et al. 2006). The analysis was conducted separately for factorial combinations

of year (2005 and 2007) and community composition type (taxonomic or functional trait) with the function *varpart* in the package *vegan* (Oksanen et al. 2009) in the R statistical environment (R Development Core Team 2009). I used this analysis to compare how taxonomic and functional trait composition correlated with environmental and spatial variation.

The multiple regression model fit for each trait for each year was used to determine which individual trait most strongly interacted with the observed environmental variables used to define the habitat template. The log-likelihood of each multiple regression model for each individual trait was calculated with the *logLik* function in R (R Development Core Team 2009). Using the log-likelihoods, Akaike weights (w_i) (Burnham and Anderson 2001) were calculated for the models from the 2005 and 2007 datasets, from AIC_c scores for all individual traits. w_i is a probability that a model is the best fit model out of a set of models, and penalizes models with more parameters. Thus, for each year w_i indicated which multiple regression model was the best fit model, and consequently which trait most strongly interacted with the habitat template, given the dataset.

Separate models of the interactions among observed environmental variables were created for pre- and post-disturbance datasets. The resulting models were then used to discern which aspects of the habitat template interacted to translate the disturbance effect to a change in macroinvertebrate composition. The model building process is illustrated for the 2005 dataset in Appendix G. A specification search was used to determine which environmental variables were influenced by the treatment (for 2005 data, this indicates whether reference sites were different than all other sites with respect to each environmental variable, prior to logging) and distance downstream by determining which causal pathways in model A (Appendix G) were statistically significant, yielding model B (Appendix G). Path model B constrains covariance among environmental variables not explained by either Treatment or Reach to be 0. Covariances, which are drawn as double headed arrows representing unexplained correlations among environmental variables, were added to model B if their modification index exceeded 4 (Arbuckle 2007). Model C (Appendix G) shows the among-environmental variable relationships and the interactions between environmental variables and treatment and distance downstream.

The covariance structure modeled in step C was used to explain variation in a composite variable (PC1_2005) representing functional community composition, producing model D (Appendix G). A specification search was used to select significant direct causal relationships

between environmental variables and community composition, resulting in model E (Appendix G). Model E is similar to a multiple regression model, where the 10 environmental variables are predictor variables of the community composition variable (PC1_2005); however, this model is different from a multiple regression model in that relationships among predictor variables are constrained to 0 unless they are connected through a common causal parent variable (Treatment or Reach) or a double headed covariance arrow. The standardized path coefficients are standardized regression coefficients, which are conditioned on any other indirect causal pathways between a given predictor and response variable. Any bivariate relationships not considered statistically significant are set to zero, and provide additional degrees of freedom to calculate model goodness of fit. Environmental variables were then removed from the model if they were not involved in any direct or indirect causal pathways that predicted variation in PC1_2005, and covariances among environmental variables were redrawn as causal relationships (one-way arrows) if such a change was judged as ecologically justifiable (this was done for 2007 models that included chlorophyll *a* concentrations as an endogenous variable).

Model F (Appendix G) represents the final simplified model and provides a coefficient of determination for all endogenous and response variables and a goodness of fit statistic for the entire model. Any indirect path from treatment or distance downstream through an environmental variable to the response variable indicates a possible mechanism by which the treatment or distance downstream affects community composition. These relationships must only be interpreted ecologically as a treatment effect in the context of the ANCOVA models (described above).

Steps A through C, illustrated in Appendix G, were used to create models for pre (2005) and post (2007) logging datasets. Steps D, F and E were used to create models describing the influence of the different components of the habitat template on community composition for composite variables (principal components) calculated from the 2005 and 2007 community composition data and individual traits that were considered likely candidates to interact with the habitat template.

Results

Habitat template

Measurements of variables used to quantify the reach scale habitat template are summarized in Table 4.1. The strongest treatment effect was a warming of treatment sites (Table 4.2, ANCOVA, $p = 0.02$). Other treatment effects included a decrease in canopy cover ($p = 0.11$) and an increase in chlorophyll *a* standing crop ($p = 0.07$). The 84th percentile of the bed particle size distribution, a metric to describe substrate size, was significantly larger at treatment sites prior to logging ($p = 0.04$). Following logging, the bed particle distribution appeared to be smaller at treatment sites ($p = 0.12$). The ANCOVA path model also indicated that CBOM standing crops may have been greater at the reference site prior to logging ($p = 0.17$), but there was no detectable difference between treatment and reference sites following the disturbance. There was, however, a strong longitudinal trend indicating greater CBOM standing crops in the upstream reaches ($p < 0.001$). The availability of large woody debris (LWD) as habitat, and the amount of particulate material (organic and inorganic) in transport (Trans) were both greater in upstream reaches before and after logging ($p < 0.05$). Hydraulic radius was strongly consistent over time ($p < 0.001$) and gradient was not tested with the ANCOVA model because it was only measured in the field once, and I assumed reach scale gradient measurements would not be influenced by the disturbance.

Table 4.1. Observed environmental and community composition variables.

Variable description		2005		2007		2007	
		Reference		Reference		Treatment	
		mean	SE	mean	SE	mean	SE
%Canopy cover	Canopy*	0.81	0.07	0.89	0.02	0.67	0.07
Daily temperature (°C)							
		mean	0.10	12.01	0.05	12.24	0.12
		median	0.21	11.90	0.07	12.54	0.16
	Temp_med*	12.35					
		SE	0.00	0.15	0.01	0.15	0.00
Particulate transport							
		mean transport (mg/L)	0.09	0.02	0.01	0.03	0.01
	Trans*	0.36					

Variable description	2005		2007		2007		
	Reference		Reference		Treatment		
	mean	SE	mean	SE	mean	SE	
Periphyton							
AFDM (mg/cm ²)		0.17	0.01	0.11	0.02	0.11	0.01
Chl a (ug/cm ²)	Chla*	0.14	0.03	0.08	0.04	0.13	0.02
Benthic organic matter							
Fine (g AFDM FBOM/m ²)	FBOM*	26.33	10.81	44.40	11.22	35.94	3.72
Coarse (g AFDM CBOM/m ²)	CBOM*	86.63	4.00	212.80	159.61	100.60	29.16
Large woody debris (ratio)	LWD*	0.06	0.01	0.07	0.01	0.08	0.01
Geomorphology							
Mean hydraulic radius (m)	HydRad*	0.31	0.05	0.29	0.04	0.32	0.03
Gradient (% grade)	Gradient*	0.12	0.01	0.12	0.01	0.13	0.01
Bed particle size distribution (mm)							
D26 (26 th percentile)		7.61	0.77	9.35	0.23	15.06	3.61
median		15.85	2.45	35.00	4.10	36.89	5.28
D84 (84 th percentile)	D84*	59.54	6.01	104.85	7.95	106.89	9.74
Macroinvertebrate community							
Density (no./m ²)		626.5	150.6	2119.4	472.7	1722.9	273.2
Richness (no. taxonomic groups)		27.3	1.4	33.0	1.7	30.9	1.3

*indicates variables included in path analysis

Table 4.2. ANCOVA of environmental and macroinvertebrate response to logging.

		A [†]		B [†]		C [†]		D [†]		E [†]	
		DD-->2005		DD-->2007		2005-->2007		Trt-->2005		Trt-->2007	
		Estimate	p	Estimate	p	Estimate	p	Estimate	p	Estimate	p
Environmental variable											
	Canopy									-0.38	0.11
	CBOM			-0.66	***			-0.38	0.17		
	Chla					-0.35	0.11			0.40	0.07
	D84					0.67	0.02	0.63	0.04	-0.43	0.12
	FBOM										
	HydRad					0.90	***				
	LWD	-0.61	0.00	-0.65	***						
	Temp_med									0.53	0.02
	Trans	-0.87	***	-0.51	0.02						
Fucntional Trait											
<i>Ecology</i>	FFG.CF					-0.63	0.00				
	FFG.CG	0.61	0.00			0.39	0.04			0.56	0.00
	FFG.Pred					0.48	0.04				
	FFG.SC			0.30	0.14					0.53	0.01
	FFG.SH	-0.51	0.01			0.40	0.08	0.36	0.19	-0.53	0.02
	Hab.Burrow							-0.48	0.10	-0.59	0.01
	Hab.Climb	-0.35	0.14							-0.38	0.11
	Hab.Cling	0.43	0.07							0.61	0.00
	Hab.Sprawl							0.39	0.16	-0.37	0.13
	Hab.Swim										
	Rheo	-0.36	0.14							0.48	0.04
	Ther	-0.42	0.04					0.46	0.11		
<i>Life History</i>	Desi	-0.40	0.09	-0.41	0.06					-0.39	0.07
	Devl					-0.38	0.08			0.33	0.13
	Exit			-0.57	0.00	0.46	0.01	0.38	0.17		

		A [†]		B [†]		C [†]		D [†]		E [†]	
		DD-->2005		DD-->2007		2005-->2007		Trt-->2005		Trt-->2007	
		Estimate	p	Estimate	p	Estimate	p	Estimate	p	Estimate	p
	Life										
	Sync	0.36	0.14	0.38	0.11						
	Volt										
<i>Mobility</i>	Crwl			-0.37	0.12			-0.42	0.14		
	Disp			-0.45	0.05						
	Drft					0.65	***				
	Flgt					0.34	0.17				
	Swim									0.37	0.12
<i>Morphology</i>	Armr	0.57	0.00					0.36	0.19	0.39	0.10
	Atch										
	Resp	-0.42	0.08								
	Shpe									-0.45	0.05
	Size			-0.41	0.02	0.58	0.00				
Principal component (CFT scores)											
	PC1					0.60	0.01	0.38	0.17	-0.51	0.02
	PC2			0.32	0.12					0.53	0.01
	PC3									-0.55	0.01

***p-value < 0.001

[†]Corresponds to a path in the model in Figure 4.2.

Path models (Figure 4.3) illustrate the correlations among the environmental variables used to represent the reach scale habitat template before (2005) and after (2007) logging. Prior to logging, chlorophyll *a* and FBOM standing crops were positively correlated, independent of treatment and distance downstream. CBOM and D84 were negatively correlated, and the negative covariance was accounted for by a difference in the treatment and reference reaches prior to logging. Covariance among gradient, LWD, and particles in transport was accounted for by a common negative correlation with distance downstream. The goodness of fit for the entire model in 2005 ($p = 0.35$) is better than the 2007 path model ($p = 0.03$), but comparable goodness of fit statistics are observed when subsets of interacting variables in 2007 are analyzed separately (models not shown).

In the post-disturbance dataset (2007), canopy cover and chlorophyll *a* standing crop, D84 and FBOM standing crops, and hydraulic radius and median temperature were negatively correlated independent of distance downstream and treatment. The positive relationship between gradient and LWD increased beyond what was previously explained by a common negative correlation with distance downstream. Treatment was negatively correlated with canopy cover and positively correlated with median temperature. Distance downstream was negatively correlated with CBOM, Gradient, LWD, and the amount of particulate transport.

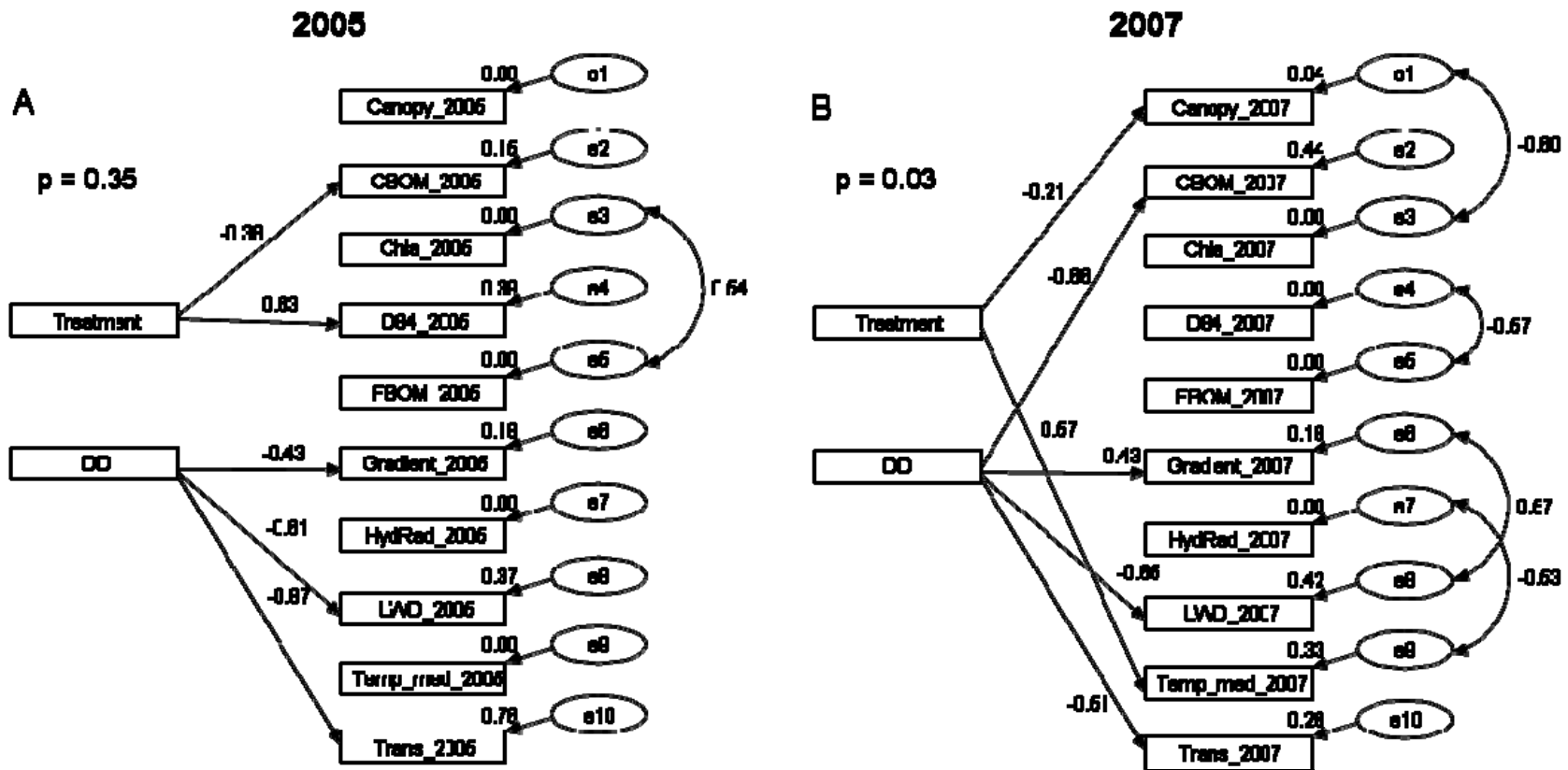


Figure 4.3. Path models summarizing the covariance structure of observed environmental variables in 2005 (A) and 2007 (B), and the affect of treatment and distance downstream (DD). Environmental variables are described in Table 2.2. Boxes represent variables with observed values and ovals represent unexplained error. Single headed arrows indicate direct causal relationships, and standardized path coefficients are reported. Coefficients of determination are displayed for endogenous variables. Double headed arrows represent significant correlation among endogenous variables that is not explained by any other variable included in the model. Displayed p-values represent the goodness of fit for each model.

Community composition

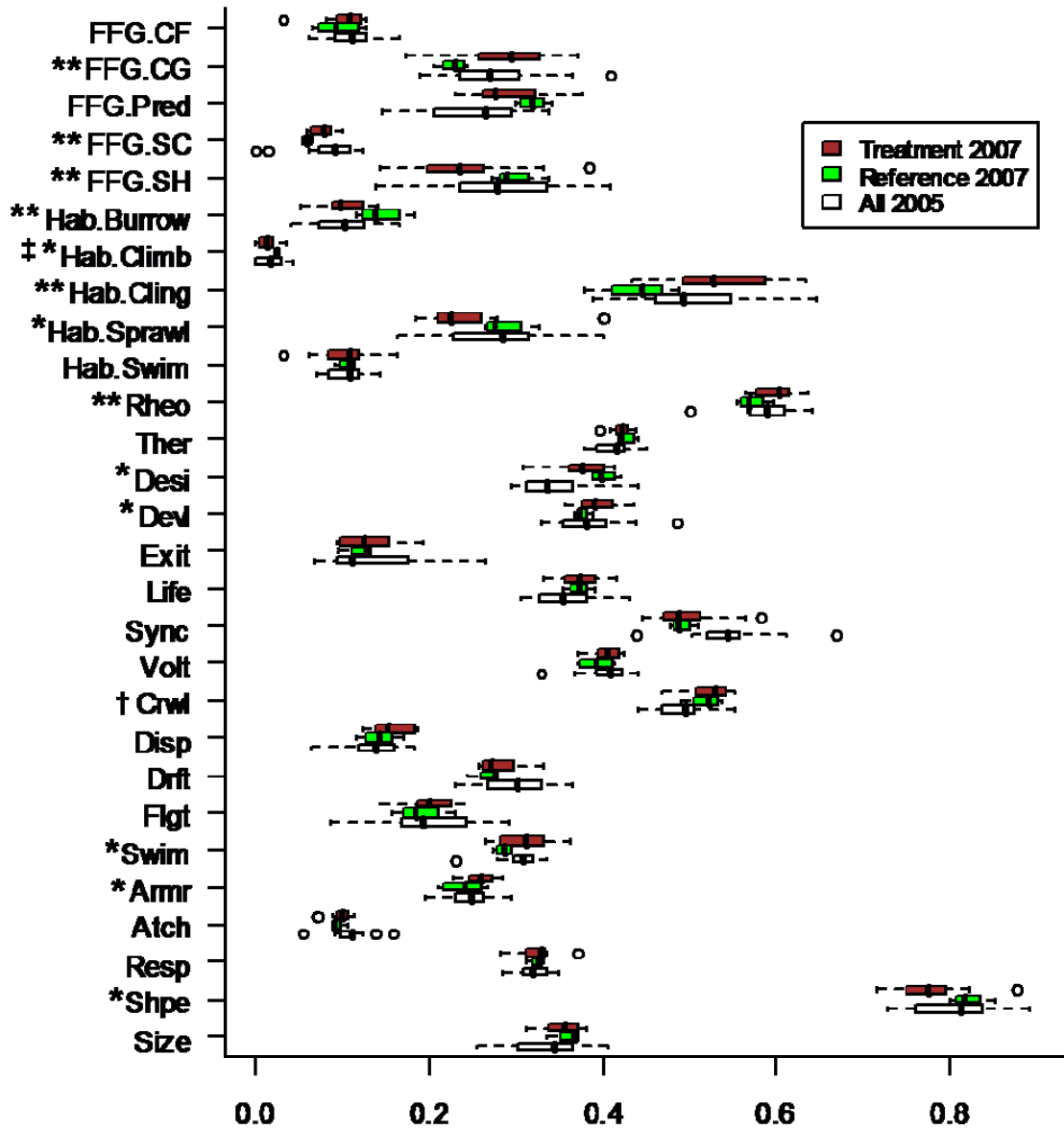


Figure 4.4. The observed distribution of CFT scores for each trait in 2005 and 2007. Post disturbance distributions are plotted separately for reference and treatment sites.

** significant treatment effect ($p < 0.05$).

* treatment effect indicated by specification search ($p < 0.10$)

† trait best predicted by environmental variables in 2005

‡ trait best predicted by environmental variables in 2007

Prior to logging (2005), and including only taxonomic groups for which trait scores were available, sites had a mean density of 724 (± 120 SE) no./m², and an average richness of 26 (± 1.9 SE) out of the 55 possible taxa included in the trait database (Table 4.1). Following logging (2007), reference reaches had a mean density of 2119 (± 473 SE) no./m² and an average richness of 33 (± 1.7 SE) taxa, and treatment reaches had a mean density of 1723 (± 273 SE) no./m² and an average richness of 31 (± 1.3 SE). The distributions of community-aggregate functional trait (CFT) scores for each trait in 2005 and 2007 are illustrated in Figure 4.4, where treatment and reference CFT score distributions are shown separately for the post logging data. A paired t-test indicates there was an overall increase in mean reach macroinvertebrate density ($p < 0.001$) from 2005 to 2007 among all sites, but there was no detectable difference between reference and treatment mean reach densities within a sampling season when they were compared with a t-test. A Wilcoxon Signed Rank Test indicated an increase in richness ($p = 0.012$) from 2005 and 2007 as well, but a Mann-Whitney Rank Sum Test showed no difference between reference and treatment within a sampling season. A mantel correlation of 0.82 ($p < 0.001$) indicated a strong similarity in the organization of sites in taxonomic space and functional trait space.

Distributions of trait scores (Figure 4.4) related to functional feeding group (FFG), habit, and rheophily showed the strongest response to the treatment (Table 4.2). Traits related to resistance of desiccation, development time, swimming ability, armoring, and shape were also indicated to be marginally influence by the treatment by the ANCOVA analysis. The ANCOVA also indicated that CFT scores at treatment sites relating to thermal preference, exit ability as an adult, and crawling ability became more similar to reference sites following the disturbance. CFT scores for armoring were marginally greater at treatment sites in both years. The ANCOVA also indicates a longitudinal pattern in functional composition that changes from 2005 to 2007, and most strongly affects distributions of CFT scores related to functional feeding group (collector gatherers and shredders), thermal preference, exit ability, dispersal ability, and armoring.

The first three principal components of an ordination of sites in functional trait space account for 22, 18, and 15% of the variation in functional composition, respectively (Table 4.3). Functional trait loading on each of the first three principal components are listed in Table 4.3. Principal component 1 (PC1) is a composite variable that is positively correlated with trait scores indicating a sprawling habit and shredding functional feeding group and is negatively correlated

with collector gatherer dominance, mobility via crawling, and size. PC2 is positively correlated with traits indicative of multivoltinism, rheophily, an affinity to attach to substrate, and synchronized emergence and negatively correlated with burrowing habit. PC3 is negatively correlated with traits indicating occurrence in drift, adult flight ability, female dispersal distance before oviposition, swimming ability, and ability to exit the water as an adult.

The principal components of the ordination of sites in trait space served as composite variables to describe how groups of multicollinear traits responded collectively to environmental gradients. The ANCOVA indicates a significant treatment effect in 2007 on PC1, PC2 and PC3. PC1 had greater values at treatment sites prior to disturbance, a relationship which was reversed in 2007. PC2 showed a weak longitudinal pattern in 2007.

Table 4.3. Trait loading on the first three principal components of a PCA of functional composition.

Trait Class	Trait	PC1	PC2	PC3
Ecology	FFG.CF	-0.04	0.19	-0.20
	FFG.CG	-0.29	0.03	-0.24
	FFG.Pred	-0.24	-0.20	0.26
	FFG.SC	0.11	0.26	0.05
	FFG.SH	0.36	-0.04	0.04
	Hab.Burrow	-0.04	-0.29	0.25
	Hab.Climb	0.06	0.04	0.12
	Hab.Cling	-0.24	0.22	-0.17
	Hab.Sprawl	0.37	-0.10	0.09
	Hab.Swim	-0.18	0.02	-0.13
	Rheo	-0.04	0.31	0.05
	Ther	0.19	-0.11	0.03
	Life History	Desi	0.07	-0.27
Devl		-0.24	-0.16	-0.09
Exit		0.17	-0.18	-0.31
Life		-0.22	-0.21	-0.06
Sync		0.17	0.29	0.03
Volt		-0.02	0.31	0.16
Mobility	Crwl	-0.27	-0.21	-0.03
	Disp	0.05	-0.12	-0.33
	Drft	0.23	0.01	-0.36
	Flgt	0.14	-0.14	-0.35

Trait Class	Trait	PC1	PC2	PC3
	Swim	-0.04	0.10	-0.32
Morphology	Armr	-0.05	-0.03	-0.13
	Atch	0.07	0.30	0.08
	Resp	-0.15	0.02	-0.10
	Shpe	0.20	-0.25	0.13
	Size	-0.25	0.05	0.19
Var. Explained		0.22	0.18	0.15
Cumulative		0.22	0.40	0.55

Interactions between the habitat template and community composition

Variance partitioning (Table 4.4) showed that in 2005 variation in taxonomic composition was not organized by observed environmental variables ($X1$, adj. $R^2 = 0.12$, $p = 0.28$), but spatial organization did significantly affect taxonomic composition (adj. $R^2 = 0.20$, $p < 0.01$). However, spatial patterns did not significantly explain variation in taxonomic composition when the effect of environmental variation was statistically controlled for ($X2|X1$, adj. $R^2 = 0.08$, $p = 0.29$). Variation in functional composition was influenced by the environment ($X1$, adj. $R^2 = 0.23$, $p = 0.07$) and space ($X2$, adj. $R^2 = 0.11$, $p = 0.01$), but neither accounted for variation in functional composition independent of the other. In 2007, spatial variation ($X2$) organized both taxonomic (adj. $R^2 = 0.26$, $p < 0.01$) and functional trait (adj. $R^2 = 0.11$, $p = 0.01$) composition, but not independent of the environment ($X1$), and environmental variation may have influenced functional composition independent of space ($X1|X2$, adj. $R^2 = 0.28$, $p = 0.08$).

Table 4.4. Variance partitioning of raw data matrices of taxonomic and functional trait composition using redundancy analysis (RDA). The adjusted R^2 values represent the proportion of variance explained by variation in the environmental data matrix ($X1$) or the spatial data matrix ($X2$, where $X2$ is a matrix of arbitrary xy coordinates in geographic space calculated from GPS coordinates). [a] is variance in the response variable that is solely accounted for by environmental variation, [b] is variance explained by both environment and spatial structure, [c] is variance explained only by spatial structure. The significance (p -values) of RDA ordinations were calculated with the function *permutest*, available in the *vegan* package for R (Oksanen et al. 2009), with 10000 iterations.

2005		2007	
Adj. R^2	p	Adj. R^2	p

Taxonomic composition				
[a+b] = X1	0.12	0.28	0.11	0.18
[b+c] = X2	0.20	< 0.01	0.15	< 0.01
[a+b+c] = X1+X2	0.20		0.27	
[a] = X1 X2	-0.01	0.46	0.12	0.24
[c] = X2 X1	0.08	0.29	0.16	0.21
Functional composition				
[a+b] = X1	0.23	0.07	0.11	0.23
[b+c] = X2	0.11	0.01	0.11	0.01
[a+b+c] = X1+X2	0.23		0.39	
[a] = X1 X2	0.12	0.31	0.28	0.08
[c] = X2 X1	0.01	0.53	0.28	0.18

The best fit multiple regression models for individual traits indicate that at least 1 environmental variable is significantly correlated with most of the functional traits, but w_i scores show that Crwl and Hab.Climb are the best individual traits to describe how community functional composition was affected by the observed environmental variables in 2005 and 2007, respectively (Table 4.5). A paired t-test indicates AIC_c scores for individual traits tended to decrease from 2005 to 2007 (lower AIC_c scores indicate better model fit). Six environmental variables are correlated with variation in CFT scores related to crawling ability (Crwl) in 2005 (Figure 4.5A). The path model also indicates indirect effects linking Crwl to both treatment and distance downstream prior to logging. Model B (Figure 4.5) indicates indirect effects of treatment and distance downstream (DD) on Crwl through a different set of environmental variables in 2007, and is a poorer ($p = 0.42$) fit than model A ($p = 0.87$). Both models show high coefficients of determination for Crwl ($R^2 = 0.99$ and 0.83 for models A and B, respectively), and low variance inflation factors for the analogous multiple regression models suggest multicollinearity is not driving the high R^2 .

Table 4.5. Multiple regression model fits for each functional trait. The coefficient of determination and p-value for the best fit multiple regression model of functional composition on environmental variables for each trait is reported. Akaike weights (w_i) were then calculated for the set of best fit models for all traits for both years, and indicate the probability for each model that it is the best model of the relationship between observed environmental variables and functional composition in a given year. The trait best predicted by

environmental variation for each year is in bold. AIC_c scores tended to be lower in 2007 (paired t-test, p = 0.004).

Trait Class	Trait	2005				2007			
		adj.R ²	p	AIC _c	w _i	adj.R ²	p	AIC _c	w _i
Ecology	FFG.CF	0.36	0.11	-47.3	0.00	0.16	0.29	-45.6	0.00
	FFG.CG	0.60	0.01	-39.3	0.00	0.71	0.01	-31.7	0.00
	FFG.Pred	0.38	0.01	-47.0	0.00	0.19	0.22	-40.3	0.00
	FFG.SC	0.86	0.00	-66.5	0.00	0.33	0.08	-81.3	0.00
	FFG.SH	0.16	0.07	-29.8	0.00	0.50	0.02	-38.6	0.00
	Hab.Burrow	0.45	0.03	-56.5	0.00	0.27	0.12	-54.7	0.00
	Hab.Climb	0.44	0.01	-90.0	0.01	0.65	0.01	-97.0	0.30
	Hab.Cling	0.45	0.05	-29.1	0.00	0.32	0.03	-37.8	0.00
	Hab.Sprawl	0.54	0.05	-17.6	0.00	0.64	0.01	-43.7	0.00
	Hab.Swim	0.87	0.00	-56.9	0.00	0.52	0.04	-50.3	0.00
	Rheo	0.59	0.03	-40.7	0.00	0.36	0.08	-60.7	0.00
	Ther	0.58	0.01	-75.9	0.00	0.42	0.08	-80.4	0.00
Life History	Desi	0.64	0.04	-22.6	0.00	0.24	0.13	-57.0	0.00
	Devl	0.37	0.11	-37.0	0.00	0.75	0.00	-77.0	0.00
	Exit	0.69	0.00	-42.4	0.00	0.72	0.00	-69.0	0.00
	Life	0.18	0.23	-42.2	0.00	0.52	0.02	-68.9	0.00
	Sync	0.50	0.03	-40.4	0.00	0.58	0.05	-24.2	0.00
	Volt	0.65	0.00	-70.6	0.00	0.14	0.08	-79.0	0.00
Mobility	Crwl	0.98	0.00	-98.4	0.61	0.54	0.02	-66.3	0.00
	Disp	0.46	0.04	-54.9	0.00	0.96	0.00	-73.7	0.00
	Drft	0.53	0.01	-54.0	0.00	0.34	0.05	-71.3	0.00
	Flgt	0.37	0.17	-2.4	0.00	0.55	0.02	-62.3	0.00
	Swim	0.70	0.01	-55.2	0.00	0.86	0.00	-48.7	0.00
Morphology	Armr	0.20	0.14	-63.7	0.00	0.54	0.03	-62.2	0.00
	Atch	0.62	0.01	-65.5	0.00	0.09	0.21	-93.4	0.05
	Resp	0.87	0.01	-3.5	0.00	0.95	0.00	-92.3	0.03
	Shpe	0.68	0.01	-31.9	0.00	0.61	0.01	-55.5	0.00
	Size	0.60	0.02	-42.9	0.00	0.44	0.07	-61.8	0.00

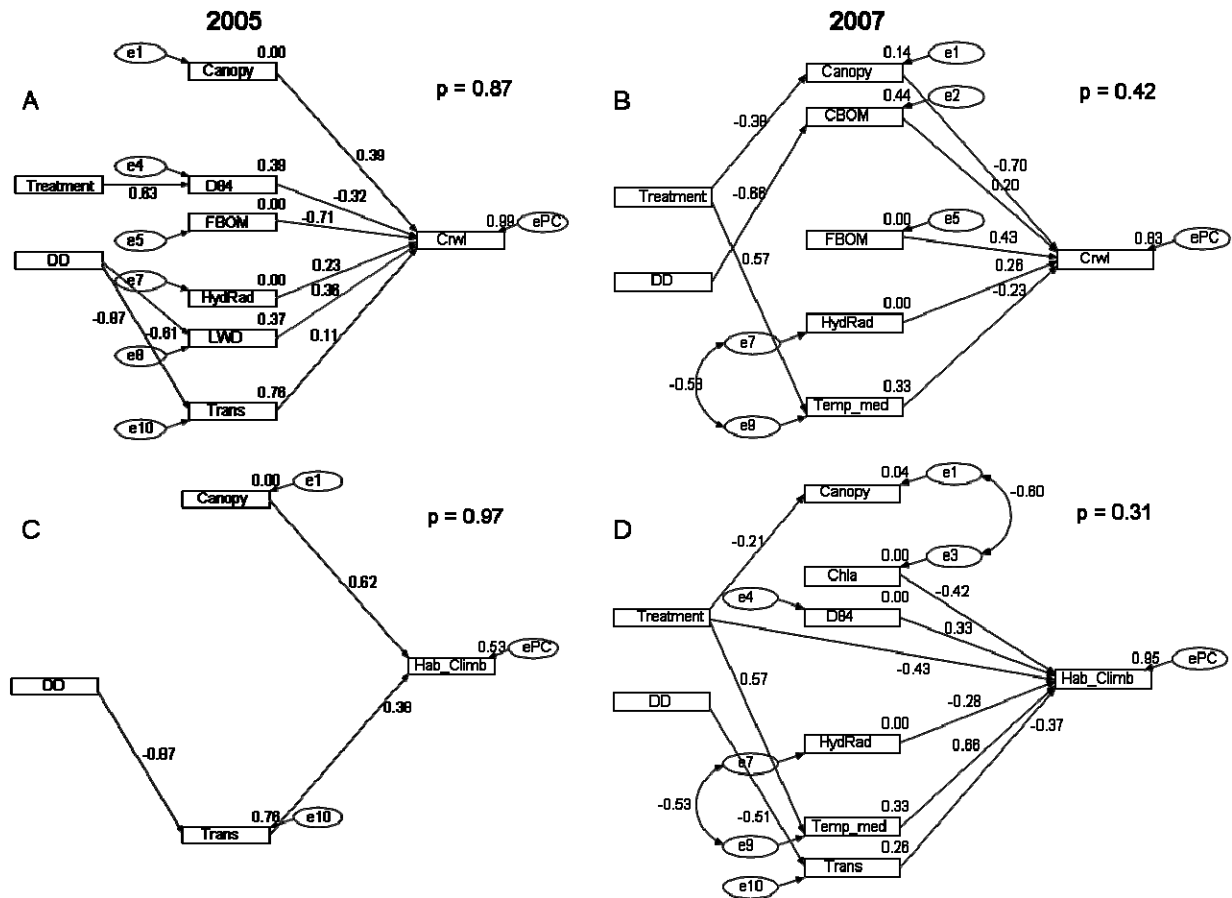


Figure 4.5. Path models showing the effect of treatment and distance downstream (DD) and important relationships between environmental variables and the variation in functional composition for the traits Crwl and Hab.Climb in 2005 and 2007.

CFT scores relating to climbing habit (Hab.Climb) were correlated with canopy cover (Canopy) and particulate transport (Trans), and indirectly with distance downstream (DD) in 2005 (Figure 4.5C). The indirect influence of distance downstream on Hab.Climb through particulate transport remained in 2007, but there were also significant direct and indirect treatment effects via canopy cover (Canopy), chlorophyll *a* standing crops (Chla) and median temperature (Temp_med) (Figure 4.5D). Bed particle size (D84) and hydraulic radius (HydRad) had direct effects on Hab.Climb, independent of treatment or distance downstream. Model C had a better goodness of fit ($p = 0.97$) than model D ($p = 0.31$), and a smaller coefficient of determination for Hab.Climb ($R^2 = 0.53$) than model D ($R^2 = 0.95$).

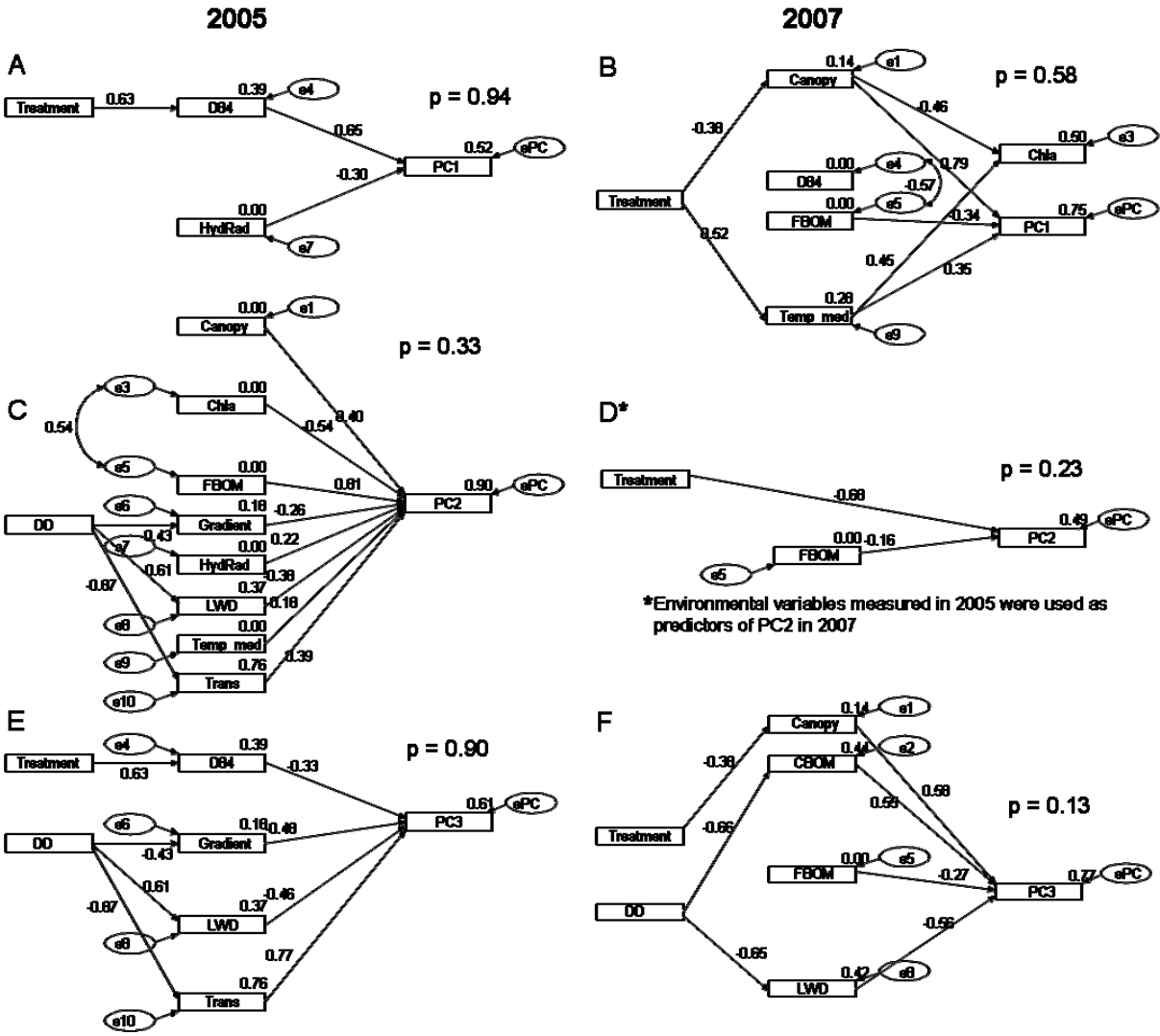


Figure 4.6. Path models showing the effect of treatment and distance downstream (DD) and important relationships between environmental variables and the variation in functional composition for the traits principal components of functional trait composition in 2005 and 2007. See Table 4.3 for trait loading for principal components.

The best fit path model for the 2005 dataset for PC1 (Figure 4.6A) indicates an indirect causal path from the treatment through bed particle size (D84), and a negative correlation between hydraulic radius (HydRad) and PC1. The best fit model for the 2007 dataset (Figure 4.6B) suggests two indirect pathways by which treatment influences PC1 (through canopy and median temperature), and correlation with FBOM that is independent of treatment. Model B also shows chlorophyll *a* standing crop (Chla) is indirectly related to treatment by the same environmental variables (canopy cover and median temperature) as PC1.

PC2 correlates with all observed environmental variables except bed particle size (D84) and coarse benthic organic matter (CBOM) in the 2005 dataset (Figure 4.6C), and is indirectly influenced by distance downstream through gradient, the presence of large woody debris (LWD), and particulate transport (Trans). None of the observed environmental variables in the 2007 dataset are correlated with PC2; however, variation in the 2007 values of PC2 is directly affected by treatment and correlates with the 2005 measures of fine benthic organic matter standing crop (FBOM) (Figure 4.6D).

Path analysis indicates PC3 is indirectly affected by treatment via bed particle size, and indirectly affected by distance downstream through gradient, large woody debris, and particulate transport in the 2005 dataset (Figure 4.6E). The 2007 dataset shows an indirect effect of treatment via canopy, separate indirect effects of distance downstream via CBOM and LWD, and a direct effect of FBOM on PC3 (Figure 4.6F). PC3 has a coefficient of determination over 0.60 in both models, and model E has a better goodness of fit ($p = 0.90$) than model F ($p = 0.13$).

Discussion

Effects of logging on the reach scale habitat template

The reach scale habitat template of forested headwater streams, as quantified by the environmental variables measured in this study (Table 4.1, Figure 4.3), exhibited a complicated and dynamic set of interacting environmental gradients. The ANCOVA model (Figure 4.2) showed two distinct treatment effects on the reach scale habitat template. An interaction between distance downstream and the logging treatment indicates upstream treatment sites realized an increase in CBOM standing crop, relative to the reference sites, but this change in CBOM was not detected in downstream reaches in treatment watersheds. The trend of increased CBOM standing crops at treatment sites directly adjacent to logged areas is likely to reverse in subsequent years due to the reduced influence of canopy tree cover as a CBOM source (Webster et al. 1990, Kiffney et al. 2003).

The resultant decrease in canopy cover in the treatment watersheds correlated with an increase in chlorophyll a standing crop and median temperature (Table 4.2). The lack of a longitudinal effect, especially in temperature, shows how this treatment effect is perpetuated up to 200m downstream from the logged area. The weak correlation between canopy cover and treatment, and lack of a detectable longitudinal pattern, is likely due to the strong influence, and

unimodal distribution of *Rhododendron* in the study watersheds with distance downstream. The observed decrease in canopy cover at upstream sites was great enough to be detected with the specification search, but I did not survey enough sampling points along each reach to account for the non-linear spatial patterns in canopy cover.

The slope of the channel bed along the thalweg (Gradient), the proportion of habitat provided by large woody debris (LWD), and particulate matter in transport (Trans) all covaried longitudinally, but were unaffected by the treatment (Gradient was assumed to be unaffected by the treatment). The path models in Figure 4.3 illustrate how these gradients remained consistently negatively correlated with distance downstream between 2005 and 2007.

Shifts in community composition

The use of functional traits to quantify shifts in community can be easily compared across studies that use similar trait scoring methods, even among sites spanning multiple provinces with different faunal pools (Poff 1997, Stutzner et al. 2001a, Cummins et al. 2008). Trait scores also provide ecologically interpretable characterizations of community composition, and the distribution of functional types of a particular trait provides a measure of how physiological characteristics of the organisms that make up assemblages correlate with particular environmental constraints (Poff 1997, Lamouroux et al. 2004).

Caveats related to the functional trait approach include a lack of phylogenetic independence among traits, and rudimentary scoring schemes that oversimplify some aspects of functional diversity. Poff et al. (2006) showed some subsets of trait categories that are scored separately in the North American benthic macroinvertebrate functional trait dataset are innately linked evolutionarily, thus interpretation of trends in functional trait composition must proceed with caution. I used principal components as composite variables to describe trends in functional composition that incorporate multiple traits that covary among sites, and to account for correlated trends in functional composition among traits that may occur merely from a phylogenetic association.

The distribution of trait scores (Figure 4.4) indicates that communities at these sites were dominated by collector gatherer, predator, and shredder functional feeding groups; however, the ANCOVA model indicates collector gatherers and scrapers, increased in dominance at treatment sites, while shredder dominance decreased, hinting at a shift in resource availability. This shift in functional feeding group dominance was consistent with the response reported by Gurtz and

Wallace (1984). Other studies have also reported shifts in community composition relating to resource availability as a response to a logging disturbance (Kiffney et al. 2004, Jackson et al. 2007).

The results from the ANCOVA of the principal coordinates of CFT scores indicates a shift in community composition occurred along at least three separate, ecologically meaningful, functional axes. The collective relationship between CFT scores correlating with PC1 (Table 4.3) and treatment was reversed, indicating an extreme shift in the relative differences in functional composition between the reference and treatment sites following disturbance. Functional shifts also occurred along PC2 and PC3, with PC2 developing a weakly detectable longitudinal pattern following disturbance. Collectively, these treatment effects indicate that logging influences different aspects of the habitat template at different scales, where some functional responses only occur locally in stream reaches located within the disturbed area (PC2), while other treatment effects may influence community composition at sites located downstream of logging.

Dominant community assembly processes

The mantel correlation (0.82, $p < 0.001$) between site organization in taxonomic and functional trait space indicates much of the variation in taxonomic community composition among sites is preserved, in general, when using CFT scores to describe community composition. Variance partitioning indicates taxonomic and functional composition are similarly influenced by environmental (X1) and spatial (X2) multivariate predictors (Table 4.4). Variation in both taxonomic and functional trait composition correlates with spatial structure (X2), but not spatial structure independent of environmental variation (X2|X1).

Overall, I found that shelterwood logging altered the stream habitat template in a manner that was detectable in environmental variables at the reach scale, primarily canopy cover, CBOM standing crop, area specific chlorophyll *a* concentrations, and stream temperature. Response in functional composition suggests the shift in these dimensions of the habitat template augmented the filtering effect of some environmental variables and increased the relative importance of niche assembly processes. Distributions of CFT scores were generally better predicted by environmental variables in 2007 ($p = 0.004$), and the trait most strongly correlated with the habitat template shifted from a mobility trait (Crwl – crawling ability) in 2005 to an ecology trait (Hab.Climb – habitat preference) (Table 4.5).

While the results of this study suggest an increased importance of environmental filtering following a disturbance, this conclusion must be placed in the context of the study system. Lotic ecosystems are rather unique in that they experience a strong background perturbation intensity (constantly shifting bedmaterial, changing hydrograph, etc.) (Allan and Castillo 2007). Consequently, dispersal assembly mechanisms may be sorting community composition at a scale smaller than the observational scale used in this study (a 10 m reach), and the importance of dispersal assembly may vary among reaches depending on the local perturbation level (e.g., local hydrological characteristics). This interaction between the habitat template and dispersal assembly mechanisms at the microhabitat scale (<1 m) would be manifested as a correlation between a habitat characteristic (e.g., bed particle size, hydrologic regime) and functional composition with respect to dispersal traits at the reach or watershed scale. The distribution of Crwl, a trait related to mobility, correlated with variables that relate can relate to the hydrologic regime (D84, LWD, HydRad, Trans) (Figure 4.5A). D84 and LWD affect local hydrodynamics by adding complexity to water flow paths or by constricting the channel to alter flow velocity (Gordon et al. 1992), and Trans and D84 represent environmental parameters that correlate with water velocity (Gordon et al. 1992, Allan and Castillo 2007). The decrease in model fit for Crwl in 2007 (multiple regression model – Table 4.5, path model – Figure 4.5B) indicates a waning importance of these dynamics as organizers of community composition following disturbance.

Hab.Climb is an indicator of a preference for habitat complexity produced by debris dams, submerged roots and branches (Merritt and Cummins 1996). The direct causal path from treatment to Hab.climb (Figure 4.5D) suggests the habitat template was altered in a manner that affected Hab.climb CFT score distribution that was not accounted for in the environmental variables that were sampled. This model also shows indirect effects of treatment through temperature and chlorophyll *a* standing crop.

Chlorophyll *a* standing crop and PC1 were both modeled as response variables in model B (Figure 4.6) to illustrate how both were indirectly affected by the treatment through canopy cover and temperature. Any covariance between these two variables is explained by the common causal parents (canopy cover and temperature). As expected, the model shows logging results in less canopy cover and warmer median temperature, and ultimately an increase in chlorophyll *a* standing crop. This effect covaries negatively with PC1, and thus providing a

context for the community compositional shifts detected with the ANCOVA for the variables that load most strongly on PC1 (see Table 4.3 for PCA loadings).

The change in the relationship between PC2 and the observed components of the habitat template indicate a disruption in the connection between some aspects of the reach scale habitat template and community composition. PC2 was significantly correlated with a number of variables prior to disturbance (Figure 4.6C), but the connection between variation in the functional composition represented by PC2 and the observed environmental variables was lost in 2007. PC2 did exhibit a treatment effect (Table 4.2), suggesting logging led to a compositional shift along this component by altering an aspect of the habitat template not measured in this study.

PC3 showed a functional shift in an aspect of community composition that also covaried with distance downstream. Logging affected the functional composition of upstream sites, with respect to PC3, through CBOM standing crop and canopy cover.

Conclusions

The shift in community composition in these headwater stream reaches indicate that landscape scale disturbances, such as logging, affect community composition in lotic ecosystems by increasing the filtering effect of various aspects of the local habitat template. Thus, disturbance increased the relative importance of niche assembly in streams, similar to the effect of drought on macroinvertebrate communities in ponds reported by Chase (2007). In headwater streams, one of the main organizing environmental variables to fill this role in the post-disturbance habitat seems to be insolation (Kiffney et al. 2003, 2004), as indicated by the importance of canopy cover, chlorophyll *a* standing crops, and temperature as conduits for the treatment effect in the path models.

Disturbance is classically thought to act on community composition as a mass mortality event, reducing richness, and creating a clean slate for early successional species (Connell and Slatyer 1977). The influence of landscape scale disturbance on lotic ecosystems appears to have the opposite effect, by creating more pronounced environmental filters in a habitat that is regularly dominated by instability.

Chapter 5 - Conclusions

Niche and neutral theory provide endpoints for a continuum of community assembly processes, and make specific predictions about spatially explicit patterns in community composition (Gilbert and Lechowicz 2004, Gravel et al. 2006, Chase 2007, Chu et al. 2007). In Chapter Two, I developed a framework that used methods for describing patterns in community composition created by Whittaker (1975), to evaluate patterns in both taxonomic and functional community composition.

Taxonomic and functional trait identifications provide two complimentary descriptions of community composition. I used α -, β -, and γ -diversity patterns in functional and taxonomic community composition to develop criteria for two diagnostics of community assembly based on community composition patterns. Diagnostic 1, β -diversity type, is a measure of whether taxonomic turnover occurs along an environmental gradient (type I) or within a functional niche (type II). Diagnostic 2 uses a trait-neutral lottery model as a null model to test the relationship between the regional source pool (γ_0), the local “effective source pool” (γ_i), and observed local community composition (α_i).

I used these diagnostics to assess the community composition patterns of benthic macroinvertebrates in forested headwater streams in the southern Blue Ridge Physiographic Province. From the spatially explicit patterns in community composition, I inferred that benthic macroinvertebrate communities in the study system are largely organized by the community assembly processes outlined by niche theory. When variation in functional composition with respect to individual traits was considered, community composition appeared to be organized by environmental gradients affecting resource and habitat preference throughout the study region; whereas, functional variation related to dispersal and size traits was only relevant locally (<30km).

While metacommunity organization is generally thought to be influenced by both niche-based and dispersal-based community assembly processes (Leibold et al. 2004, Chase 2007), the regional scale analysis of benthic macroinvertebrate communities in Chapter Two suggests that niche-based community assembly is the dominant process organizing the metacommunity in headwater streams in the southern Blue Ridge, and stream reaches likely share a common source pool of colonizers. Therefore, variation in both functional and taxonomic composition should

correlate with variation in measures of reach scale habitat characteristics that act as environmental filters, but not spatial structure independent of environmental variation (Dray et al. 2006, Laliberte et al. 2009).

In Chapter Three, I used taxonomic- and trait-based measures of β -diversity as metrics for compositional variation in the benthic macroinvertebrate metacommunity along a local (<10km study extent) disturbance (logging) gradient in the Ray Branch watershed in western North Carolina to test the conclusions from Chapter Two. Variance partitioning indicated that both taxonomic and functional β -diversity were predominantly organized by environmental variation among sites, corroborating my prediction that niche-based processes dominated community assembly at these sites. Trait-neutral lottery models were used to predict null distributions of functional composition, which were compared against observed distributions of trait scores to rank traits as candidates for interacting with the environmental gradients thought to be organizing the metacommunity. Multiple linear regression models predicting the variation in functional composition with respect to each trait were constructed using two-way stepwise linear regression. Traits ranked most likely to be sorted generally correlated best with environmental variation, corroborating the diagnostic framework from Chapter Two, which predicted community sorting processes from β -diversity patterns in taxonomic and functional composition. After establishing the importance of niche-based community assembly in this system, I used path analysis to show factors that organize physical habitat structure (gradient, channel velocity, large wood) play the dominant role in organizing community composition in these headwater streams.

The relative importance of niche-based and dispersal-based assembly processes is linked to the prevalence of disturbance (Chase 2007, Chu et al. 2007, Lepori and Malmqvist 2009). In Chapter Four, I reported an enhanced relationship between reach scale environmental gradients and the functional composition of benthic macroinvertebrate communities following disturbance (shelterwood logging) in the Ray Branch watershed.

ANCOVA showed environmental variables and community composition were affected by logging (primarily by a decrease in canopy cover, and an increase in temperature, chlorophyll *a* concentrations, and CBOM standing crops) with an interaction with distance downstream from the logging treatment. Path analysis helped to elucidate the multivariate relationship between shifts in community functional composition and shifts in the habitat template. Model comparisons with AIC_c showed stronger relationships between environmental variables and

individual functional traits following logging, indicating an increased influence of environmental filters following logging.

These results corroborate the conclusions of other recent studies in lotic systems (Chase 2007, Lepori and Malmqvist 2009) that in dynamic systems, such as headwater streams, a disturbance can augment the relative importance of niche-based community assembly. Additionally I was able to identify the particular environmental filters and functional traits that organize the reach scale response in streams to a landscape scale disturbance within the watershed.

Literature Cited

- Ackerly, D. D. and W. K. Cornwell. 2007. A trait-based approach to community assembly: Partitioning of species trait values into within- and among-community components. *Ecology Letters* **10**:135-145.
- Allan, J. D. and M. M. Castillo. 2007. *Stream ecology: Structure and function of running waters*. 2nd edition. Springer, Dordrecht, The Netherlands.
- Apha, Awwa, and Wef. 1998. *Standard methods for the examination of water and wastewater*. 20th edition. American Public Health Association, Washington, D.C.
- Arbuckle, J. L. 2007. *Amos 16.0 user's guide*. SPSS, Chicago, IL.
- Baas Becking, L. G. M. 1934. *Geobiologie of inleiding tot de milieukunde*. W.P. Van Stockum & Zoon, The Hague, the Netherlands.
- Bady, P., S. Doledec, C. Fesl, et al. 2005. Use of invertebrate traits for the biomonitoring of european large rivers: The effects of sampling effort on genus richness and functional diversity. *Freshwater Biology* **50**:159-173.
- Bell, G. 2001. Ecology - neutral macroecology. *Science* **293**:2413-2418.
- Bell, G., M. J. Lechowicz, and M. J. Waterway. 2006. The comparative evidence relating to functional and neutral interpretations of biological communities. *Ecology* **87**:1378-1386.
- Benke, A. C., T. C. Van Arsdall, D. M. Gillespie, et al. 1984. Invertebrate productivity in a subtropical blackwater river: The importance of habitat and life history. *Ecological Monographs* **54**:25-63.
- Borcard, D. and P. Legendre. 2002. All-scale spatial analysis of ecological data by means of principal coordinates of neighbour matrices. *Ecological Modelling* **153**:51-68.

- Borcard, D., P. Legendre, and P. Drapeau. 1992. Partialling out the spatial component of ecological variation. *Ecology* **73**:1045-1055.
- Buffington, J. M., R. D. Woodsmith, D. B. Booth, et al. 2003. Fluvial processes in puget sound rivers and the pacific northwest. Pages 46-78 *in* D. R. Montgomery, S. Bolton, D. B. Booth, et al., editors. Restoration of puget sound rivers. University of Washington Press, Seattle.
- Bunte, K. and S. R. Abt. 2001. Sampling surface and subsurface particle-size distributions in wadable gravel- and cobble-bed streams for analyses in sediment transport, hydraulics, and streambed monitoring. U.S. Department of Agriculture, Fort Collins, CO.
- Burnham, K. P. and D. R. Anderson. 2001. Model selection and multimodel inference: A practical information-theoretic approach. 2nd edition. Springer-Verlag, New York.
- Charvet, S., A. Kosmala, and B. Statzner. 1998. Biomonitoring through biological traits of benthic macroinvertebrates: Perspectives for a general tool in stream management. *Archiv Fur Hydrobiologie* **142**:415-432.
- Chase, J. M. 2003. Community assembly: When should history matter? *Oecologia* **136**:489-498.
- Chase, J. M. 2005. Towards a really unified theory for metacommunities. *Functional Ecology* **19**:182-186.
- Chase, J. M. 2007. Drought mediates the importance of stochastic community assembly. *Proceedings of the National Academy of Sciences of the United States of America* **104**:17430-17434.
- Chase, J. M. and M. A. Leibold. 2003. Ecological niches: Linking classical and contemporary approaches. University of Chicago Press, Chicago, Ill.

- Chu, C. J., Y. S. Wang, G. Z. Du, et al. 2007. On the balance between niche and neutral processes as drivers of community structure along a successional gradient: Insights from alpine and sub-alpine meadow communities. *Annals of Botany* **100**:807-812.
- Clements, F. E. 1916. *Plant succession*. Carnegie Institution of Washington, Washington.
- Connell, J. H. and R. O. Slatyer. 1977. Mechanisms of succession in natural communities and their role in community stability and organization. *American Naturalist* **111**:1119-1144.
- Cook, K. R. 2003. Livestock exclusion effects on the structure and function of headwater streams. M. Sc. Virginia Tech, Blacksburg.
- Cummins, K. W., R. W. Merritt, and M. B. Berg. 2008. Ecology and distribution of aquatic insects. *in* R. W. Merritt, K. W. Cummins, and M. B. Berg, editors. *An introduction to the aquatic insects of north america*. Kendall/Hunt, Dubuque, IA.
- Diamond, J. M. 1975. Assembly of species communities. Pages 342-444 *in* M. L. Cody and J. M. Diamond, editors. *Ecology and evolution of communities*. Harvard University Press.
- Diaz, A. M., M. L. S. Alonso, and M. Gutierrez. 2008. Biological traits of stream macroinvertebrates from a semi-arid catchment: Patterns along complex environmental gradients. *Freshwater Biology* **53**:1-21.
- Doledec, S., N. Phillips, M. Scarsbrook, et al. 2006. Comparison of structural and functional approaches to determining landuse effects on grassland stream invertebrate communities. *Journal of the North American Benthological Society* **25**:44-60.
- Doledec, S., B. Statzner, and M. Bournard. 1999. Species traits for future biomonitoring across ecoregions: Patterns along a human-impacted river. *Freshwater Biology* **42**:737-758.

- Dray, S., P. Legendre, and P. R. Peres-Neto. 2006. Spatial modelling: A comprehensive framework for principal coordinate analysis of neighbour matrices (pcnm). *Ecological Modelling* **196**:483-493.
- Driscoll, D. A. and D. B. Lindenmayer. 2009. Empirical tests of metacommunity theory using an isolation gradient. *Ecological Monographs* **79**:485-501.
- Ely, D. in prep. Secondary production of macroinvertebrates in coweeta watersheds. in Prep.
- Finlay, B. J. 2002. Global dispersal of free-living microbial eukaryote species. *Science* **296**:1061-1063.
- Frissell, C. A., W. J. Liss, C. E. Warren, et al. 1986. A hierarchical framework for stream habitat classification - viewing streams in a watershed context. *Environmental Management* **10**:199-214.
- Gilbert, B. and M. J. Lechowicz. 2004. Neutrality, niches, and dispersal in a temperate forest understory. *Proceedings of the National Academy of Sciences of the United States of America* **101**:7651-7656.
- Gleason, H. A. 1939. The individualistic concept of the plant association. *American Midland Naturalist* **21**:92-110.
- Gordon, N. D., T. A. McMahon, B. L. Finlayson, et al. 1992. *Stream hydrology: An introduction for ecologists*. 2nd. edition. Wiley, New York.
- Goslee, S. and D. Urban. 2007a. The ecodist package for dissimilarity-based analysis of ecological data. *Journal of Statistical Software* **22**:1-19.
- Goslee, S. and D. Urban. 2007b. The ecodist package: Dissimilarity-based functions for ecological analysis.

- Grace, J. B. 2006. Structural equation modeling and natural systems. Cambridge University Press, Cambridge.
- Gravel, D., C. D. Canham, M. Beaudet, et al. 2006. Reconciling niche and neutrality: The continuum hypothesis. *Ecology Letters* **9**:399-409.
- Grime, J. P. 2006. Trait convergence and trait divergence in herbaceous plant communities: Mechanisms and consequences. *Journal of Vegetation Science* **17**:255-260.
- Gurtz, M. E. and J. B. Wallace. 1984. Substrate-mediated response of stream invertebrates to disturbance. *Ecology* **65**:1556-1569.
- Hanski, I. 1994. A practical model of metapopulation dynamics. *Journal of Animal Ecology* **63**:151-162.
- Hanski, I. 1999. *Metapopulation ecology*. Oxford University Press, Oxford.
- Harding, J. S., E. F. Benfield, P. V. Bolstad, et al. 1998. Stream biodiversity: The ghost of land use past. *Proceedings of the National Academy of Sciences of the United States of America* **95**:14843-14847.
- Harding, J. S. and M. J. Winterbourn. 1995. Effects of contrasting land use on physico-chemical conditions and benthic assemblages of streams in a canterbury (south island, new zealand) river system. *New Zealand Journal of Marine and Freshwater Research* **29**:479-492.
- Hauer, F. R. and G. A. Lamberti, editors. 2006. *Methods in stream ecology*. 2nd edition. Elsevier.
- Heino, J. and H. Mykra. 2008. Control of stream insect assemblages: Roles of spatial configuration and local environmental factors. *Ecological Entomology* **33**:614-622.

- Holyoak, M. and M. Loreau. 2006. Reconciling empirical ecology with neutral community models. *Ecology* **87**:1370-1377.
- Hubbell, S. P. 2001. A unified theory of biodiversity and biogeography. Princeton University Press.
- Hubbell, S. P. 2006. Neutral theory and the evolution of ecological equivalence. *Ecology* **87**:1387-1398.
- Hutchinson, G. E. 1957. Concluding remarks. Pages 15-427 *in* Cold Spring Harbor Symposia on Quantitative Biology.
- Jackson, C. R., D. P. Batzer, S. S. Cross, et al. 2007. Headwater streams and timber harvest: Channel, macroinvertebrate, and amphibian response and recovery. *Forest Science* **53**:356-370.
- Janzen, D. H., W. Hallwachs, P. Blandin, et al. 2009. Integration of DNA barcoding into an ongoing inventory of complex tropical biodiversity. *Molecular Ecology Resources* **9**:1-26.
- Keddy, P. A. 1992. Assembly and response rules: Two goals for predictive community ecology. *Journal of Vegetation Science* **3**:157-164.
- Kiffney, P. M., J. S. Richardson, and J. P. Bull. 2003. Responses of periphyton and insects to experimental manipulation of riparian buffer width along forest streams. *Journal of Applied Ecology* **40**:1060-1076.
- Kiffney, P. M., J. S. Richardson, and J. P. Bull. 2004. Establishing light as a causal mechanism structuring stream communities in response to experimental manipulation of riparian buffer width. *Journal of the North American Benthological Society* **23**:542-555.
- Lachance, M. A. 2004. Here and there or everywhere? *BioScience* **54**:884-884.

- Laliberte, E. 2008. Analyzing or explaining beta diversity? Comment. *Ecology* **89**:3232-3237.
- Laliberte, E., A. Paquette, and P. Legendre. 2009. Assessing the scale-specific importance of niches and other spatial processes on beta diversity: A case study from a temperate forest. *Oecologia* **159**:337-388.
- Lamouroux, M., S. Doledec, and S. Gayraud. 2004. Biological traits of stream macroinvertebrate communities: Effects of microhabitat, reach, and basin filters. *Journal of the North American Benthological Society* **23**:449-466.
- Lane, E. W. 1955. Design of stable alluvial channels. *Transactions of the American Society of Civil Engineers* **120**:1234-1260.
- Legendre, P., D. Borcard, and P. R. Peres-Neto. 2005. Analyzing beta diversity: Partitioning the spatial variation of community composition data. *Ecological Monographs* **75**:435-450.
- Legendre, P., D. Borcard, and P. R. Peres-Neto. 2008. Analyzing or explaining beta diversity? Comment. *Ecology* **89**:3238-3244.
- Legendre, P. and E. D. Gallagher. 2001. Ecologically meaningful transformations for ordination of species data. *Oecologia* **129**:271-280.
- Legendre, P. and L. Legendre. 1998. *Numerical ecology*. Second English edition. Elsevier, Amsterdam.
- Leibold, M. A., M. Holyoak, N. Mouquet, et al. 2004. The metacommunity concept: A framework for multi-scale community ecology. *Ecology Letters* **7**:601-613.
- Leibold, M. A. and M. A. Mcpeek. 2006. Coexistence of the niche and neutral perspectives in community ecology. *Ecology* **87**:1399-1410.
- Lepori, F. and B. Malmqvist. 2009. Deterministic control on community assembly peaks at intermediate levels of disturbance. *Oikos* **118**:471-479.

- Linares-Palomino, R. and M. Kessler. 2009. The role of dispersal ability, climate and spatial separation in shaping biogeographical patterns of phylogenetically distant plant groups in seasonally dry andean forests of bolivia. *Journal of Biogeography* **36**:280-290.
- Martiny, J. B. H., B. J. M. Bohannan, J. H. Brown, et al. 2006. Microbial biogeography: Putting microorganisms on the map. *Nature Reviews Microbiology* **4**:102-112.
- Mccune, B. and J. B. Grace. 2002. Analysis of ecological communities. MjM Software Design, Gleneden Beach, OR.
- Mcgill, B. J., B. A. Maurer, and M. D. Weiser. 2006. Empirical evaluation of neutral theory. *Ecology* **87**:1411-1423.
- Merritt, R. W. and K. W. Cummins, editors. 1996. An introduction to the aquatic insects of north america. 3 edition. Kendall/Hunt, Dubuque, IA.
- Nekola, J. C. and P. S. White. 1999. The distance decay of similarity in biogeography and ecology. *Journal of Biogeography* **26**:867-878.
- Oksanen, J., R. Kindt, P. Legendre, et al. 2009. Vegan: Community ecology package.
- Pacala, S. W. and D. Tilman. 1994. Limiting similarity in mechanistic and spatial models of plant competition in heterogeneous environments. *American Naturalist* **143**:222-257.
- Peres-Neto, P. R., P. Legendre, S. Dray, et al. 2006. Variation partitioning of species data matrices - estimation and comparison of fractions. *Ecology* **87**:2614-2625.
- Poff, N. L. 1997. Landscape filters and species traits: Towards mechanistic understanding and prediction in stream ecology. *Journal of the North American Benthological Society* **16**:391-409.

- Poff, N. L., J. D. Olden, N. K. M. Vieira, et al. 2006. Functional trait niches of north american lotic insects: Traits-based ecological applications in light of phylogenetic relationships. *Journal of the North American Benthological Society* **25**:730-755.
- R Development Core Team. 2007. R: A language and environment for statistical computing. R Foundation for Statistical Computing, Vienna, Austria.
- R Development Core Team. 2009. R: A language and environment for statistical computing. R Foundation for Statistical Computing, Vienna, Austria.
- Richards, C., R. J. Haro, L. B. Johnson, et al. 1997. Catchment and reach-scale properties as indicators of macroinvertebrate species traits. *Freshwater Biology* **37**:219-&.
- Southwood, T. R. E. 1977. Habitat, the templet for ecological strategies? *Journal of Animal Ecology* **46**:337-365.
- Sponseller, R. A., E. F. Benfield, and H. M. Valett. 2001. Relationships between land use, spatial scale and stream macroinvertebrate communities. *Freshwater Biology* **46**:1409-1424.
- Statzner, B., P. Bady, S. Doledec, et al. 2005. Invertebrate traits for the biomonitoring of large european rivers: An initial assessment of trait patterns in least impacted river reaches. *Freshwater Biology* **50**:2136-2161.
- Statzner, B., B. Bis, S. Doledec, et al. 2001a. Perspectives for biomonitoring at large spatial scales: A unified measure for the functional composition on invertebrate communities in european running waters. *Basic and Applied Ecology* **2**:73-85.
- Statzner, B., A. G. Hildrew, and V. H. Resh. 2001b. Species traits and environmental constraints: Entomological research and the history of ecological theory. *Annual Review of Entomology* **46**:291-316.

- Statzner, B., K. Hoppenhaus, M. F. Arens, et al. 1997. Reproductive traits, habitat use and templet theory: A synthesis of world-wide data on aquatic insects. *Freshwater Biology* **38**:109-135.
- Stewart, K. W., B. P. Stark, and J. A. Stanger. 1993. Nymphs of north american stonefly genera (plecoptera). University of North Texas Press, Denton, TX.
- Stone, M. K. and J. B. Wallace. 1998. Long-term recovery of a mountain stream from clearcut logging: The effects of forest succession on benthic invertebrate community structure. *Freshwater Biology* **39**:151-169.
- Thompson, R. and C. Townsend. 2006. A truce with neutral theory: Local deterministic factors, species traits and dispersal limitation together determine patterns of diversity in stream invertebrates. *Journal of Animal Ecology* **75**:476-484.
- Tilman, D., S. S. Kilham, and P. Kilham. 1982. Phytoplankton community ecology - the role of limiting nutrients. *Annual Review of Ecology and Systematics* **13**:349-372.
- Tonn, W. M., J. J. Magnuson, M. Rask, et al. 1990a. Intercontinental comparison of small-lake fish assemblages: The balance between local and regional processes. *American Naturalist* **136**:345-375.
- Tonn, W. M., J. J. Magnuson, M. Rask, et al. 1990b. Intercontinental comparison of small-lake fish assemblages - the balance between local and regional processes. *American Naturalist* **136**:345-375.
- Tuomisto, H. and K. Ruokolainen. 2006. Analyzing or explaining beta diversity? Understanding the targets of different methods of analysis. *Ecology* **87**:2697-2708.
- Tuomisto, H., K. Ruokolainen, and M. Yli-Halla. 2003. Dispersal, environment, and floristic variation of western amazonian forests. *Science* **299**:241 - 244.

- Usseglio-Polatera, P., M. Bournaud, P. Richoux, et al. 2000. Biological and ecological traits of benthic freshwater macroinvertebrates: Relationships and definition of groups with similar traits. *Freshwater Biology* **43**:175-205.
- Venables, W. N. and B. D. Ripley. 2002. *Modern applied statistics with s*. Fourth edition. Springer, New York.
- Webster, J. R., S. W. Golladay, E. F. Benfield, et al. 1990. Effects of forest disturbance on particulate organic matter budgets of small streams. *Journal of the North American Benthological Society* **9**:120-140.
- Weiher, E., G. D. P. Clarke, and P. A. Keddy. 1998. Community assembly rules, morphological dispersion, and the coexistence of plant species. *Oikos* **81**:309-322.
- Weiher, E. and P. A. Keddy. 2001. *The scope and goals of research on assembly rules. Ecological assembly rules*. Cambridge University Press, Cambridge.
- Westoby, M. and I. J. Wright. 2006. Land-plant ecology on the basis of functional traits. *Trends in Ecology & Evolution* **21**:261-268.
- Whittaker, R. H. 1975. *Communities and ecosystems*. 2nd edition. MacMillan Publishing Co., Inc., New York.
- Wiggins, G. B. 1977. *Larvae of the north american caddisfly genera (trichoptera)*. University of Toronto Press, Buffalo.
- Wright, I. J., P. B. Reich, M. Westoby, et al. 2004. The worldwide leaf economics spectrum. *Nature* **428**:821-827.
- Zhou, S. R. and D. Y. Zhang. 2008. A nearly neutral model of biodiversity. *Ecology* **89**:248-258.

Appendix A – Taxonomic groups and observed relative abundances

Table A.1. Estimates of benthic macroinvertebrate densities (no./m²) from 26 headwater streams in the southern Blue Ridge Physiographic Province.

Order	Family	Genus	Site ID												
			Ely1	Ely2	Sponseller7	Sponseller8	Sponseller9	Cook1	Cook2	Cook3	Harding1	Harding2	Harding3	Harding4	Harding5
Coleoptera	Elmidae		380.2	297.0	2451.1	295.6	648.8	667.4	592.0	387.5	26.9	61.5	47.4	39.5	7.2
Coleoptera	Psephenidae	<i>Ectopria</i>	4.1	37.7	11.6	0.0	30.2	10.8	0.0	0.0	0.0	4.6	0.0	0.0	0.0
Coleoptera	Psephenidae	<i>Psephenus</i>	0.0	0.0	9.3	72.1	46.5	0.0	0.0	0.0	0.0	4.6	4.3	0.0	3.6
Diptera	Athericidae	<i>Atherix</i>	0.0	0.0	11.6	0.0	14.0	0.0	0.0	0.0	0.0	4.6	0.0	0.0	0.0
Diptera	Blephariceridae	<i>Blepharicera</i>	0.5	3.4	455.8	83.7	267.4	0.0	0.0	0.0	0.0	0.0	2.2	5.4	46.6
Diptera	Ceratopogonidae	<i>Ceratopogonidae</i>	619.7	667.5	25.6	107.0	16.3	301.4	236.8	258.3	12.6	9.2	8.6	1.8	10.8
Diptera	Deuterophlebiidae	<i>Deuterophlebia</i>	0.0	0.0	0.0	0.0	0.0	0.0	0.0	0.0	0.0	0.0	0.0	0.0	0.0
Diptera	Empididae		81.9	17.6	39.5	16.3	58.1	484.4	1151.8	215.3	9.0	26.1	99.0	0.0	9.0
Diptera	Psychodidae	<i>Pericoma</i>	0.0	0.0	0.0	0.0	0.0	43.1	0.0	43.1	0.0	0.0	0.0	0.0	0.0
Diptera	Simuliidae	<i>Simuliidae</i>	304.7	128.4	786.1	9.3	1772.1	0.0	0.0	0.0	19.7	6.2	68.9	9.0	3.6
Diptera	Tipulidae		456.1	381.6	65.1	193.0	32.6	2217.4	1528.5	2088.3	25.1	60.0	86.1	14.4	12.6
Ephemeroptera	Ameletidae	<i>Ameletus</i>	0.3	2.4	0.0	0.0	0.0	86.1	236.8	387.5	0.0	0.0	2.2	9.0	1.8
Ephemeroptera	Baetidae	<i>Acentrella</i>	0.0	0.0	0.0	0.0	0.0	0.0	0.0	0.0	0.0	0.0	0.0	0.0	0.0
Ephemeroptera	Baetidae	<i>Baetis</i>	380.5	261.1	148.8	125.6	23.3	0.0	0.0	0.0	52.0	44.6	226.0	28.7	116.6
Ephemeroptera	Caenidae	<i>Caenis</i>	0.0	0.0	0.0	0.0	0.0	0.0	0.0	0.0	3.6	0.0	0.0	0.0	0.0
Ephemeroptera	Ephemerellidae	<i>Attenella</i>	0.0	0.0	0.0	0.0	0.0	0.0	0.0	0.0	0.0	0.0	0.0	48.4	0.0
Ephemeroptera	Ephemerellidae	<i>Drunella</i>	0.0	0.0	165.1	60.5	153.5	0.0	0.0	0.0	7.2	63.0	6.5	3.6	0.0
Ephemeroptera	Ephemerellidae	<i>Ephemerella</i>	0.0	0.0	476.7	251.2	1402.3	1646.9	1797.6	4887.0	181.2	395.2	426.3	68.2	175.8
Ephemeroptera	Ephemerellidae	<i>Eurylophella</i>	0.0	0.0	0.0	0.0	0.0	96.9	0.0	21.5	1.8	0.0	8.6	0.0	0.0
Ephemeroptera	Ephemerellidae	<i>Serratella</i>	745.6	278.1	0.0	0.0	0.0	0.0	32.3	0.0	0.0	0.0	0.0	0.0	0.0
Ephemeroptera	Ephemeridae	<i>Ephemerella</i>	0.0	0.0	27.9	0.0	0.0	0.0	0.0	0.0	0.0	0.0	0.0	0.0	0.0
Ephemeroptera	Heptageniidae	<i>Cinygmula</i>	0.0	0.0	0.0	0.0	0.0	0.0	0.0	0.0	71.8	0.0	60.3	0.0	0.0
Ephemeroptera	Heptageniidae	<i>Epeorus</i>	59.5	31.9	393.0	1174.4	111.6	21.5	21.5	43.1	89.7	116.9	174.4	125.6	14.4
Ephemeroptera	Heptageniidae	<i>Heptagenia</i>	0.0	0.0	0.0	0.0	0.0	0.0	0.0	0.0	0.0	0.0	0.0	0.0	0.0
Ephemeroptera	Heptageniidae	<i>Rhithrogena</i>	0.0	0.0	0.0	0.0	0.0	0.0	10.8	0.0	17.9	4.6	90.4	0.0	245.8
Ephemeroptera	Heptageniidae	<i>Stenacron</i> <i>Stenonema</i>	0.0	0.0	0.0	0.0	0.0	0.0	0.0	0.0	0.0	0.0	0.0	0.0	0.0
Ephemeroptera	Heptageniidae	<i>Maccaffertium</i>	16.7	61.8	14.0	446.5	39.5	139.9	333.7	172.2	3.6	75.3	75.3	35.9	30.5
Ephemeroptera	Isonychiidae	<i>Isonychia</i>	0.4	0.9	0.0	0.0	0.0	0.0	0.0	0.0	0.0	0.0	10.8	0.0	0.0
Ephemeroptera	Leptophlebiidae	<i>Habrophlebia</i>	0.0	33.6	0.0	0.0	0.0	0.0	0.0	0.0	0.0	0.0	0.0	0.0	0.0
Ephemeroptera	Leptophlebiidae	<i>Leptophlebia</i>	0.0	0.0	0.0	0.0	0.0	0.0	0.0	0.0	0.0	0.0	28.0	0.0	0.0

Ephemeroptera	Leptophlebiidae	<i>Paraleptophlebia</i>	394.5	231.6	0.0	30.2	2.3	3240.0	1625.4	1786.9	12.6	30.8	21.5	0.0	14.4
Hemiptera	Gerridae	<i>Trepobates</i>	0.0	0.0	0.0	0.0	0.0	0.0	0.0	21.5	0.0	0.0	0.0	0.0	0.0
Hemiptera	Veliidae	<i>Microvelia</i>	0.0	0.0	0.0	0.0	0.0	0.0	0.0	0.0	0.0	0.0	0.0	0.0	0.0
Hemiptera	Veliidae	<i>Rhagovelia</i>	0.0	0.0	0.0	0.0	0.0	0.0	0.0	0.0	0.0	0.0	0.0	0.0	0.0
Lepidoptera	Pyralidae	<i>Petrophila</i>	0.0	0.0	0.0	0.0	0.0	0.0	0.0	0.0	0.0	0.0	0.0	0.0	0.0
Megaloptera	Corydalidae	<i>Corydalus</i>	0.0	0.0	0.0	4.7	0.0	0.0	0.0	0.0	0.0	0.0	0.0	0.0	1.8
Megaloptera	Corydalidae	<i>Nigronia</i>	0.0	0.0	2.3	0.0	0.0	0.0	0.0	0.0	0.0	7.7	0.0	0.0	0.0
Megaloptera	Sialidae	<i>Sialis</i>	0.0	0.0	0.0	0.0	0.0	0.0	0.0	0.0	0.0	0.0	0.0	0.0	1.8
Odonata	Cordulegastridae	<i>Cordulegaster</i>	11.2	12.1	0.0	2.3	0.0	226.0	10.8	86.1	0.0	0.0	0.0	0.0	0.0
Odonata	Gomphidae	<i>Dromogomphus</i>	0.0	0.0	0.0	0.0	0.0	0.0	0.0	0.0	0.0	0.0	2.2	0.0	0.0
Odonata	Gomphidae	<i>Gomphus</i>	0.0	0.0	0.0	0.0	0.0	0.0	0.0	0.0	0.0	0.0	0.0	0.0	0.0
Odonata	Gomphidae	<i>Lanthus</i>	72.6	17.2	0.0	0.0	0.0	871.9	21.5	215.3	0.0	0.0	0.0	0.0	0.0
Odonata	Gomphidae	<i>Stylogomphus</i>	0.0	0.0	0.0	0.0	0.0	0.0	0.0	0.0	0.0	4.6	0.0	0.0	0.0
Plecoptera	Capniidae	<i>Allocaupnia</i>	0.0	0.0	151.2	0.0	0.0	0.0	0.0	0.0	0.0	0.0	0.0	14.4	0.0
Plecoptera	Chloroperlidae	<i>Alloperla</i>	0.0	0.0	0.0	0.0	0.0	0.0	0.0	0.0	0.0	0.0	8.6	0.0	23.3
Plecoptera	Chloroperlidae	<i>Haploperla</i>	0.0	0.0	0.0	0.0	0.0	183.0	86.1	0.0	0.0	0.0	0.0	0.0	0.0
Plecoptera	Chloroperlidae	<i>Sweltsa</i>	44.8	47.9	0.0	467.5	9.3	43.1	0.0	667.4	0.0	6.2	0.0	0.0	0.0
Plecoptera	Chloroperlidae	<i>Utaperla</i>	0.0	0.0	0.0	0.0	0.0	0.0	0.0	0.0	0.0	0.0	0.0	0.0	0.0
Plecoptera	Leuctridae	<i>Leuctra</i>	1079.6	1032.6	0.0	14.0	14.0	2368.1	516.7	1743.8	0.0	215.3	0.0	0.0	0.0
Plecoptera	Nemouridae	<i>Amphinemura</i>	382.5	370.6	18.6	23.3	314.0	398.3	247.6	495.2	3.6	13.8	0.0	0.0	0.0
Plecoptera	Nemouridae	<i>Paranemoura</i>	0.0	0.0	0.0	0.0	0.0	0.0	0.0	0.0	0.0	0.0	0.0	0.0	0.0
Plecoptera	Nemouridae	<i>Soyedina</i>	203.3	262.5	0.0	0.0	0.0	0.0	0.0	0.0	3.6	0.0	0.0	0.0	0.0
Plecoptera	Peltoperlidae	<i>Peltoperlidae</i>	208.1	255.4	9.3	7.0	65.1	3692.1	1474.7	1076.4	16.1	3.1	19.4	28.7	0.0
Plecoptera	Perlidae	<i>Acroperla</i>	0.0	0.0	9.3	27.9	18.6	0.0	0.0	0.0	35.9	21.5	12.9	3.6	12.6
Plecoptera	Perlidae	<i>Agnetina</i>	0.0	0.0	0.0	0.0	0.0	0.0	0.0	0.0	0.0	0.0	0.0	0.0	0.0
Plecoptera	Perlidae	<i>Beloneuria</i>	2.1	7.1	0.0	0.0	0.0	10.8	21.5	0.0	0.0	53.8	0.0	0.0	0.0
Plecoptera	Perlidae	<i>Hansonoperla</i>	0.0	0.0	0.0	0.0	0.0	0.0	0.0	0.0	1.8	0.0	0.0	3.6	0.0
Plecoptera	Perlidae	<i>Paragnetina</i>	0.0	0.0	0.0	2.3	0.0	0.0	0.0	0.0	0.0	0.0	0.0	0.0	0.0
Plecoptera	Perlidae	<i>Perlesta</i>	0.0	0.0	0.0	0.0	0.0	0.0	0.0	0.0	0.0	0.0	0.0	0.0	0.0
Plecoptera	Perlodidae	<i>Clioperla</i>	0.0	0.0	0.0	0.0	0.0	0.0	0.0	0.0	0.0	0.0	0.0	0.0	0.0
Plecoptera	Perlodidae	<i>Cultus</i>	0.0	0.0	0.0	0.0	0.0	0.0	0.0	0.0	0.0	26.1	8.6	0.0	0.0
Plecoptera	Perlodidae	<i>Helopicus</i>	0.0	0.0	0.0	0.0	0.0	0.0	0.0	0.0	0.0	27.7	0.0	0.0	55.6
Plecoptera	Perlodidae	<i>Hydroperla</i>	0.0	0.0	0.0	0.0	0.0	0.0	0.0	0.0	5.4	0.0	0.0	0.0	0.0
Plecoptera	Perlodidae	<i>Isogenoides</i>	0.0	0.0	0.0	0.0	0.0	0.0	0.0	0.0	1.8	0.0	2.2	0.0	0.0
Plecoptera	Perlodidae	<i>Isoperla</i>	474.7	181.3	41.9	18.6	34.9	0.0	64.6	0.0	3.6	41.5	94.7	0.0	95.1
Plecoptera	Perlodidae	<i>Kogotus</i>	0.0	0.0	0.0	0.0	0.0	0.0	0.0	0.0	0.0	0.0	0.0	0.0	0.0

Plecoptera	Perlodidae	<i>Malirekus</i>	31.8	8.1	0.0	0.0	0.0	0.0	0.0	0.0	1.8	0.0	0.0	3.6	0.0
Plecoptera	Perlodidae	<i>Remenus</i>	0.0	0.0	0.0	0.0	0.0	0.0	559.7	193.8	0.0	0.0	0.0	0.0	0.0
Plecoptera	Perlodidae	<i>Yugus</i>	0.0	0.0	0.0	4.7	0.0	0.0	0.0	0.0	0.0	0.0	0.0	14.4	0.0
Plecoptera	Pteronarcyidae	<i>Pteronarcys</i>	0.0	0.0	65.1	7.0	162.8	0.0	0.0	0.0	9.0	4.6	0.0	16.1	0.0
Plecoptera	Taeniopterygidae	<i>Oemopteryx</i>	0.0	0.0	20.9	2.3	0.0	0.0	0.0	0.0	41.3	206.1	0.0	66.4	21.5
Plecoptera	Taeniopterygidae	<i>Taeniopteryx</i>	28.9	0.0	0.0	0.0	0.0	0.0	0.0	0.0	0.0	0.0	0.0	0.0	0.0
Trichoptera	Brachycentridae	<i>Brachycentrus</i>	0.0	0.0	0.0	16.3	0.0	0.0	0.0	0.0	3.6	0.0	2.2	0.0	1.8
Trichoptera	Brachycentridae	<i>Micrasema</i>	42.6	30.9	0.0	0.0	0.0	0.0	0.0	0.0	0.0	0.0	0.0	0.0	0.0
Trichoptera	Glossosomatidae	<i>Agapetus</i>	0.0	0.0	0.0	0.0	23.3	0.0	0.0	0.0	0.0	0.0	15.1	3.6	0.0
Trichoptera	Glossosomatidae	<i>Glossosoma</i>	1.1	1.9	9.3	18.6	7.0	0.0	10.8	0.0	3.6	0.0	0.0	0.0	0.0
Trichoptera	Glossosomatidae	<i>Matrioptila</i>	0.0	0.0	9.3	0.0	2.3	0.0	0.0	0.0	0.0	0.0	0.0	0.0	0.0
Trichoptera	Hydropsychidae	<i>Arctopsyche</i>	0.0	0.0	0.0	0.0	0.0	0.0	0.0	0.0	0.0	0.0	0.0	3.6	0.0
Trichoptera	Hydropsychidae	<i>Ceratopsyche</i>	0.0	0.0	0.0	0.0	0.0	0.0	0.0	0.0	344.5	49.2	0.0	0.0	1.8
Trichoptera	Hydropsychidae	<i>Cheumatopsyche</i>	0.0	0.0	32.6	23.3	11.6	0.0	0.0	0.0	3.6	0.0	0.0	0.0	1.8
Trichoptera	Hydropsychidae	<i>Diplectrona</i>	477.9	371.0	44.2	7.0	65.1	0.0	0.0	0.0	62.8	0.0	2.2	17.9	0.0
Trichoptera	Hydropsychidae	<i>Hydropsyche</i>	0.0	0.0	0.0	0.0	0.0	721.2	2669.5	322.9	0.0	227.6	28.0	3.6	34.1
Trichoptera	Hydropsychidae	<i>Parapsyche</i>	356.7	356.6	0.0	0.0	0.0	0.0	0.0	0.0	3.6	0.0	0.0	26.9	0.0
Trichoptera	Hydroptilidae	<i>Hydroptila</i>	0.0	0.0	0.0	0.0	0.0	0.0	0.0	0.0	0.0	0.0	0.0	0.0	0.0
Trichoptera	Hydroptilidae	<i>Leucotrichia</i>	0.0	0.0	0.0	0.0	0.0	0.0	0.0	0.0	0.0	0.0	0.0	0.0	0.0
Trichoptera	Lepidostomatidae	<i>Lepidostoma</i>	98.9	115.7	0.0	0.0	0.0	0.0	0.0	0.0	3.6	0.0	2.2	0.0	0.0
Trichoptera	Lepidostomatidae	<i>Theliopsyche</i>	0.0	0.0	0.0	0.0	0.0	0.0	0.0	0.0	0.0	0.0	4.3	0.0	0.0
Trichoptera	Limnephilidae	<i>Pycnopsyche</i>	64.9	153.8	0.0	0.0	0.0	635.1	215.3	107.6	9.0	0.0	12.9	0.0	0.0
Trichoptera	Odontoceridae	<i>Pseudogoera</i>	1.9	2.4	0.0	0.0	0.0	0.0	0.0	0.0	0.0	0.0	0.0	0.0	0.0
Trichoptera	Odontoceridae	<i>Psilotreta</i>	0.0	2.6	0.0	0.0	0.0	10.8	10.8	64.6	0.0	0.0	0.0	0.0	0.0
Trichoptera	Philopotamidae	<i>Dolophilodes</i>	12.3	9.8	14.0	0.0	4.7	0.0	0.0	0.0	3.6	0.0	0.0	0.0	0.0
Trichoptera	Philopotamidae	<i>Wormaldia</i>	0.0	0.0	0.0	0.0	0.0	0.0	0.0	0.0	0.0	0.0	47.4	0.0	0.0
Trichoptera	Polycentropodidae	<i>Cyrmellus</i>	0.0	0.0	0.0	0.0	0.0	0.0	0.0	21.5	1.8	0.0	4.3	0.0	0.0
Trichoptera	Polycentropodidae	<i>Neureclipsis</i>	0.0	0.0	0.0	0.0	0.0	0.0	0.0	0.0	1.8	0.0	0.0	0.0	0.0
Trichoptera	Polycentropodidae	<i>Polycentropus</i>	0.4	2.4	0.0	14.0	30.2	43.1	0.0	0.0	1.8	3.1	0.0	7.2	0.0
Trichoptera	Psychomyiidae	<i>Lype</i>	44.6	15.1	0.0	0.0	0.0	172.2	43.1	43.1	0.0	0.0	0.0	0.0	0.0
Trichoptera	Rhyacophilidae	<i>Rhyacophila</i>	107.8	37.3	32.6	7.0	44.2	269.1	538.2	430.6	7.2	33.8	43.1	21.5	0.0
Trichoptera	Uenoidae	<i>Neophylax</i>	95.6	19.8	2.3	0.0	7.0	236.8	107.6	21.5	0.0	0.0	4.3	0.0	0.0

Table A.1. (Continued)

Order	Family	Genus	Site ID												
			Harding6	Harding7	Harding8	Harding9	Harding10	Harding11	Harding12	Harding13	Harding14	Sokol1	Sokol2	Sokol3	Sokol4
Coleoptera	Elmidae		19.4	93.8	27.7	47.7	113.8	64.6	70.7	32.3	18.5	43.6	65.7	60.6	49.0
Coleoptera	Psephenidae	<i>Ectopria</i>	0.0	1.5	0.0	0.0	0.0	4.6	0.0	0.0	1.5	5.4	15.1	34.0	10.8
Coleoptera	Psephenidae	<i>Psephenus</i>	2.2	0.0	0.0	0.0	0.0	0.0	0.0	3.1	0.0	0.0	0.0	0.0	0.0
Diptera	Athericidae	<i>Atherix</i>	0.0	3.1	0.0	6.2	12.3	3.1	0.0	1.5	4.6	0.0	0.0	0.0	0.0
Diptera	Blephariceridae	<i>Blepharicera</i>	49.5	0.0	6.2	26.1	40.0	1.5	0.0	10.8	0.0	0.0	0.0	0.0	0.0
Diptera	Ceratopogonidae	Ceratopogonidae	0.0	1.5	23.1	3.1	4.6	24.6	7.7	32.3	3.1	17.8	13.5	6.8	40.9
Diptera	Deuterophlebiidae	<i>Deuterophlebia</i>	0.0	0.0	0.0	0.0	0.0	0.0	0.0	0.0	0.0	0.5	0.0	0.0	0.0
Diptera	Empididae		15.1	3.1	26.1	1.5	6.2	20.0	1.5	1.5	3.1	14.5	2.2	2.3	3.8
Diptera	Psychodidae	<i>Pericoma</i>	0.0	0.0	0.0	0.0	0.0	0.0	0.0	0.0	0.0	0.0	0.0	0.0	0.0
Diptera	Simuliidae	<i>Simuliidae</i>	6.5	55.4	289.1	127.6	269.1	53.8	86.1	84.6	46.1	5.9	10.2	192.6	12.9
Diptera	Tipulidae		10.8	89.2	123.0	66.1	75.3	33.8	69.2	13.8	30.8	37.1	26.4	10.2	38.8
Ephemeroptera	Ameletidae	<i>Ameletus</i>	2.2	6.2	0.0	4.6	30.8	29.2	16.9	0.0	3.1	0.0	0.0	0.0	0.0
Ephemeroptera	Baetidae	<i>Acentrella</i>	0.0	0.0	0.0	0.0	3.1	315.2	0.0	0.0	0.0	0.0	0.0	0.0	0.0
Ephemeroptera	Baetidae	<i>Baetis</i>	30.1	296.8	876.5	219.9	861.1	10.8	70.7	482.9	96.9	26.4	58.1	106.5	54.4
Ephemeroptera	Caenidae	<i>Caenis</i>	0.0	0.0	0.0	0.0	0.0	0.0	0.0	0.0	0.0	0.0	0.0	0.0	0.0
Ephemeroptera	Ephemerellidae	<i>Attenella</i>	0.0	0.0	0.0	0.0	0.0	0.0	0.0	0.0	1.5	0.0	0.0	0.0	0.0
Ephemeroptera	Ephemerellidae	<i>Drunella</i>	4.3	24.6	33.8	3.1	15.4	13.8	12.3	1.5	33.8	0.0	2.2	2.3	1.1
Ephemeroptera	Ephemerellidae	<i>Ephemerella</i>	2555.4	859.6	550.5	542.8	1399.4	253.7	467.5	507.5	250.7	0.5	1.6	1.1	1.6
Ephemeroptera	Ephemerellidae	<i>Eurylophella</i>	0.0	0.0	0.0	0.0	0.0	13.8	0.0	0.0	0.0	0.0	0.0	0.0	0.0
Ephemeroptera	Ephemerellidae	<i>Serratella</i>	0.0	9.2	0.0	0.0	0.0	0.0	0.0	0.0	7.7	0.0	0.0	0.0	0.0
Ephemeroptera	Ephemeridae	<i>Ephemera</i>	0.0	0.0	0.0	0.0	0.0	0.0	0.0	0.0	0.0	0.0	0.0	0.6	0.0
Ephemeroptera	Heptageniidae	<i>Cinygmula</i>	2.2	558.2	0.0	0.0	0.0	40.0	644.3	176.8	339.8	0.0	0.0	0.0	0.0
Ephemeroptera	Heptageniidae	<i>Epeorus</i>	198.1	129.2	80.0	183.0	232.2	112.3	361.4	161.5	263.0	3.2	4.8	2.3	7.5
Ephemeroptera	Heptageniidae	<i>Heptagenia</i>	0.0	1.5	0.0	0.0	0.0	0.0	0.0	0.0	1.5	0.0	0.0	0.0	0.0
Ephemeroptera	Heptageniidae	<i>Rhithrogena</i>	211.0	49.2	173.8	346.0	21.5	0.0	0.0	63.0	0.0	0.0	0.0	0.0	0.0
Ephemeroptera	Heptageniidae	<i>Stenacron</i>	0.0	1.5	0.0	0.0	0.0	0.0	0.0	0.0	0.0	0.0	1.6	2.3	0.5
Ephemeroptera	Heptageniidae	<i>Stenonema/ Maccaffertium</i>	232.5	27.7	33.8	63.0	29.2	38.4	4.6	50.7	18.5	0.0	0.0	0.0	0.5
Ephemeroptera	Isonychiidae	<i>Isonychia</i>	0.0	0.0	38.4	0.0	3.1	0.0	6.2	4.6	0.0	9.7	1.6	23.8	1.6
Ephemeroptera	Leptophlebiidae	<i>Habrophlebia</i>	0.0	0.0	0.0	0.0	0.0	0.0	0.0	0.0	0.0	0.0	0.0	0.0	0.0
Ephemeroptera	Leptophlebiidae	<i>Leptophlebia</i>	0.0	7.7	0.0	0.0	0.0	0.0	50.7	0.0	0.0	0.0	0.0	0.0	0.0
Ephemeroptera	Leptophlebiidae	<i>Paraleptophlebia</i>	17.2	27.7	3.1	152.2	0.0	27.7	166.1	9.2	23.1	0.0	0.0	0.0	1.1
Hemiptera	Gerridae	<i>Trepobates</i>	0.0	0.0	0.0	0.0	0.0	0.0	0.0	0.0	0.0	0.0	0.0	0.0	0.0
Hemiptera	Veliidae	<i>Microvelia</i>	0.0	0.0	0.0	0.0	0.0	0.0	0.0	0.0	0.0	0.0	0.0	1.7	0.0

Hemiptera	Veliidae	<i>Rhagovelia</i>	0.0	0.0	0.0	0.0	0.0	0.0	0.0	0.0	0.0	0.0	0.0	0.6	0.0
Lepidoptera	Pyrilidae	<i>Petrophila</i>	0.0	0.0	0.0	0.0	0.0	0.0	0.0	0.0	0.0	1.6	0.0	0.6	0.0
Megaloptera	Corydalidae	<i>Corydalus</i>	4.3	0.0	9.2	0.0	0.0	0.0	0.0	0.0	0.0	0.0	0.0	0.0	0.0
Megaloptera	Corydalidae	<i>Nigronia</i>	0.0	3.1	0.0	0.0	18.5	0.0	0.0	3.1	0.0	0.0	0.0	0.0	0.0
Megaloptera	Sialidae	<i>Sialis</i>	0.0	0.0	6.2	0.0	0.0	0.0	0.0	0.0	0.0	0.0	0.0	0.0	0.0
Odonata	Cordulegastridae	<i>Cordulegaster</i>	0.0	0.0	0.0	0.0	0.0	0.0	0.0	0.0	0.0	0.0	0.0	0.0	0.0
Odonata	Gomphidae	<i>Dromogomphus</i>	0.0	0.0	0.0	0.0	0.0	0.0	0.0	0.0	0.0	0.0	0.0	0.0	0.0
Odonata	Gomphidae	<i>Gomphus</i>	0.0	0.0	0.0	0.0	0.0	6.2	0.0	0.0	0.0	7.0	3.8	3.4	0.5
Odonata	Gomphidae	<i>Lanthus</i>	0.0	0.0	0.0	0.0	0.0	0.0	0.0	0.0	0.0	0.0	0.0	0.0	0.0
Odonata	Gomphidae	<i>Stylogomphus</i>	0.0	0.0	0.0	0.0	0.0	0.0	0.0	0.0	0.0	0.0	0.0	0.0	0.0
Plecoptera	Capniidae	<i>Allocapnia</i>	4.3	3.1	0.0	23.1	0.0	0.0	3.1	0.0	0.0	0.0	0.0	0.0	0.0
Plecoptera	Chloroperlidae	<i>Alloperla</i>	8.6	13.8	6.2	0.0	0.0	0.0	0.0	0.0	0.0	0.0	0.0	0.0	0.0
Plecoptera	Chloroperlidae	<i>Haploperla</i>	0.0	3.1	0.0	0.0	0.0	0.0	0.0	0.0	12.3	0.0	0.0	0.0	0.0
Plecoptera	Chloroperlidae	<i>Sweltsa</i>	0.0	7.7	0.0	26.1	13.8	0.0	135.3	6.2	35.4	13.5	4.8	1.7	1.1
Plecoptera	Chloroperlidae	<i>Utaperla</i>	0.0	0.0	0.0	0.0	7.7	0.0	0.0	0.0	0.0	0.0	0.0	0.0	0.0
Plecoptera	Leuctridae	<i>Leuctra</i>	0.0	32.3	0.0	0.0	1.5	0.0	0.0	0.0	0.0	13.5	19.4	10.8	19.9
Plecoptera	Nemouridae	<i>Amphinemura</i>	0.0	13.8	1.5	7.7	6.2	3.1	12.3	6.2	36.9	21.0	2.2	3.4	5.9
Plecoptera	Nemouridae	<i>Paranemoura</i>	40.9	0.0	0.0	0.0	0.0	0.0	0.0	0.0	0.0	0.0	0.0	0.0	0.0
Plecoptera	Nemouridae	<i>Soyedina</i>	0.0	6.2	0.0	0.0	0.0	0.0	3.1	0.0	0.0	0.0	0.0	0.0	0.0
Plecoptera	Peltoperlidae	<i>Peltoperlidae</i>	6.5	18.5	0.0	70.7	29.2	13.8	10.8	7.7	7.7	128.1	47.4	45.9	30.7
Plecoptera	Perlidae	<i>Acroneuria</i>	15.1	9.2	307.6	47.7	43.1	9.2	15.4	7.7	23.1	31.8	23.1	2.8	28.0
Plecoptera	Perlidae	<i>Agnentina</i>	0.0	0.0	0.0	0.0	0.0	0.0	0.0	0.0	0.0	0.5	0.0	0.0	0.0
Plecoptera	Perlidae	<i>Beloneuria</i>	2.2	7.7	0.0	0.0	30.8	0.0	7.7	21.5	0.0	1.6	0.0	0.0	0.0
Plecoptera	Perlidae	<i>Hansonoperla</i>	0.0	0.0	0.0	0.0	0.0	4.6	0.0	0.0	12.3	0.0	0.0	0.0	0.0
Plecoptera	Perlidae	<i>Paragnetina</i>	0.0	0.0	0.0	0.0	0.0	0.0	0.0	0.0	0.0	0.0	0.0	0.0	0.0
Plecoptera	Perlidae	<i>Perlesta</i>	0.0	0.0	0.0	0.0	0.0	0.0	0.0	0.0	0.0	0.0	1.1	0.6	0.5
Plecoptera	Perlodidae	<i>Clioperla</i>	0.0	0.0	0.0	0.0	0.0	0.0	0.0	0.0	0.0	5.9	8.6	0.0	4.3
Plecoptera	Perlodidae	<i>Cultus</i>	2.2	1.5	0.0	0.0	0.0	7.7	0.0	40.0	7.7	0.0	0.0	0.0	0.0
Plecoptera	Perlodidae	<i>Helopicus</i>	34.4	1.5	1.5	0.0	0.0	0.0	0.0	0.0	0.0	0.0	0.0	0.0	0.0
Plecoptera	Perlodidae	<i>Hydroperla</i>	0.0	0.0	0.0	0.0	0.0	0.0	0.0	0.0	1.5	0.0	0.0	0.0	0.0
Plecoptera	Perlodidae	<i>Isogenoides</i>	0.0	0.0	0.0	0.0	0.0	0.0	0.0	0.0	0.0	0.0	0.0	0.0	0.0
Plecoptera	Perlodidae	<i>Isoperla</i>	163.6	52.3	3.1	0.0	10.8	20.0	43.1	24.6	20.0	0.0	0.0	0.0	0.0
Plecoptera	Perlodidae	<i>Kogotus</i>	0.0	0.0	0.0	0.0	0.0	0.0	0.0	4.6	0.0	0.0	0.0	0.0	0.0
Plecoptera	Perlodidae	<i>Malirekus</i>	0.0	0.0	0.0	0.0	0.0	0.0	0.0	0.0	0.0	14.0	14.5	1.1	16.7
Plecoptera	Perlodidae	<i>Remenus</i>	0.0	1.5	0.0	0.0	0.0	20.0	0.0	0.0	0.0	0.0	0.0	0.0	0.0
Plecoptera	Perlodidae	<i>Yugus</i>	0.0	12.3	0.0	16.9	20.0	0.0	9.2	12.3	0.0	0.0	0.0	0.0	0.0

Plecoptera	Pteronarcyidae	<i>Pteronarcys</i>	4.3	21.5	0.0	20.0	0.0	27.7	1.5	16.9	9.2	0.0	0.0	0.0	0.0
Plecoptera	Taeniopterygidae	<i>Oemopteryx</i>	0.0	73.8	116.9	84.6	6.2	426.0	24.6	27.7	43.1	0.0	0.0	0.0	0.0
Plecoptera	Taeniopterygidae	<i>Taeniopteryx</i>	0.0	0.0	0.0	0.0	0.0	30.8	0.0	0.0	0.0	0.0	0.0	0.0	0.0
Trichoptera	Brachycentridae	<i>Brachycentrus</i>	0.0	0.0	0.0	10.8	18.5	13.8	0.0	1.5	0.0	0.0	0.0	0.0	0.0
Trichoptera	Brachycentridae	<i>Micrasema</i>	0.0	0.0	0.0	0.0	0.0	0.0	0.0	0.0	0.0	0.0	0.0	0.0	0.0
Trichoptera	Glossosomatidae	<i>Agapetus</i>	0.0	1.5	0.0	0.0	1.5	0.0	0.0	0.0	0.0	0.0	0.0	0.0	0.0
Trichoptera	Glossosomatidae	<i>Glossosoma</i>	0.0	0.0	0.0	0.0	0.0	0.0	0.0	0.0	0.0	1.6	3.8	3.4	5.4
Trichoptera	Glossosomatidae	<i>Matrioptila</i>	0.0	0.0	0.0	0.0	0.0	0.0	0.0	0.0	0.0	0.0	0.0	0.0	0.0
Trichoptera	Hydropsychidae	<i>Arctopsyche</i>	0.0	0.0	0.0	0.0	0.0	0.0	0.0	0.0	0.0	14.0	8.1	138.8	19.4
Trichoptera	Hydropsychidae	<i>Ceratopsyche</i>	0.0	21.5	127.6	26.1	6.2	107.6	36.9	0.0	10.8	0.0	0.0	0.0	0.0
Trichoptera	Hydropsychidae	<i>Cheumatopsyche</i>	4.3	29.2	0.0	4.6	1.5	1.5	3.1	370.6	3.1	0.0	0.0	0.0	0.0
Trichoptera	Hydropsychidae	<i>Diplectrona</i>	0.0	3.1	0.0	0.0	0.0	1.5	0.0	0.0	0.0	40.4	38.2	32.3	19.9
Trichoptera	Hydropsychidae	<i>Hydropsyche</i>	101.2	13.8	0.0	27.7	170.2	3.1	1.5	132.2	13.8	0.0	0.0	0.0	0.0
Trichoptera	Hydropsychidae	<i>Parapsyche</i>	0.0	0.0	0.0	0.0	0.0	1.5	0.0	0.0	0.0	2.7	0.5	0.0	2.2
Trichoptera	Hydroptilidae	<i>Hydroptila</i>	0.0	0.0	3.1	0.0	3.1	0.0	0.0	0.0	0.0	0.5	0.5	0.0	0.0
Trichoptera	Hydroptilidae	<i>Leucotrichia</i>	0.0	0.0	0.0	0.0	0.0	1.5	0.0	0.0	0.0	0.0	0.0	0.0	0.0
Trichoptera	Lepidostomatidae	<i>Lepidostoma</i>	0.0	0.0	0.0	0.0	0.0	0.0	13.8	0.0	3.1	2.2	0.5	0.0	0.5
Trichoptera	Lepidostomatidae	<i>Theliopsyche</i>	0.0	0.0	0.0	0.0	0.0	0.0	0.0	0.0	0.0	0.0	0.0	0.0	0.0
Trichoptera	Limnephilidae	<i>Pycnopsyche</i>	0.0	3.1	0.0	1.5	0.0	12.3	0.0	0.0	0.0	4.3	0.5	0.0	0.5
Trichoptera	Odontoceridae	<i>Pseudogoera</i>	0.0	0.0	0.0	0.0	0.0	0.0	0.0	0.0	0.0	0.0	0.0	0.0	0.0
Trichoptera	Odontoceridae	<i>Psilotreta</i>	0.0	0.0	0.0	0.0	0.0	0.0	0.0	3.1	0.0	0.5	0.5	2.3	0.0
Trichoptera	Philopotamidae	<i>Dolophilodes</i>	0.0	1.5	106.1	12.3	502.8	15.4	0.0	1.5	0.0	0.5	3.2	0.6	0.0
Trichoptera	Philopotamidae	<i>Wormaldia</i>	0.0	0.0	0.0	0.0	81.5	0.0	0.0	0.0	0.0	4.3	1.6	0.0	4.8
Trichoptera	Polycentropodidae	<i>Cyrnellus</i>	0.0	0.0	0.0	0.0	0.0	9.2	0.0	0.0	0.0	0.0	0.0	0.0	0.0
Trichoptera	Polycentropodidae	<i>Neureclipsis</i>	0.0	0.0	0.0	0.0	0.0	0.0	0.0	0.0	0.0	0.0	0.5	0.6	0.0
Trichoptera	Polycentropodidae	<i>Polycentropus</i>	8.6	24.6	0.0	4.6	0.0	0.0	1.5	7.7	1.5	0.0	0.0	0.0	0.0
Trichoptera	Psychomyiidae	<i>Lype</i>	0.0	0.0	0.0	0.0	0.0	0.0	0.0	0.0	0.0	1.6	0.0	0.0	0.0
Trichoptera	Rhyacophilidae	<i>Rhyacophila</i>	2.2	96.9	0.0	109.2	192.2	47.7	20.0	16.9	30.8	14.5	11.8	5.7	17.2
Trichoptera	Uenoidae	<i>Neophylax</i>	0.0	0.0	0.0	0.0	0.0	0.0	0.0	0.0	0.0	0.0	0.0	0.6	1.1

Appendix B – Functional trait scores for the southern Blue Ridge Physiographic Province

Table B.1. Functional trait scores for North American benthic macroinvertebrates, modified from Poff et al. (2006), used for analysis in Chapter Two.

Order	Family	Genus	ECOLOGY													LIFE HISTORY					MOBILITY				MORPHOLOGY										
			Functional Feeding					Habit								Rheo	Ther	Desi	Devl	Exit	Life	Sync	Volt	Crwl	Disp	Drft	Flgt	Swim	Armr	Atch	Resp	Shpe	Size		
			CG	CF	SC	Pred	SH	Burrow	Climb	Sprawl	Cling	Swim	Skate																						
Coleoptera	Dryopidae	<i>Helichus</i>	0	0	1	0	0	0	0	0	0	1	0	0	0	1	0.5	0	0.5	0	1	0	0	0	0	0	0	0	0	0	1	0	1	1	0
Coleoptera	Dryopidae	<i>Pelonomus</i>	0	0	1	0	0	0	1	0	0	0	0	0	0	0.5	0.5	0	1	0	1	0	0	0	0	0	0	0	0	0	1	0	1	1	0
Coleoptera	Dytiscidae	<i>Agabus</i>	0	0	0	1	0	0	0	0	0	0	1	0	0	0.5	0.5	0	0.5	1	1	0	0	1	1	0	1	1	1	1	0	1	0	0.5	
Coleoptera	Dytiscidae	<i>Hydroporus</i>	0	0	0	1	0	0	0	0	0	1	0	0	0	0.5	0.5	0	0.5	1	1	0	0	1	1	0	1	1	1	0	1	0	0.5		
Coleoptera	Dytiscidae	<i>Oreodytes</i>	0	0	0	1	0	0	0	0	0	0	1	0	0	0	0.5	0	0.5	1	1	0	0	1	1	0	1	1	1	0	1	0	0.5		
Coleoptera	Elmidae	<i>Elmidae</i>	1	0	0	0	0	0	0	0	0	1	0	0	0	0.5	0.5	1	1	0	1	0	0	0.5	0	0.5	0	0	0.5	0	0	1	0		
Coleoptera	Haliplidae	<i>Brychius</i>	0	0	1	0	0	0	0	0	0	1	0	0	0	1	0	0	0.5	1	1	1	0.5	0.5	0	0	1	0.5	1	0	0.5	1	0		
Coleoptera	Psephenidae	<i>Ectopria</i>	0	0	1	0	0	0	0	0	0	1	0	0	0	1	0.5	0	0.5	0	0.5	1	0	1	0	0	0	0	0	1	0.5	0.5	0	0.5	
Coleoptera	Psephenidae	<i>Psephenus</i>	0	0	1	0	0	0	0	0	0	1	0	0	0	1	0.5	0	0.5	0	0.5	1	0	0	0	0	0	0	0.5	0.5	0.5	0	0.5		
Diptera	Athericidae	<i>Atherix</i>	0	0	0	1	0	0	0	0	0	1	0	0	0	0.5	0.5	0	0.5	0	0	1	0.5	0.5	0	0	0	0	0.5	0	0	1	0.5		
Diptera	Blephariceridae	<i>Agathon</i>	0	0	1	0	0	0	0	0	0	1	0	0	0	0.5	0	0	0.5	0	0	1	0.5	0	0	0	0	0	0	1	0.5	0.5	0	0	
Diptera	Blephariceridae	<i>Bibiocephala</i>	0	0	1	0	0	0	0	0	0	1	0	0	0	1	0	0	0.5	0	0	1	0.5	0	0	0	0	0	1	0.5	0.5	0	0.5		
Diptera	Blephariceridae	<i>Blepharicera</i>	0	0	1	0	0	0	0	0	0	1	0	0	0	1	0	0	0.5	0	0	1	0.5	0	0	0	0	0	1	0.5	0.5	0	0		
Diptera	Blephariceridae	<i>Philorus</i>	0	0	1	0	0	0	0	0	0	1	0	0	0	1	0	0	0.5	0	0	1	0.5	0	0	0	0	0	1	0.5	0.5	0	0		
Diptera	Ceratopogonidae	<i>gen1</i>	0	0	0	1	0	0	0	0	1	0	0	0	0	0.5	0.5	0	0	0	0	0	0.5	0	0	0	0	0	0.5	0	0	1	0		
Diptera	Deuterothlebiidae	<i>Deuterothlebia</i>	0	0	1	0	0	0	0	0	0	1	0	0	0	1	0	0	0.5	0	0	1	0.5	0	0	0	0	1	0.5	0	0	0	0		
Diptera	Empididae	<i>Empididae</i>	0	0	0	1	0	0	0	0	1	0	0	0	0	0.5	0.5	0	0.5	1	0	1	0.5	0.5	0	0	0	0	0	0	0	1	0.5		
Diptera	Psychodidae	<i>Maruina</i>	0	0	1	0	0	0	0	0	0	1	0	0	0	1	0	0	0	0	0	1	0.5	0	0	0	0	0	0.5	0.5	0	0	0		
Diptera	Psychodidae	<i>Pericoma</i>	1	0	0	0	0	1	0	0	0	0	0	0	0	0	0.5	0	0	0	0	0	0.5	0	0	0	0	0	0.5	0	0	1	0		
Diptera	Simuliidae	<i>Simuliidae</i>	0	1	0	0	0	0	0	0	0	1	0	0	0	1	0.5	0	0	0	0	1	1	0.5	0	0.5	1	0	0	0.5	0	1	0		
Diptera	Tipulidae	<i>gen1</i>	0	0	0	0	1	0	0	0	1	0	0	0	0	0.5	0.5	1	0.5	0	0.5	0	0.5	0.5	0	0	0	0	0	0	0.5	1	0.5		
Diptera	Tipulidae	<i>gen2</i>	0	0	0	0	1	1	0	0	0	0	0	0	0	0.5	0.5	1	0.5	0	0.5	0	0.5	0.5	0	0	0	0	0	0.5	1	0.5			
Ephemeroptera	Acanthametropodidae	<i>Acanthametropus</i>	0	0	0	1	0	0	0	0	0	1	0	0	0	0	0	0	0.5	0	0.5	0	0.5	1	0.5	1	0	0	0	0.5	0	0.5	1	0	
Ephemeroptera	Ameletidae	<i>Ameletus</i>	1	0	0	0	0	0	0	0	0	0	1	0	0	0.5	0	0	0	0	0.5	1	0.5	1	0	0	0	1	0	0	0.5	0	0		
Ephemeroptera	Ametropodidae	<i>Ametropus</i>	0	1	0	0	0	1	0	0	0	0	0	0	0	0.5	0	0	0	0	1	0.5	0	0	0.5	0	0	0	0	0	0.5	0	0		
Ephemeroptera	Baetidae	<i>Acentrella</i>	1	0	0	0	0	0	0	0	0	1	0	0	0	0.5	0.5	0	0	0	0	0	1	0	0	0.5	0	1	0	0	0.5	0	0		
Ephemeroptera	Baetidae	<i>Acerpenna</i>	1	0	0	0	0	0	0	0	0	0	1	0	0	0.5	0.5	0	0	0	0	0	1	0	0	1	0	1	0	0	0.5	0	0		
Ephemeroptera	Baetidae	<i>Apobaetis</i>	1	0	0	0	0	0	0	0	0	0	1	0	0	0.5	0.5	0	0	0	0	1	0	0	0	0	1	0	0	0.5	0	0			
Ephemeroptera	Baetidae	<i>Baetis</i>	1	0	0	0	0	0	0	0	0	0	1	0	0	0.5	0.5	0	0	0	0	0	1	0	0	1	0	1	0	0	0.5	0	0		
Ephemeroptera	Baetidae	<i>Callibaetis</i>	1	0	0	0	0	0	0	0	0	0	1	0	0	0	0.5	0	0	0	0	0	1	0.5	0	0	0	1	0	0	0.5	0	0		
Ephemeroptera	Baetidae	<i>Camelobaetidius</i>	1	0	0	0	0	0	0	0	0	0	1	0	0	0	0.5	0	0	0	0	0	1	0.5	0	1	0	1	0	0	0.5	0	0		
Ephemeroptera	Baetidae	<i>Centroptilum/</i>																																	
Ephemeroptera	Baetidae	<i>Proclaoon</i>	1	0	0	0	0	0	0	0	0	0	1	0	0	0.5	0.5	0	0	0	0	0	1	0.5	0	0	0	1	0	0	0.5	0	0		
Ephemeroptera	Baetidae	<i>Cloodes</i>	1	0	0	0	0	0	0	0	0	0	1	0	0	0.5	0.5	0	0	0	0	0	1	0.5	0	0	0	1	0	0	0.5	0	0		
Ephemeroptera	Baetidae	<i>Dipheter</i>	1	0	0	0	0	0	0	0	0	0	1	0	0	0.5	0.5	0	0	0	0	0	1	0.5	0	0	0	1	0	0	0.5	0	0		
Ephemeroptera	Baetidae	<i>Fallceon</i>	1	0	0	0	0	0	0	0	0	0	1	0	0	0.5	0.5	0	0	0	0	0	1	0.5	0	1	0	1	0	0	0.5	0	0		
Ephemeroptera	Baetidae	<i>Heterocloeon</i>	0	0	1	0	0	0	0	0	0	0	1	0	0	1	0.5	0	0	0	0	0	1	0.5	0	0	0	1	0	0	0.5	0	0		
Ephemeroptera	Baetidae	<i>Paracloodes</i>	0	0	1	0	0	0	0	0	0	0	1	0	0	0	1	0	0	0	0	0	1	0.5	0	0	0	1	0	0	0.5	0	0		
Ephemeroptera	Baetidae	<i>Pseudocloeon</i>	1	0	0	0	0	0	0	0	0	0	1	0	0	0.5	0.5	0	0	0	0	0	1	0.5	0	1	0	0.5	0	0	0.5	0	0		
Ephemeroptera	Baetiscidae	<i>Baetisca</i>	1	0	0	0	0	0	0	0	1	0	0	0	0	0	0.5	0	0	0	0	1	0.5	0	0	0	0	0.5	0	0	0.5	1	0.5		
Ephemeroptera	Caenidae	<i>Amercaenis</i>	0	1	0	0	0	0	0	0	0	1	0	0	0	0	0.5	0	0	0	0	1	0.5	0.5	0	0	0	0.5	0	0	0.5	1	0		
Ephemeroptera	Caenidae	<i>Brachycercus</i>	1	0	0	0	0	0	0	0	1	0	0	0	0	0	0.5	0	0.5	0	0	1	0.5	0.5	0	0	0	0.5	0	0	0.5	1	0		
Ephemeroptera	Caenidae	<i>Caenis</i>	1	0	0	0	0	0	0	0	1	0	0	0	0	0	1	0	0.5	0	0	1	1	0.5	0	0	0	0.5	0	0	0.5	1	0		
Ephemeroptera	Ephemerellidae	<i>Attenella</i>	1	0	0	0	0	0	0	0	0	1	0	0	0	1	0.5	0	0.5	0	0	1	0.5	0.5	0	0	0	0.5	0	0	0.5	1	0.5		
Ephemeroptera	Ephemerellidae	<i>Caudatella</i>	1	0	0	0	0	0	0	0	0	1	0	0	0	0.5	0	0	0.5	0	0	1	0.5	0.5	0	0	0	0.5	0	0	0.5	1	0.5		
Ephemeroptera	Ephemerellidae	<i>Caurinella</i>	1	0	0	0	0	0	0	0	0	1	0	0	0	0.5	0	0	0.5	0	0	1	0.5	0.5	0	0	0	0.5	0	0	0.5	1	0.5		
Ephemeroptera	Ephemerellidae	<i>Drunella</i>	0	0	1	0	0	0	0	0	0	0	1	0	0	0	0.5	0.5	0	0.5	0	1	0.5	0.5	0	0	0	0.5	0	0	0.5	1	0.5		
Ephemeroptera	Ephemerellidae	<i>Ephemerella</i>	1	0	0	0	0	0	0	0	0	0	1	0	0	0.5	0.5	0	0.5	0	0	1	0.5	0.5	0	0.5	0	0.5	0	0	0.5	1	0.5		

Ephemeroptera	Ephemerellidae	<i>Eurylophella</i>	1	0	0	0	0	0	0	0	0	0.5	0.5	0	0.5	0	0	1	0.5	0.5	0	0.5	0	0.5	0	0.5	1	0.5		
Ephemeroptera	Ephemerellidae	<i>Serratella</i>	1	0	0	0	0	0	0	1	0	0	0.5	0.5	0	0.5	0	0	1	0.5	0.5	0	0.5	0	0.5	0	0.5	1	0.5	
Ephemeroptera	Ephemerellidae	<i>Timpanoga</i>	1	0	0	0	0	0	0	1	0	0	0.5	0	0	0.5	0	0	1	0.5	0.5	0	0.5	0	0.5	0	0.5	1	0	
Ephemeroptera	Ephemeridae	<i>Ephemerella</i>	1	0	0	0	0	1	0	0	0	0	0	0.5	0	0.5	0	0	0	0	0.5	0	0	0.5	0	0	0.5	1	0.5	
Ephemeroptera	Ephemeridae	<i>Hexagenia</i>	1	0	0	0	0	1	0	0	0	0	0	0.5	0	0.5	0	0	0	0.5	0	0	0.5	0	0	0.5	1	0.5		
Ephemeroptera	Ephemeridae	<i>Litobranchia</i>	1	0	0	0	0	1	0	0	0	0	0	0	0	0.5	0	0	0	0.5	0	0	0.5	0	0	0.5	1	0.5		
Ephemeroptera	Ephemeridae	<i>Pentagenia</i>	1	0	0	0	0	1	0	0	0	0	0	0	1	0	0.5	0	0	0	0.5	0	0	0.5	0	0	0.5	1	0.5	
Ephemeroptera	Heptageniidae	<i>Cinygma</i>	0	0	1	0	0	0	0	0	1	0	0	0.5	0	0	0	0	1	0.5	0.5	0	0.5	0	0.5	0	0.5	0	0.5	
Ephemeroptera	Heptageniidae	<i>Cinygmula</i>	0	0	1	0	0	0	0	0	1	0	0	0.5	0	0	0	0	1	0.5	0.5	0	0.5	0	0.5	0	0	0.5	0	
Ephemeroptera	Heptageniidae	<i>Epeorus</i>	1	0	0	0	0	0	0	0	1	0	0	0.5	0	0	0	0	1	0.5	0.5	0	0	0.5	0	0	0.5	0	0.5	
Ephemeroptera	Heptageniidae	<i>Heptagenia</i>	0	0	1	0	0	0	0	0	1	0	0	0.5	0	0	0	0	1	0.5	0.5	0	0.5	0	0.5	0	0	0.5	0	
Ephemeroptera	Heptageniidae	<i>Ironodes</i>	0	0	1	0	0	0	0	0	1	0	0	0.5	0.5	0	0	0	1	0.5	0.5	0	0.5	0	0.5	0	0	0.5	0	
Ephemeroptera	Heptageniidae	<i>Leucrocota</i>	0	0	1	0	0	0	0	0	1	0	0	0.5	0	0	0	0	1	0.5	0.5	0	0.5	0	0.5	0	0	0.5	0	
Ephemeroptera	Heptageniidae	<i>Macdunnoa</i>	0	0	1	0	0	0	0	0	1	0	0	0.5	0.5	0	0	0	1	0.5	0.5	0	0.5	0	0.5	0	0	0.5	0	
Ephemeroptera	Heptageniidae	<i>Nixe</i>	0	0	1	0	0	0	0	0	1	0	0	0.5	0.5	0	0	0	1	0.5	0.5	0	0.5	0	0.5	0	0	0.5	0	
Ephemeroptera	Heptageniidae	<i>Raptoheptagenia</i>	0	0	0	1	0	0	0	0	0	1	0	0.5	0	0	0	0	1	0.5	0.5	0	0	0.5	0	0	0.5	0	0	
Ephemeroptera	Heptageniidae	<i>Rhithrogena</i>	1	0	0	0	0	0	0	0	1	0	0	0.5	0	0	0	0	1	0.5	0.5	0	0.5	0	0.5	0	0	0.5	0	
Ephemeroptera	Heptageniidae	<i>Stenacron</i>	1	0	0	0	0	0	0	1	0	0	0	0.5	0.5	0	0	0	1	0.5	0.5	0	0.5	0	0.5	0	0	0.5	0	
Ephemeroptera	Heptageniidae	<i>Stenonema</i>	0	0	1	0	0	0	0	0	1	0	0	0.5	0.5	0	0	0	0.5	0.5	0	0.5	0	0.5	0	0	0.5	0	0.5	
Ephemeroptera	Isonychiidae	<i>Isonychia</i>	0	1	0	0	0	0	0	0	1	0	1	0.5	0	0.5	0	0	0.5	1	0	1	0	1	0	0	0.5	0	0.5	
Ephemeroptera	Leptohyphidae	<i>Leptohyphes</i>	1	0	0	0	0	0	0	1	0	0	0	1	0	0	0	0	0.5	0.5	0	0.5	0	0.5	0	0	0.5	1	0	
Ephemeroptera	Leptohyphidae	<i>Tricorythodes</i>	1	0	0	0	0	0	0	1	0	0	0	0.5	0	0	0	0	0.5	0.5	0	1	0	0.5	0	0	0.5	1	0	
Ephemeroptera	Leptophlebiidae	<i>Choroterpes</i>	1	0	0	0	0	0	0	0	1	0	0	0.5	1	0	0	0.5	0	0.5	0.5	0	0.5	0	0.5	0	0	0.5	0	
Ephemeroptera	Leptophlebiidae	<i>Habrophlebia</i>	1	0	0	0	0	0	0	0	1	0	0.5	0	0	0	0	1	0.5	0	0	0.5	0	0.5	0	0	0.5	0	0	
Ephemeroptera	Leptophlebiidae	<i>Habrophlebiodes</i>	0	0	1	0	0	0	0	0	1	0	0.5	0	0	0	0	1	0.5	0	0	0.5	0	0.5	0	0	0.5	0	0	
Ephemeroptera	Leptophlebiidae	<i>Leptophlebia</i>	1	0	0	0	0	0	0	0	1	0	1	0.5	0	0.5	0	0	0.5	0.5	0	0.5	0	0.5	0	0	0.5	0	0	
Ephemeroptera	Leptophlebiidae	<i>Neochoroterpes</i>	1	0	0	0	0	0	0	0	1	0	0.5	1	0	0	0	0	0.5	0.5	0	0.5	0	0.5	0	0	0.5	0	0	
Ephemeroptera	Leptophlebiidae	<i>Paraleptophlebia</i>	1	0	0	0	0	0	0	0	1	0	0.5	0.5	0	0	0	0	0.5	0.5	0	0.5	0	0.5	0	0	0.5	0	0.5	
Ephemeroptera	Leptophlebiidae	<i>Thraulodes</i>	1	0	0	0	0	0	0	0	1	0	0	0.5	1	0	0	0	0	0.5	0.5	0	0.5	0	0.5	0	0	0.5	0	
Ephemeroptera	Leptophlebiidae	<i>Traverella</i>	0	1	0	0	0	0	0	0	1	0	0	0.5	1	0	0	0	0	0.5	0.5	0	0.5	0	0.5	0	0	0.5	0	
Ephemeroptera	Metretopodidae	<i>Siphloplecton</i>	1	0	0	0	0	0	0	0	1	0	0.5	0.5	0	0	0	0	1	0.5	1	0	0	1	0	0	0.5	0	0.5	
Ephemeroptera	Oligoneuridae	<i>Homoeoneuria</i>	0	1	0	0	0	1	0	0	0	0	0	0.5	0	0.5	0	0.5	0	1	0.5	1	0	0	1	0	0	0.5	0	
Ephemeroptera	Polymitarciidae	<i>Ephoron</i>	1	0	0	0	0	1	0	0	0	0	0.5	1	0	0.5	0	0	0.5	0.5	0	0	0.5	0	0	0.5	0	0.5	0	
Ephemeroptera	Polymitarciidae	<i>Tortopus</i>	1	0	0	0	0	1	0	0	0	0	1	0.5	0	0.5	0	0	0.5	0.5	0	0	0.5	0	0	0.5	0	0.5	0	
Ephemeroptera	Potamanthidae	<i>Anthopotamus</i>	0	1	0	0	0	1	0	0	0	0	0	0	0.5	0	0.5	0	0	0.5	0.5	0	0	0.5	0	0	0.5	1	0.5	
Ephemeroptera	Pseudironidae	<i>Pseudiron</i>	0	0	0	1	0	0	0	1	0	0	0	0	1	0	0.5	0	0	1	0.5	0.5	0	0	0.5	0	0	0.5	1	0.5
Ephemeroptera	Siphonuridae	<i>Siphonurus</i>	1	0	0	0	0	0	0	0	1	0	0	0.5	0	0.5	0	0	0	0.5	1	0	0.5	0	1	0	0	0.5	0	
Hemiptera	Belostomatidae	<i>Abedus</i>	0	0	0	1	0	0	1	0	0	0	0	0	1	1	0	1	0.5	1	0.5	1	1	0	1	1	0	1	0	
Hemiptera	Belostomatidae	<i>Belostoma</i>	0	0	0	1	0	0	1	0	0	0	0	0	1	1	0	1	1	0.5	1	1	0	1	1	1	0	1	0	
Hemiptera	Corixidae	<i>Corixidae</i>	0	0	1	0	0	0	0	0	1	0	0	0.5	1	0	1	1	1	1	1	1	0	1	1	1	0	1	0	
Hemiptera	Gerridae	<i>Aquarius</i>	0	0	0	1	0	0	0	0	0	1	0	0.5	1	0	1	1	1	1	1	0	0	0	1	0	0	1	0.5	
Hemiptera	Gerridae	<i>Gerris</i>	0	0	0	1	0	0	0	0	0	1	0	0.5	1	0	1	1	1	1	1	0	0	0	1	0	0	1	0.5	
Hemiptera	Gerridae	<i>Metrobates</i>	0	0	0	1	0	0	0	0	0	0	1	0.5	0.5	1	0	1	1	0.5	1	0	0	0	1	0	0	1	0	
Hemiptera	Gerridae	<i>Rheumatobates</i>	0	0	0	1	0	0	0	0	0	0	1	0	0.5	1	0	1	1	1	0.5	1	0	0	0	1	0	0	1	0
Hemiptera	Gerridae	<i>Trepobates</i>	0	0	0	1	0	0	0	0	0	0	1	0	0.5	1	0	1	1	1	0.5	1	0	0	0	1	0	0	1	0
Hemiptera	Nepidae	<i>Curicta</i>	0	0	0	1	0	0	1	0	0	0	0	0.5	1	0.5	1	1	0	1	1	0	0	0	0	0.5	0	1	1	1
Hemiptera	Nepidae	<i>Nepa</i>	0	0	0	1	0	0	1	0	0	0	0	0.5	1	0.5	1	1	0	1	1	0	0	0	0	0.5	0	1	1	1
Hemiptera	Veliidae	<i>Microvelia</i>	0	0	0	1	0	0	0	0	0	1	0	0.5	1	0	1	1	1	1	1	0	0	0	1	0	0	1	0	
Hemiptera	Veliidae	<i>Rhagovelia</i>	0	0	0	1	0	0	0	0	0	1	0.5	0.5	1	0	1	1	1	1	1	0	0	0	1	0	0	1	0	
Lepidoptera	Pyrallidae	<i>Petrophila</i>	0	0	1	0	0	0	0	0	1	0	0	1	0.5	0	0.5	0	0	1	0.5	0	0	0	0	0.5	0.5	0.5	1	0.5
Megaloptera	Corydalidae	<i>Corydalus</i>	0	0	0	1	0	0	0	0	1	0	0	0.5	0.5	0	0.5	0	0.5	1	0	1	0	0	0	0	0.5	0	0	1
Megaloptera	Corydalidae	<i>Nigronia</i>	0	0	0	1	0	0	0	0	1	0	0	0.5	0.5	0	0.5	0	0.5	1	0	1	0	0	0	0	0.5	0	0	1
Megaloptera	Sialidae	<i>Sialis</i>	0	0	0	1	0	1	0	0	0	0	0	0.5	0.5	0	0.5	0	0.5	1	0.5	1	0	0	0	0	0.5	0	0	1
Neuroptera	Sisyridae	<i>Climacia</i>	0	0	0	1	0	0	1	0	0	0	0	0.5	0.5	0	0.5	0	0.5	1	0.5	1	0	0	0	0	0.5	0	0	1
Neuroptera	Sisyridae	<i>Sisyra</i>	0	0	0	1	0	0	1	0	0	0	0	0.5	0.5	0	0.5	0	0.5	1	0.5	1	0	0	0	0	0.5	0	0	1
Odonata	Aeshnidae	<i>Aeshna</i>	0	0	0	1	0	0	1	0	0	0	0	0.5	0.5	0	0.5	0	1	1	0	1	1	0	1	0.5	0	0.5	1	1
Odonata	Aeshnidae	<i>Basiaeschna</i>	0	0	0	1	0	0	1	0	0	0	0	0	0.5	0	0.5	0	1	1	0	1	1	0	1	1	0.5	0	0.5	1

Odonata	Aeshnidae	<i>Boyeria</i>	0	0	0	1	0	0	0	1	0	0	0	0	0	0.5	0.5	0	0.5	0	1	1	0	1	1	0	1	1	0.5	0	0.5	1	1	
Odonata	Aeshnidae	<i>Epiaeschna</i>	0	0	0	1	0	0	1	0	0	0	0	0	0.5	0.5	0	0.5	0	1	1	0	1	1	0	1	0	1	1	0.5	0	0.5	1	1
Odonata	Aeshnidae	<i>Nasiaeschna</i>	0	0	0	1	0	0	1	0	0	0	0	0	1	0.5	0	0.5	0	1	1	0	1	1	0	1	1	0.5	0	0.5	1	1		
Odonata	Calopterygidae	<i>Calopteryx</i>	0	0	0	1	0	0	1	0	0	0	0	0	0.5	0.5	0	0.5	0	0.5	1	0	1	0	0	1	0.5	0	0	0.5	0	1		
Odonata	Calopterygidae	<i>Hetaerina</i>	0	0	0	1	0	0	1	0	0	0	0	0	0.5	0.5	0	0.5	0	0.5	1	0	1	0	0	1	0.5	0	0	0.5	0	1		
Odonata	Coenagrionidae	<i>Argia</i>	0	0	0	1	0	0	0	0	1	0	0	0	0.5	0.5	0	0.5	0	0.5	1	0.5	1	0	0	0	0.5	0	0	0	0.5	0	0.5	
Odonata	Coenagrionidae	<i>Chromagrion</i>	0	0	0	1	0	0	1	0	0	0	0	0	1	0.5	0	0.5	0	0.5	1	0.5	1	0	0	0	0.5	0	0	0	0.5	0	0.5	
Odonata	Coenagrionidae	<i>Coenagrion</i>	0	0	0	1	0	0	1	0	0	0	0	0	0.5	0.5	0	0.5	0	0.5	1	0.5	1	0	0	0	0.5	0	0	0	0.5	0	0.5	
Odonata	Coenagrionidae	<i>Enallagma</i>	0	0	0	1	0	0	1	0	0	0	0	0	0	0.5	0	0.5	0	0.5	1	0.5	1	0	0	0	0.5	0	0	0	0.5	0	0.5	
Odonata	Coenagrionidae	<i>Hesperagrion</i>	0	0	0	1	0	0	1	0	0	0	0	0	0	0.5	0	0.5	0	0.5	1	0.5	1	0	0	0	0.5	0	0	0	0.5	0	0.5	
Odonata	Coenagrionidae	<i>Ischnura</i>	0	0	0	1	0	0	1	0	0	0	0	0	0	0.5	0	0.5	0	0.5	1	0.5	1	0	0	0	0.5	0	0	0	0.5	0	0.5	
Odonata	Cordulegasteridae	<i>Cordulegaster</i>	0	0	0	1	0	0	1	0	0	0	0	0	0	0.5	0	0.5	0	0.5	1	1	0.5	1	1	0	1	0.5	0.5	0	0.5	1	0.5	
Odonata	Corduliidae	<i>Didymops</i>	0	0	0	1	0	0	0	1	0	0	0	0	0.5	0.5	0	0.5	0	1	1	0	1	1	0	1	0	0.5	0	0.5	1	1		
Odonata	Corduliidae	<i>Epicordulia</i>	0	0	0	1	0	0	0	1	0	0	0	0	0	0.5	0	0.5	0	1	1	0	1	1	0	1	0.5	0.5	0	0.5	1	1		
Odonata	Corduliidae	<i>Epiheca</i>	0	0	0	1	0	0	1	0	0	0	0	0	0	0.5	0	0.5	0	1	1	0	1	1	0	1	0.5	0.5	0	0.5	1	1		
Odonata	Corduliidae	<i>Helocordulia</i>	0	0	0	1	0	0	0	1	0	0	0	0	0	0.5	0	0.5	0	1	1	0	1	1	0	1	0.5	0.5	0	0.5	1	0.5		
Odonata	Corduliidae	<i>Macromia</i>	0	0	0	1	0	0	0	1	0	0	0	0	0.5	0.5	0	0.5	0	1	1	0	1	1	0	1	0	0.5	0	0.5	1	1		
Odonata	Corduliidae	<i>Neurocordulia</i>	0	0	0	1	0	0	1	0	0	0	0	0	0	0.5	0	0.5	0	1	1	0	1	1	0	1	0.5	0.5	0	0.5	1	0.5		
Odonata	Corduliidae	<i>Somatochlora</i>	0	0	0	1	0	0	0	1	0	0	0	0	0	0.5	0	0.5	0	1	1	0	1	1	0	1	0.5	0.5	0	0.5	1	1		
Odonata	Gomphidae	<i>Aphylla</i>	0	0	0	1	0	1	0	0	0	0	0	0	0.5	0.5	0	0.5	0	1	1	0	1	1	0	1	0.5	0.5	0	0.5	1	1		
Odonata	Gomphidae	<i>Arigomphus</i>	0	0	0	1	0	1	0	0	0	0	0	0	0	0.5	0	0.5	0	1	1	0	1	0	0	1	0.5	0.5	0	0.5	1	0.5		
Odonata	Gomphidae	<i>Dromogomphus</i>	0	0	0	1	0	1	0	0	0	0	0	0	0	0.5	0	0.5	0	1	1	0	1	0	0	1	0.5	0.5	0	0.5	1	0.5		
Odonata	Gomphidae	<i>Erpetogomphus</i>	0	0	0	1	0	1	0	0	0	0	0	0	0	0.5	0	0.5	0	1	1	0	1	0	0	1	0.5	0.5	0	0.5	1	1		
Odonata	Gomphidae	<i>Gomphus</i>	0	0	0	1	0	1	0	0	0	0	0	0	0	0.5	0	0.5	0	1	1	0	1	0	0	1	0.5	0.5	0	0.5	1	0.5		
Odonata	Gomphidae	<i>Hagenius</i>	0	0	0	1	0	0	1	0	0	0	0	0	0	0.5	0	0.5	0	1	1	0	1	0	0	1	0.5	0.5	0	0.5	1	0.5		
Odonata	Gomphidae	<i>Lanthus</i>	0	0	0	1	0	1	0	0	0	0	0	0	0	0	0	0.5	0	1	1	0	1	0	0	1	0.5	0.5	0	0.5	1	0.5		
Odonata	Gomphidae	<i>Octogomphus</i>	0	0	0	1	0	1	0	0	0	0	0	0	0	0	0	0.5	0	1	1	0	1	0	0	1	0.5	0.5	0	0.5	1	1		
Odonata	Gomphidae	<i>Ophiogomphus</i>	0	0	0	1	0	1	0	0	0	0	0	0	0	0.5	0	0.5	0	1	1	0	1	0	0	1	0.5	0.5	0	0.5	1	0.5		
Odonata	Gomphidae	<i>Phyllogomphoides</i>	0	0	0	1	0	1	0	0	0	0	0	0	0	0.5	0	0.5	0	1	1	0	1	0	0	1	0.5	0.5	0	0.5	1	1		
Odonata	Gomphidae	<i>Progomphus</i>	0	0	0	1	0	1	0	0	0	0	0	0	0	0.5	0	0.5	0	1	1	0	1	0	0	1	0.5	0.5	0	0.5	1	0.5		
Odonata	Gomphidae	<i>Stylogomphus</i>	0	0	0	1	0	1	0	0	0	0	0	0	0	0.5	0	0.5	0	1	1	0	1	0	0	1	0.5	0.5	0	0.5	1	0.5		
Odonata	Gomphidae	<i>Stylurus</i>	0	0	0	1	0	1	0	0	0	0	0	0	0	0.5	0	0.5	0	1	1	0	1	0	0	1	0.5	0.5	0	0.5	1	0.5		
Odonata	Lestidae	<i>Archilestes</i>	0	0	0	1	0	0	1	0	0	0	0	0	0	0.5	0	0	0	0.5	1	0.5	1	0	0	0	0.5	0	0	0	0	1		
Odonata	Lestidae	<i>Lestes</i>	0	0	0	1	0	0	1	0	0	0	0	0	0	0.5	0	0	0	0.5	1	0.5	1	0	0	0	0.5	0	0	0	0	1		
Plecoptera	Capniidae	<i>Allocapnia</i>	0	0	0	0	1	0	0	0	1	0	0	0	0.5	0.5	1	0	0	0	1	0.5	0.5	0	0.5	0	0.5	0	0	0	1	0		
Plecoptera	Capniidae	<i>Capnia</i>	0	0	0	0	1	0	0	1	0	0	0	0	0.5	0	1	0	0	0	1	0.5	0.5	0	0.5	0	0.5	0	0	0	1	0		
Plecoptera	Capniidae	<i>Capnura</i>	0	0	0	0	1	0	0	1	0	0	0	0	0.5	0.5	1	0	0	0	1	0.5	0.5	0	0	0	0.5	0	0	0	1	0		
Plecoptera	Capniidae	<i>Eucapnopsis</i>	0	0	0	0	1	0	0	1	0	0	0	0	0.5	0	1	0	0	0	1	0.5	0.5	0	0	0	0.5	0	0	0	1	0		
Plecoptera	Capniidae	<i>Isocapnia</i>	0	0	0	0	1	0	0	1	0	0	0	0	1	0	1	0	0	0	1	0.5	0.5	0	0	0	0.5	0	0	0	1	0		
Plecoptera	Capniidae	<i>Mesocapnia</i>	0	0	0	0	1	0	0	1	0	0	0	0	0.5	0.5	1	0	0	0	1	0.5	0.5	0	0	0	0.5	0	0	0	1	0		
Plecoptera	Capniidae	<i>Nemocapnia</i>	0	0	0	0	1	0	0	1	0	0	0	0	0.5	1	1	0	0	0	1	0.5	0.5	0	0	0	0.5	0	0	0	1	0		
Plecoptera	Capniidae	<i>Paracapnia</i>	0	0	0	0	1	0	0	1	0	0	0	0	0.5	0	1	0	0	0	1	0.5	0.5	0	0	0	0.5	0	0	0	1	0		
Plecoptera	Capniidae	<i>Utacapnia</i>	0	0	0	0	1	0	0	1	0	0	0	0	0.5	0	1	0	0	0	1	0.5	0.5	0	0	0	0.5	0	0	0	1	0		
Plecoptera	Chloroperlidae	<i>Alaskaperla</i>	0	0	0	1	0	0	0	0	1	0	0	0	1	0	0	0.5	0	0.5	0	0.5	1	0.5	0.5	0	0	0.5	0	0	1	0.5		
Plecoptera	Chloroperlidae	<i>Alloperla</i>	1	0	0	0	0	0	0	0	1	0	0	0	0.5	0	0	0.5	0	0.5	1	0.5	0.5	0	0.5	0	0.5	0	0	0	1	0.5		
Plecoptera	Chloroperlidae	<i>Bisancora</i>	1	0	0	0	0	0	0	0	1	0	0	0	0.5	0.5	0	0.5	0	0.5	1	0.5	0.5	0	0	0	0.5	0	0	0	1	0		
Plecoptera	Chloroperlidae	<i>Haploperla</i>	0	0	0	1	0	0	0	0	1	0	0	0	0.5	0.5	0	0.5	0	0.5	1	0.5	0.5	0	1	0	0.5	0	0	0	1	0		
Plecoptera	Chloroperlidae	<i>Kathroperla</i>	1	0	0	0	0	0	0	0	1	0	0	0	1	0	0	0.5	0	0.5	0.5	1	0.5	0.5	0	0	0	0.5	0.5	0	0	1	1	
Plecoptera	Chloroperlidae	<i>Paraperla</i>	0	0	0	1	0	0	0	0	1	0	0	0	1	0	0	0.5	0	0.5	1	0.5	0.5	0	0	0	0.5	0.5	0	0	1	0.5		
Plecoptera	Chloroperlidae	<i>Plumiperla</i>	1	0	0	0	0	0	0	0	1	0	0	0	0.5	0	0	0.5	0	0.5	1	0.5	0.5	0	0.5	0	0.5	0	0	0	1	0		
Plecoptera	Chloroperlidae	<i>Suwalia</i>	0	0	0	1	0	0	0	0	1	0	0	0	0.5	0.5	0	0.5	0	0.5	1	0.5	0.5	0	0.5	0	0.5	0	0	0	1	0.5		
Plecoptera	Chloroperlidae	<i>Sweltsa</i>	0	0	0	1	0	0	0	0	1	0	0	0	0.5	0.5	0	0.5	0	0.5	1	0	0.5	0	0.5	0	0.5	0	0	0	1	0.5		
Plecoptera	Chloroperlidae	<i>Triznaka</i>	0	0	0	1	0	0	0	0	1	0	0	0	0.5	0	0	0.5	0	0.5	1	0.5	0.5	0	0.5	0	0.5	0	0	0	1	0.5		
Plecoptera	Chloroperlidae	<i>Utaperla</i>	0	0	0	1	0	0	0	0	1	0	0	0	0.5	0	0	0.5	0	0.5	1	0.5	0.5	0	0	0	0.5	0	0	0	1	0.5		
Plecoptera	Leuctridae	<i>Despaxia</i>	0	0	0	0	1	0	0	1	0																							

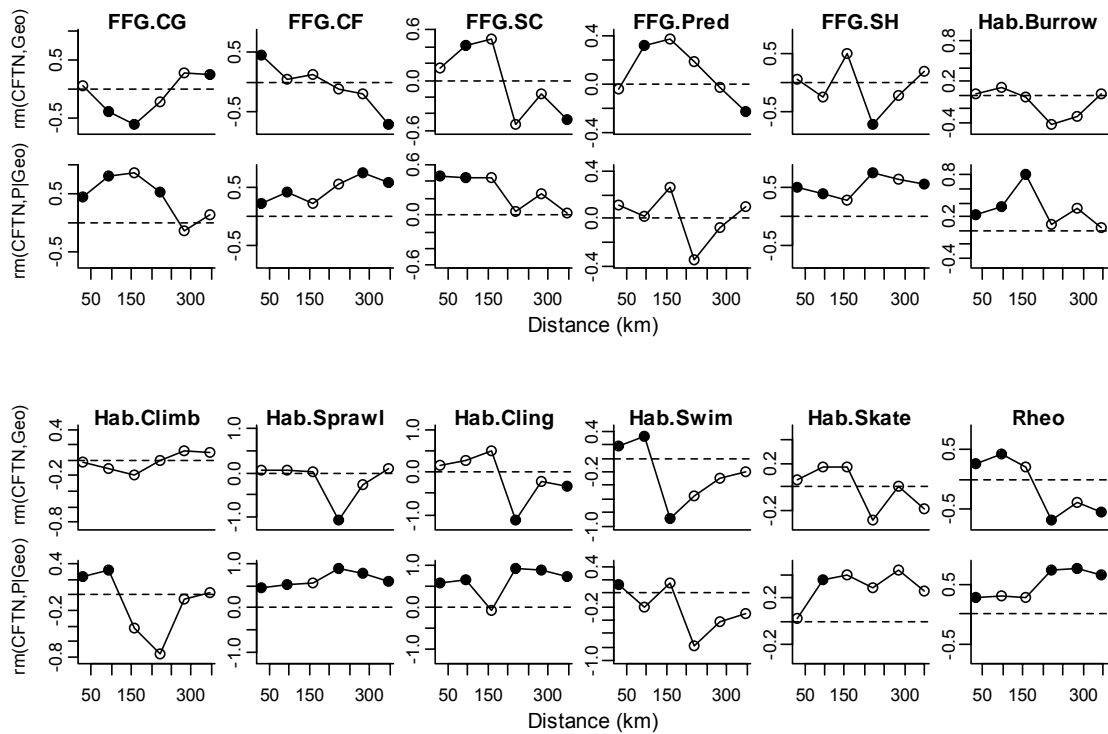
Plecoptera	Leuctridae	<i>Perlomyia</i>	0	0	0	0	1	0	0	1	0	0	0	0	0.5	0	1	0	0	0	1	0.5	0.5	0	0.5	0	0.5	0	0	0	1	0	
Plecoptera	Leuctridae	<i>Zealeuctra</i>	0	0	0	0	1	0	0	1	0	0	0	0	0.5	0	1	0	0	0	1	0.5	0.5	0	0.5	0	0.5	0	0	0	1	0	
Plecoptera	Nemouridae	<i>Amphinemura</i>	0	0	0	0	1	0	0	1	0	0	0	0	0.5	0.5	1	0	0	0	1	0.5	0	0	0.5	0	0.5	0	0	0.5	1	0	
Plecoptera	Nemouridae	<i>Malenka</i>	0	0	0	0	1	0	0	1	0	0	0	0	0.5	0.5	0	0	0	0	1	0.5	0	0	0.5	0	0.5	0	0	0.5	1	0	
Plecoptera	Nemouridae	<i>Nemoura</i>	0	0	0	0	1	0	0	1	0	0	0	0	0.5	0	1	0	0	0	1	0	0	0	0.5	0	0.5	0	0	0	1	0	
Plecoptera	Nemouridae	<i>Paranemoura</i>	0	0	0	0	1	0	0	1	0	0	0	0	0.5	0	0	0	0	0	1	0.5	0	0	0.5	0	0.5	0	0	0	1	0	
Plecoptera	Nemouridae	<i>Podmosta</i>	0	0	0	0	1	0	0	1	0	0	0	0	0.5	0	0	0	0	0	1	0.5	0	0	0	0.5	0	0	0	0	1	0	
Plecoptera	Nemouridae	<i>Prostoia</i>	0	0	0	0	1	0	0	1	0	0	0	0	0.5	0	1	0	0	0	1	0.5	0	0	0.5	0	0.5	0	0	0	1	0	
Plecoptera	Nemouridae	<i>Shipsa</i>	0	0	0	0	1	0	0	1	0	0	0	0	0.5	0.5	1	0	0	0	1	0.5	0	0	0.5	0	0.5	0	0	0	1	0	
Plecoptera	Nemouridae	<i>Soyedina</i>	0	0	0	0	1	0	0	1	0	0	0	0	0.5	0	1	0	0	0	1	0.5	0	0	0	0.5	0	0	0	0	1	0	
Plecoptera	Nemouridae	<i>Visoka</i>	0	0	0	0	1	0	0	1	0	0	0	0	0.5	0	0	0	0	0	1	0.5	0	0	0	0.5	0	0	0	0.5	1	0	
Plecoptera	Nemouridae	<i>Zapada</i>	0	0	0	0	1	0	0	1	0	0	0	0	0.5	0	0	0	0	0	1	0	0	0	0.5	0	0.5	0	0	0.5	1	0	
Plecoptera	Peltoperlidae	<i>Peltoperlidae</i>	0	0	0	0	1	0	0	0	0	0	0	0	0.5	0.5	1	0.5	1	0.5	0	0	1	1	0.5	1	0.5	0.5	0	0.5	1	0.5	
Plecoptera	Perlidae	<i>Acroneuria</i>	0	0	0	1	0	0	0	0	0	1	0	0	1	0.5	0	0.5	0	0.5	0	0.5	1	1	0	1	0.5	0.5	0	0.5	0	1	
Plecoptera	Perlidae	<i>Aagnetina</i>	0	0	0	1	0	0	0	0	0	1	0	0	1	0.5	0	1	0	0.5	0	0	1	1	0	1	0.5	0.5	0	0.5	0	1	
Plecoptera	Perlidae	<i>Attaneuria</i>	0	0	0	1	0	0	0	0	0	1	0	0	1	1	0	1	0	0.5	1	0	1	1	0	1	0.5	0.5	0	0.5	0	1	
Plecoptera	Perlidae	<i>Beloneuria</i>	0	0	0	1	0	0	0	0	0	1	0	0	1	0	0	0.5	0	0.5	1	0	1	1	0	0	0.5	0.5	0	0.5	0	1	
Plecoptera	Perlidae	<i>Calineuria</i>	0	0	0	1	0	0	0	0	0	1	0	0	1	0.5	0	1	0	0.5	0	0	1	1	0	1	0.5	0.5	0	0.5	0	1	
Plecoptera	Perlidae	<i>Claassenia</i>	0	0	0	1	0	0	0	0	0	1	0	0	1	0	0	0.5	0	0.5	0	0	1	1	0	1	0.5	0.5	0	0.5	0	1	
Plecoptera	Perlidae	<i>Doroneuria</i>	0	0	0	1	0	0	0	0	0	1	0	0	1	0	0	0.5	0	0.5	1	0	1	1	0	0	0.5	0.5	0	0.5	0	1	
Plecoptera	Perlidae	<i>Eccoptura</i>	0	0	0	1	0	0	0	0	0	1	0	0	1	0	0	0.5	0	0.5	0	0.5	1	0.5	1	1	0	1	0.5	0.5	0	1	
Plecoptera	Perlidae	<i>Hansonoperla</i>	0	0	0	1	0	0	0	0	0	1	0	0	1	0	1	1	0	0.5	1	0.5	1	0	0	0	0.5	0.5	0	0.5	0	1	
Plecoptera	Perlidae	<i>Hesperoperla</i>	0	0	0	1	0	0	0	0	0	1	0	0	1	0	0	0.5	0	0.5	1	0	1	1	0	1	0.5	0.5	0	0.5	0	1	
Plecoptera	Perlidae	<i>Neoperla</i>	0	0	0	1	0	0	0	0	0	1	0	0	1	0	0	1	0	0.5	0	0.5	1	1	0	1	0.5	0.5	0	0.5	0	0.5	
Plecoptera	Perlidae	<i>Paragnetina</i>	0	0	0	1	0	0	0	0	0	1	0	0	1	0.5	1	0.5	0	0.5	0	0	1	1	0	1	0.5	0.5	0	0.5	0	0.5	
Plecoptera	Perlidae	<i>Perlenta</i>	0	0	0	1	0	0	0	0	0	1	0	0	0.5	0.5	0	0.5	0	0.5	0	0.5	1	1	0	1	0.5	0.5	0	0.5	0	1	
Plecoptera	Perlidae	<i>Perlinella</i>	0	0	0	1	0	0	0	0	0	1	0	0	0.5	0.5	1	0.5	0	0.5	1	0.5	1	1	0	1	0.5	0.5	0	0.5	0	1	
Plecoptera	Perlidae	<i>Calliperla</i>	0	0	0	1	0	0	0	0	0	1	0	0	0.5	0.5	0	0.5	0	0.5	1	0.5	0.5	0	0	0	0.5	0.5	0	0	0	0.5	
Plecoptera	Perlidae	<i>Cascadoperla</i>	0	0	0	1	0	0	0	0	0	1	0	0	1	0.5	0	0.5	0	0.5	1	0.5	0.5	0	0	0	0.5	0.5	0	0	0	0.5	
Plecoptera	Perlidae	<i>Cliperla</i>	0	0	0	1	0	0	0	0	0	1	0	0	0.5	0	0	0.5	0	0.5	1	0.5	0.5	1	0	0	0.5	0.5	0	0	0	0.5	
Plecoptera	Perlidae	<i>Cultus</i>	0	0	0	1	0	0	0	0	0	1	0	0	1	0	0	0.5	0	0.5	1	0.5	1	0	0	0	0.5	0.5	0	0	0	0.5	
Plecoptera	Perlidae	<i>Diploperla</i>	0	0	0	1	0	0	0	0	0	1	0	0	1	0	0	0.5	0	0.5	1	0.5	1	0	0	0	0.5	0.5	0	0	0	0.5	
Plecoptera	Perlidae	<i>Diura</i>	0	0	1	0	0	0	0	0	0	1	0	0	1	0.5	0	0.5	0	0.5	1	0.5	1	0	0	0	0.5	0.5	0	0	0	0.5	
Plecoptera	Perlidae	<i>Frisonia</i>	0	0	0	1	0	0	0	0	0	1	0	0	1	0	0	0.5	0	0.5	1	0.5	1	0	0	0	0.5	0.5	0	0	0	0.5	
Plecoptera	Perlidae	<i>Helopicus</i>	0	0	0	1	0	0	0	0	0	1	0	0	1	0	0	0.5	0	0.5	0	0.5	1	1	0	0	0.5	0.5	0	0	0	1	
Plecoptera	Perlidae	<i>Hydroperla</i>	0	0	0	1	0	0	0	0	0	1	0	0	0.5	0	0	0.5	0	0.5	1	0.5	1	1	0	0	0.5	0.5	0	0	0	1	
Plecoptera	Perlidae	<i>Isogenoides</i>	0	0	0	1	0	0	0	0	0	1	0	0	0.5	0.5	0	0.5	0	0.5	1	0.5	1	1	0	0	0.5	0.5	0	0	0	1	
Plecoptera	Perlidae	<i>Isoperla</i>	0	0	0	1	0	0	0	0	0	1	0	0	0.5	0.5	1	0.5	0	0	1	0.5	1	0	0.5	0	0.5	0.5	0	0	1	0.5	
Plecoptera	Perlidae	<i>Kogotus</i>	0	0	0	1	0	0	0	0	0	1	0	0	1	0	0	0.5	0	0.5	0	0.5	1	0.5	1	0	0	0.5	0.5	0	0	0.5	
Plecoptera	Perlidae	<i>Malirekus</i>	0	0	0	1	0	0	0	0	0	1	0	0	0.5	0	0	0.5	0	0.5	1	0.5	0.5	0	0	0	0.5	0.5	0	0	0	1	
Plecoptera	Perlidae	<i>Megarcys</i>	0	0	0	1	0	0	0	0	0	1	0	0	1	0	0	0.5	0	0.5	0	0.5	1	0.5	0.5	0	0	0.5	0.5	0	0.5	0	1
Plecoptera	Perlidae	<i>Oroperla</i>	0	0	0	1	0	0	0	0	0	1	0	0	1	0	0	0.5	0	0.5	0	0.5	1	0.5	0.5	0	0	0.5	0.5	0	0.5	0	1
Plecoptera	Perlidae	<i>Osobenus</i>	0	0	0	1	0	0	0	0	0	1	0	0	1	0	0	0.5	0	0.5	0	0.5	1	0.5	0.5	0	0	0.5	0.5	0	0	0.5	
Plecoptera	Perlidae	<i>Perlinodes</i>	0	0	0	1	0	0	0	0	0	1	0	0	1	0	0	0.5	0	0.5	0	0.5	1	0.5	0.5	0	0	0.5	0.5	0	0.5	0	1
Plecoptera	Perlidae	<i>Pictetiella</i>	0	0	0	1	0	0	0	0	0	1	0	0	1	0	0	0.5	0	0.5	0	0.5	1	0.5	0.5	0	0	0.5	0.5	0	0	1	
Plecoptera	Perlidae	<i>Remenus</i>	0	0	0	1	0	0	0	0	0	1	0	0	0.5	0	0	0.5	0	0.5	1	0.5	0.5	0	0	0	0.5	0.5	0	0	0	0.5	
Plecoptera	Perlidae	<i>Rickera</i>	0	0	0	1	0	0	0	0	0	1	0	0	0.5	0	1	0.5	0	0.5	1	0.5	0.5	0	0	0	0.5	0.5	0	0	1	0.5	
Plecoptera	Perlidae	<i>Setvena</i>	0	0	0	1	0	0	0	0	0	1	0	0	0.5	0	0	0.5	0	0.5	1	0.5	0.5	0	0	0	0.5	0.5	0	0	0	1	
Plecoptera	Perlidae	<i>Skwala</i>	0	0	0	1	0	0	0	0	0	1	0	0	1	0	0	0.5	0	0.5	0	0.5	1	0.5	0.5	0	0	0.5	0.5	0	0	1	
Plecoptera	Perlidae	<i>Susulus</i>	0	0	0	1	0	0	0	0	0	1	0	0	0.5	0	0	0.5	0	0.5	1	0.5	0.5	0	0	0	0.5	0.5	0	0	0	1	
Plecoptera	Perlidae	<i>Yugus</i>	0	0	0	1	0	0	0	0	0	1	0	0	0.5	0	0	0.5	0	0.5	1	0.5	0.5	0	0	0	0.5	0.5	0	0	0	1	
Plecoptera	Pteronarcyidae	<i>Pteronarcella</i>	0	0	0	0	1	0	0	0	0	1	0	0	0.5	0.5	0	0.5	0	0.5	1	0	0.5	0	0	0	0	0.5	0	0.5	1	0.5	
Plecoptera	Pteronarcyidae	<i>Pteronarcys</i>	0	0	0	0	1	0	0	0	0	1	0	0	0.5	0	0	0.5	0	1	1	0	1	1	0.5	1	0	1	0	0.5	1	1	
Plecoptera	Taeniopterygidae	<i>Bolotoperla</i>	0	0	1	0	0	0	0	0	1	0	0	0	0.5	0.5	1	0	0	0	0	1	0.5	0	0	0	0	0.5	0	0	0	1	0.5
Plecoptera	Taeniopterygidae	<i>Doddsia</i>	0	0	1	0	0	0	0	0	0	1	0	0	0.5	0	1	0															

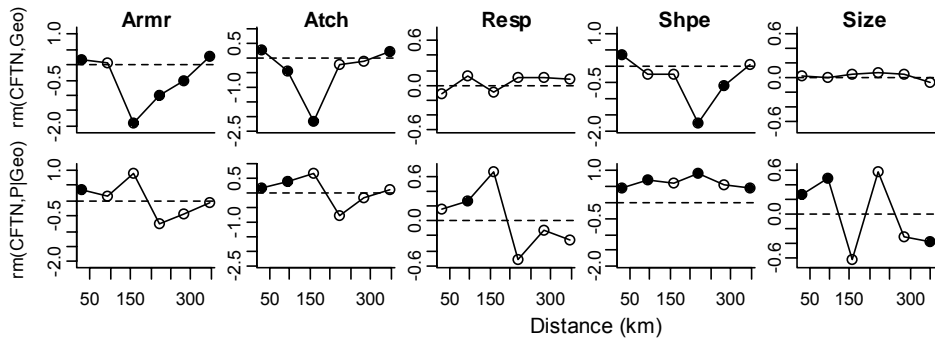
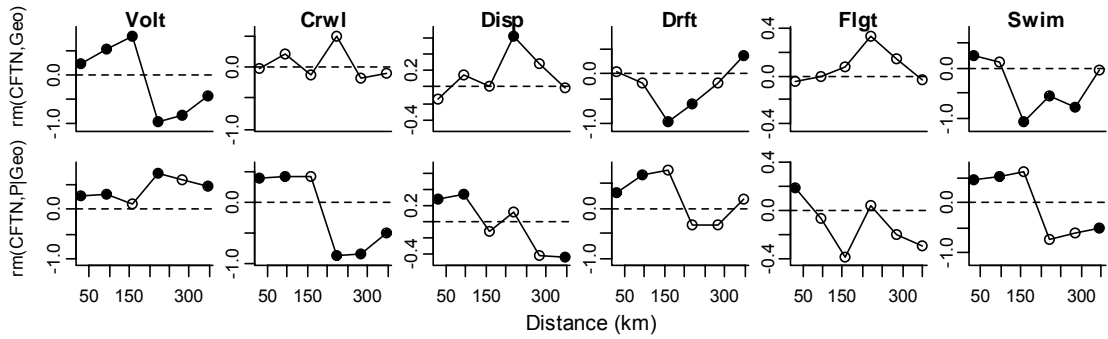
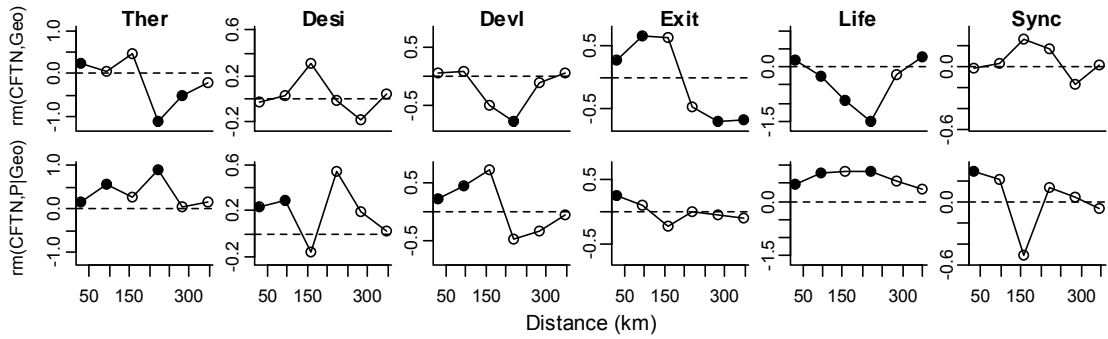
Plecoptera	Taeniopterygidae	<i>Taeniopteryx</i>	0	0	0	0	1	0	0	1	0	0	0.5	0.5	1	0	0	0	1	0.5	0	0	0	0	0.5	0	0	0.5	1	0.5		
Trichoptera	Apataniidae	<i>Allomyia</i>	0	0	1	0	0	0	0	0	1	0	0	1	0	0	0.5	0	0	0	0	0	0	0	0	0	1	0.5	0	1	0.5	
Trichoptera	Apataniidae	<i>Moselyana</i>	1	0	0	0	0	0	0	1	0	0	0	1	0	0	0.5	0	0.5	1	0.5	0.5	0	0	0	0	1	0.5	0	1	0.5	
Trichoptera	Apataniidae	<i>Pedomoecus</i>	0	0	1	0	0	0	0	0	1	0	0	1	0	0	0.5	0	0.5	1	0.5	0.5	0	0	0	0	1	0.5	0.5	1	0.5	
Trichoptera	Brachycentridae	<i>Adicrophleps</i>	0	0	0	0	1	0	0	0	0	1	0	0	1	0	0	0.5	0	0.5	1	0.5	0	0	0	0	1	1	0	1	0.5	
Trichoptera	Brachycentridae	<i>Amiocentrus</i>	1	0	0	0	0	0	0	0	1	0	0	1	0	0	0	0.5	0	0.5	1	0.5	0	0	0	0	1	1	0.5	1	0.5	
Trichoptera	Brachycentridae	<i>Brachycentrus</i>	0	1	0	0	0	0	0	0	1	0	0	1	0.5	0	0.5	0	0.5	1	0.5	0	0	0	0	0	1	1	0.5	1	0.5	
Trichoptera	Brachycentridae	<i>Micrasema</i>	0	0	1	0	0	0	0	0	1	0	0	1	0.5	0	0.5	0	0.5	1	0.5	0	0	0	0	0	1	1	0.5	1	0	
Trichoptera	Calamoceratidae	<i>Heteroplectron</i>	0	0	0	0	1	0	0	0	1	0	0	0	0.5	0	0	0.5	0	0.5	1	0.5	0	0	0	0	1	0.5	0.5	1	0.5	
Trichoptera	Calamoceratidae	<i>Phylloicus</i>	0	0	0	0	1	0	0	0	1	0	0	0	0.5	0	0	0.5	0	0.5	1	0.5	0	0	0	0	0.5	0.5	0.5	1	0.5	
Trichoptera	Glossosomatidae	<i>Agapetus</i>	0	0	1	0	0	0	0	0	1	0	0	1	0	1	0.5	0	0.5	1	0.5	0.5	0	0	0	0	1	0	0	1	0	
Trichoptera	Glossosomatidae	<i>Anagapetus</i>	0	0	1	0	0	0	0	0	1	0	0	1	0	1	0	0	0.5	0	0.5	1	0.5	0.5	0	0	0	1	0	0	1	0
Trichoptera	Glossosomatidae	<i>Culoptila</i>	0	0	1	0	0	0	0	0	1	0	0	1	0	1	0	0	0.5	0	0.5	1	0.5	0.5	0	0	0	1	0	0	1	0
Trichoptera	Glossosomatidae	<i>Glossosoma</i>	0	0	1	0	0	0	0	0	1	0	0	1	0.5	0	0.5	0	0.5	1	0.5	0.5	0	0	0	0	1	0	0	1	0	
Trichoptera	Glossosomatidae	<i>Matrioptila</i>	0	0	1	0	0	0	0	0	1	0	0	1	0.5	0	0.5	0	0.5	1	0.5	0.5	0	0	0	0	1	0	0	1	0	
Trichoptera	Glossosomatidae	<i>Protoptila</i>	0	0	1	0	0	0	0	0	1	0	0	1	0	1	0	0	0.5	0	0.5	1	0.5	0.5	0	0	0	1	0	0	1	0
Trichoptera	Goeridae	<i>Goera</i>	0	0	1	0	0	0	0	0	1	0	0	1	0	0	0.5	0	0.5	1	0.5	0	0	0	0	0	1	0	0.5	1	0.5	
Trichoptera	Goeridae	<i>Goeracea</i>	0	0	1	0	0	0	0	0	1	0	0	1	0	1	0	0	0.5	0	0.5	1	0.5	0	0	0	0	1	0	0	1	0.5
Trichoptera	Helicopsychidae	<i>Helicopsyche</i>	0	0	1	0	0	0	0	0	1	0	0	1	0.5	1	0.5	0	0.5	1	0.5	0.5	1	0	0	0	1	0.5	0.5	1	0	
Trichoptera	Hydropsychidae	<i>Arctopsyche</i>	0	1	0	0	0	0	0	0	1	0	0	1	0	0	0.5	0	0.5	1	0.5	0.5	0	0	0	0	0	0.5	0.5	1	0.5	
Trichoptera	Hydropsychidae	<i>Ceratopsyche</i>	0	1	0	0	0	0	0	0	1	0	0	1	0.5	0	0.5	1	0.5	1	0.5	0.5	1	0.5	1	0	0	0.5	0.5	1	0.5	
Trichoptera	Hydropsychidae	<i>Cheumatopsyche</i>	0	1	0	0	0	0	0	0	1	0	0	1	0.5	0	0.5	0	0.5	1	0.5	0.5	1	0.5	1	0	0	0.5	0.5	1	0.5	
Trichoptera	Hydropsychidae	<i>Dipletrona</i>	0	1	0	0	0	0	0	0	1	0	0	1	0	1	0	0	0.5	0	0.5	1	0.5	0.5	0	0	0	0	0.5	0.5	1	0.5
Trichoptera	Hydropsychidae	<i>Homoptera</i>	0	1	0	0	0	0	0	0	1	0	0	1	0	1	0	0	0.5	0	0.5	1	0.5	0.5	0	0	0	0	0.5	0.5	1	0.5
Trichoptera	Hydropsychidae	<i>Hydropsyche</i>	0	1	0	0	0	0	0	0	1	0	0	1	0.5	0	0.5	1	0.5	1	0.5	0.5	1	0.5	1	0	0	0.5	0.5	1	0.5	
Trichoptera	Hydropsychidae	<i>Macrostemum</i>	0	1	0	0	0	0	0	0	1	0	0	1	1	0	0.5	0	0.5	1	0.5	0.5	1	0.5	1	0	0	0.5	0.5	1	0.5	
Trichoptera	Hydropsychidae	<i>Oropsyche</i>	0	1	0	0	0	0	0	0	1	0	0	1	0	1	0	0	0.5	0	0.5	1	0.5	0.5	0	0	0	0	0.5	0.5	1	0.5
Trichoptera	Hydropsychidae	<i>Parapsyche</i>	0	1	0	0	0	0	0	0	1	0	0	1	0	1	0	0	0.5	0	0.5	1	0.5	0.5	0	0	0	0	0.5	0.5	1	0.5
Trichoptera	Hydropsychidae	<i>Potamya</i>	0	1	0	0	0	0	0	0	1	0	0	1	0.5	0	0.5	0	0.5	1	0.5	0.5	1	0.5	1	0	0	0.5	0.5	1	0.5	
Trichoptera	Hydropsychidae	<i>Smicridea</i>	0	1	0	0	0	0	0	0	1	0	0	1	1	0	0.5	0	0.5	1	0.5	0.5	1	0.5	1	0	0	0.5	0.5	1	0.5	
Trichoptera	Hydroptilidae	<i>Agraylea</i>	0	0	1	0	0	0	0	1	0	0	0	0	0.5	0.5	0	0.5	0	0	1	0.5	0	1	0	0	0	0.5	0.5	0	0	0
Trichoptera	Hydroptilidae	<i>Alisotrichia</i>	0	0	1	0	0	0	0	0	1	0	0	0	0.5	0.5	0	0.5	0	0	1	0.5	0	1	0	0	0	0.5	0.5	0	0	0
Trichoptera	Hydroptilidae	<i>Dibusa</i>	0	0	1	0	0	0	0	0	1	0	0	0	0.5	0.5	0	0.5	0	0	1	0.5	0	1	0	0	0	0.5	0.5	0	0	0
Trichoptera	Hydroptilidae	<i>Hydroptila</i>	0	0	1	0	0	0	0	0	1	0	0	0	0.5	0.5	0	0.5	0	0	1	0.5	0	1	0.5	0	0	0.5	0.5	0.5	0	0
Trichoptera	Hydroptilidae	<i>Ithytrichia</i>	0	0	1	0	0	0	0	0	1	0	0	1	0.5	0	0.5	0	0	1	0.5	0	1	0	0	0	0	0.5	0.5	0	0	0
Trichoptera	Hydroptilidae	<i>Leucotrichia</i>	0	0	1	0	0	0	0	0	1	0	0	1	0.5	0	0.5	0	0	1	0.5	0	1	0	0	0	0	0.5	0.5	0	0	0
Trichoptera	Hydroptilidae	<i>Mayatrichia</i>	0	0	1	0	0	0	0	0	1	0	0	1	1	0	0.5	0	0	1	0.5	0	1	0.5	0	0	0	0.5	0.5	0	0	0
Trichoptera	Hydroptilidae	<i>Neotrichia</i>	0	0	1	0	0	0	0	0	1	0	0	1	0.5	0	0.5	0	0	1	0.5	0	1	0	0	0	0	0.5	0.5	0	0	0
Trichoptera	Hydroptilidae	<i>Ochrotrichia</i>	1	0	0	0	0	0	0	0	1	0	0	0	0.5	0.5	0	0.5	0	0	1	0.5	0	1	0	0	0	0.5	0.5	0	0	0
Trichoptera	Hydroptilidae	<i>Orthotrichia</i>	0	0	1	0	0	0	0	0	1	0	0	0	0.5	0.5	0	0.5	0	0	1	0.5	0	1	0	0	0	0.5	0.5	0	0	0
Trichoptera	Hydroptilidae	<i>Oxyethira</i>	0	0	1	0	0	0	0	1	0	0	0	0	0.5	0.5	0	0.5	0	0	1	0.5	0	1	0	0	0	0.5	0.5	0	0	0
Trichoptera	Hydroptilidae	<i>Paucicalcaria</i>	0	0	1	0	0	0	0	0	0	1	0	0	0.5	0.5	0	0.5	0	0	1	0.5	0	1	0	0	0	0.5	0.5	0.5	0	0
Trichoptera	Hydroptilidae	<i>Stactobiella</i>	0	0	0	0	1	0	0	0	1	0	0	0	0.5	0.5	0	0.5	0	0	1	0.5	0	1	0	0	0	0.5	0.5	0	0	0
Trichoptera	Hydroptilidae	<i>Zumatrichia</i>	0	0	1	0	0	0	0	0	1	0	0	0	0.5	0.5	0	0.5	0	0	1	0.5	0	1	0	0	0	0.5	0.5	0	0	0
Trichoptera	Lepidostomatidae	<i>Lepidostoma</i>	0	0	0	0	1	0	1	0	0	0	0	0	0.5	0	0	0.5	0	0.5	1	0.5	0	0	0	0	0	0	0	0.5	1	0.5
Trichoptera	Lepidostomatidae	<i>Theliopsyche</i>	0	0	0	0	1	0	1	0	0	0	0	0	1	0	0	0.5	0	0.5	1	0.5	0	0	0	0	0	0	0	0.5	1	0
Trichoptera	Leptoceridae	<i>Ceraclia</i>	1	0	0	0	0	0	0	1	0	0	0	0	0.5	0.5	0	0.5	0	0.5	1	0.5	0	1	0	0	0.5	0.5	0.5	0.5	1	0.5
Trichoptera	Leptoceridae	<i>Nectopsyche</i>	0	0	1	0	0	0	0	1	0	0	0	0	0.5	0.5	0	0.5	0	0.5	1	0.5	0	1	0	0	0.5	0.5	0.5	0.5	1	0.5
Trichoptera	Leptoceridae	<i>Oecetis</i>	0	0	0	1	0	0	0	0	1	0	0	0	0.5	0.5	0	0.5	0	0.5	1	0.5	0	1	0	0	0.5	0.5	0.5	0.5	1	0.5
Trichoptera	Leptoceridae	<i>Setodes</i>	1	0	0	0	0	0	0	1	0	0	0	0	0.5	0	0	0.5	0	0.5	1	0.5	0	1	0	0	0.5	0.5	0.5	0.5	1	0
Trichoptera	Limnephilidae	<i>Allocosmoecus</i>	0	0	1	0	0	0	0	0	1	0	0	0	0.5	0	0	0.5	0	0.5	1	0.5	0.5	0	0	0	0	1	0.5	0.5	1	1
Trichoptera	Limnephilidae	<i>Amphicosmoecus</i>	0	0	0	0	1	0	0	1	0	0	0	0	0.5	0	0	0.5	0	0.5	1	0.5	0.5	0	0	0	0	1	0.5	0.5	1	1
Trichoptera	Limnephilidae	<i>Apatania</i>	0	0	1	0	0	0	0	0	1	0	0	0	1	0	0	0.5	0	0.5	1	0.5	0.5	0	0	0	0	1	0.5	0.5	1	0.5
Trichoptera	Limnephilidae	<i>Asynarchus</i>	0	0	0	0	1	0	1	0	0	0	0	0	0.5	0	1	0.5	0	0	1	0.5	0	0	0	0	0	0.5	0.5	0.5	1	0.5
Trichoptera	Limnephilidae	<i>Chyranda</i>	0	0	0	0	1	0																								

Trichoptera	Limnephilidae	<i>Ecclisomyia</i>	1	0	0	0	0	0	0	0	1	0	0	0	0.5	0	0.5	1	0	0.5	0	0	0	0	1	0.5	0.5	1	0.5		
Trichoptera	Limnephilidae	<i>Eocosmoecus</i>	0	0	0	0	1	0	0	1	0	0	0	0.5	0	0	0.5	0	0.5	1	0	0.5	0	0	0	1	0.5	0.5	1	0.5	
Trichoptera	Limnephilidae	<i>Hesperophylax</i>	0	0	0	0	1	0	0	1	0	0	0	0.5	0.5	0	0.5	0	0.5	1	0.5	0.5	0	0	0	1	0.5	0.5	1	1	
Trichoptera	Limnephilidae	<i>Homophylax</i>	0	0	0	0	1	0	0	0	1	0	0	0.5	0	0	0.5	0	0.5	1	0.5	0.5	0	0	0	1	0.5	0.5	1	1	
Trichoptera	Limnephilidae	<i>Hydatophylax</i>	0	0	0	0	1	0	0	1	0	0	0	0	0.5	0	0.5	0	0.5	1	0.5	0.5	0	0	0	1	0.5	0.5	1	1	
Trichoptera	Limnephilidae	<i>Onocosmoecus</i>	0	0	0	0	1	0	0	1	0	0	0	0	0	0	0.5	0	0.5	1	0.5	0.5	0	0	0	1	0.5	0.5	1	1	
Trichoptera	Limnephilidae	<i>Philocasca</i>	0	0	0	0	1	0	0	0	1	0	0	0.5	0	0	0.5	0	0.5	1	0.5	0.5	0	0	0	1	0.5	0.5	1	0.5	
Trichoptera	Limnephilidae	<i>Platycentropus</i>	0	0	0	0	1	0	1	0	0	0	0	0	0.5	0	0.5	0	0.5	1	0.5	0.5	0	0	0	1	0.5	0.5	1	1	
Trichoptera	Limnephilidae	<i>Pseudostenophylax</i>	0	0	0	0	1	0	0	1	0	0	0	0.5	0.5	0	0.5	0	0.5	1	0.5	0.5	0	0	0	1	0.5	0.5	1	1	
Trichoptera	Limnephilidae	<i>Psychoglypha</i>	1	0	0	0	0	0	0	1	0	0	0	1	0	0	0.5	0	1	1	0.5	0.5	0	0	0	1	0.5	0.5	1	1	
Trichoptera	Limnephilidae	<i>Psychoronia</i>	0	0	0	0	1	0	0	1	0	0	0	0.5	0	0	0.5	0	0.5	1	0.5	0.5	0	0	0	1	0.5	0.5	1	0.5	
Trichoptera	Limnephilidae	<i>Pycnopsyche</i>	0	0	0	0	1	0	0	1	0	0	0	0.5	0	0	0.5	0	0.5	1	0.5	0.5	0	0	0	1	0.5	0.5	1	1	
Trichoptera	Odontoceridae	<i>Pseudogoera</i>	0	0	0	1	0	0	0	1	0	0	0	0.5	0	0	0.5	0	0.5	1	0.5	0	0	0	0	1	0.5	0.5	1	0.5	
Trichoptera	Odontoceridae	<i>Psilotreta</i>	0	0	1	0	0	0	0	1	0	0	0	0.5	1	0	0.5	0	0.5	1	0.5	0	0	0	0	1	0.5	0.5	1	0.5	
Trichoptera	Philopotamidae	<i>Chimarra</i>	0	1	0	0	0	0	0	0	1	0	0	1	0.5	0	0.5	0	0.5	1	0.5	0	0	0	0	0	0.5	0	1	0	
Trichoptera	Philopotamidae	<i>Dolophilodes</i>	0	1	0	0	0	0	0	0	1	0	0	1	0.5	0	0.5	0	0.5	1	0.5	0	0	0	0	0	0.5	0	1	0	
Trichoptera	Philopotamidae	<i>Wormaldia</i>	0	1	0	0	0	0	0	0	1	0	0	1	0.5	0	0.5	0	0.5	1	0.5	0	0	0	0	0	0.5	0	1	0	
Trichoptera	Polycentropodidae	<i>Cyrnellus</i>	0	1	0	0	0	0	0	0	1	0	0	1	0.5	0	0.5	0	0.5	1	0.5	0	1	0	0	0	0.5	0	1	0.5	
Trichoptera	Polycentropodidae	<i>Neureclipsis</i>	0	1	0	0	0	0	0	0	1	0	0	1	0.5	0	0.5	0	0.5	1	1	0	1	0	0	0	0.5	0	1	0.5	
Trichoptera	Polycentropodidae	<i>Nyctiophylax</i>	0	0	0	1	0	0	0	0	1	0	0	0.5	0.5	0	0.5	0	0.5	1	0.5	0	1	0	0	0	0.5	0	1	0.5	
Trichoptera	Polycentropodidae	<i>Polycentropus</i>	0	0	0	1	0	0	0	0	1	0	0	1	0.5	0	0.5	0	0.5	1	0.5	0	1	0	0	0	0.5	0	1	0.5	
Trichoptera	Psychomyiidae	<i>Lype</i>	0	0	1	0	0	0	0	0	1	0	0	1	0.5	0	0.5	0	0.5	1	0.5	0	0	0	0	0	0.5	0	1	0	
Trichoptera	Psychomyiidae	<i>Psychomyia</i>	1	0	0	0	0	0	0	0	1	0	0	1	0.5	0	0.5	0	0.5	1	0.5	0	1	0	0	0	0.5	0	1	0	
Trichoptera	Rhyacophilidae	<i>Rhyacophila</i>	0	0	0	1	0	0	0	0	1	0	0	1	0.5	0	0.5	0	0.5	1	0.5	1	0	0	0	0.5	0.5	0.5	0	1	0.5
Trichoptera	Rossianidae	<i>Rossiana</i>	0	0	1	0	0	0	0	0	1	0	0	1	0	0	0.5	0	0.5	1	0.5	0.5	0	0	0	0.5	1	1	0.5	1	0.5
Trichoptera	Sericostomatidae	<i>Gumaga</i>	0	0	0	0	1	0	0	1	0	0	0	1	0	0	0.5	0	0.5	1	0.5	0.5	0	0	0	0	0.5	0.5	0.5	1	0.5
Trichoptera	Uenoidae	<i>Farula</i>	0	0	1	0	0	0	0	0	1	0	0	1	0	0	0.5	0	0.5	1	0.5	0	0	0	0	0.5	0.5	0.5	1	0	
Trichoptera	Uenoidae	<i>Neophylax</i>	0	0	1	0	0	0	0	0	1	0	0	1	0.5	0	0.5	0	0.5	1	0.5	0	0	0	0	0.5	1	0.5	0.5	1	0.5
Trichoptera	Uenoidae	<i>Neothremma</i>	0	0	1	0	0	0	0	0	1	0	0	1	0	0	0.5	0	0.5	1	0.5	0	0	0	0	0.5	0.5	0.5	1	0	
Trichoptera	Uenoidae	<i>Oligophlebodes</i>	0	0	1	0	0	0	0	0	1	0	0	1	0	0	0.5	0	0.5	1	0.5	0	0	0	0	0.5	1	0.5	0.5	1	0.5

Appendix C – Functional trait correlograms

Each plot is a correlogram of a mantel statistic (correlation of distances matrices) for successively larger spatial lags. The top plots in each row of paired (stacked) plots show similarity among watersheds in terms of functional trait composition ($r_m[\text{CFTN,Geo}]$). The bottom plots show mantel correlations between functional and taxonomic composition for subsets (defined by spatial lag classes) of watershed by watershed comparisons at different spatial lags ($r_m[\text{CFTN, P} | \text{Geo}]$). Solid points indicate statistically significant mantel correlations. Positive values mean functionally similar taxa tend to co-occur at those spatial lags, and negative values indicate taxonomic turnover within a functional niche occurs at that spatial lag.





Appendix D – Trait-neutral model fits: observed versus predicted community composition

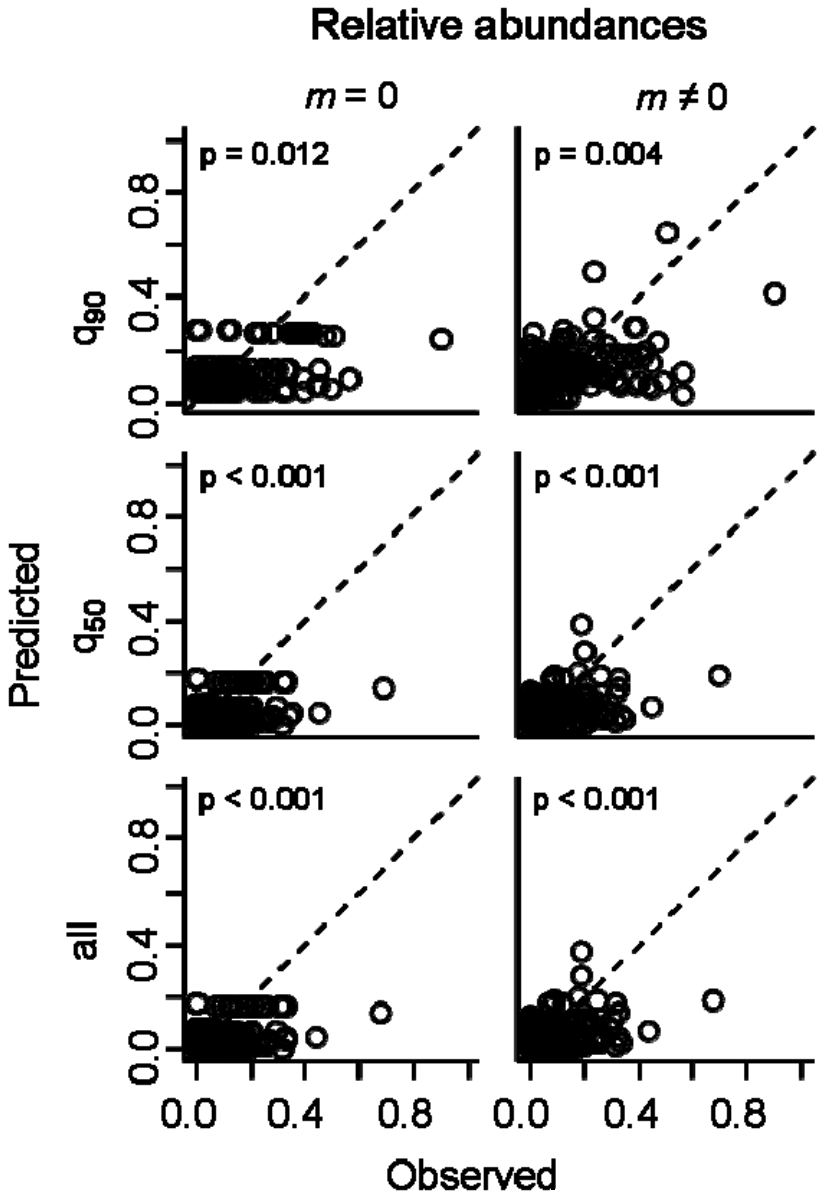


Figure D.1. Predicted relative abundances plotted against observed relative abundances for all taxa at all OUs. Column 1 ($m = 0$) are plots for estimates calculated with $f(P_{obs}, D_{geo}, m = 0)$ and column 2 ($m \neq 0$) are plots for estimates calculated with $f(P_{obs}, D_{geo}, m \neq 0)$. Row labels indicate the subset of taxa used to calculate the values (90th percentile taxa [q_{90}], 50th percentile taxa [q_{50}], all taxa [all]) p-values are goodness of fit values calculated from all predicted and observed values using a wilcox signed-rank test, 1:1 lines are plotted for reference.

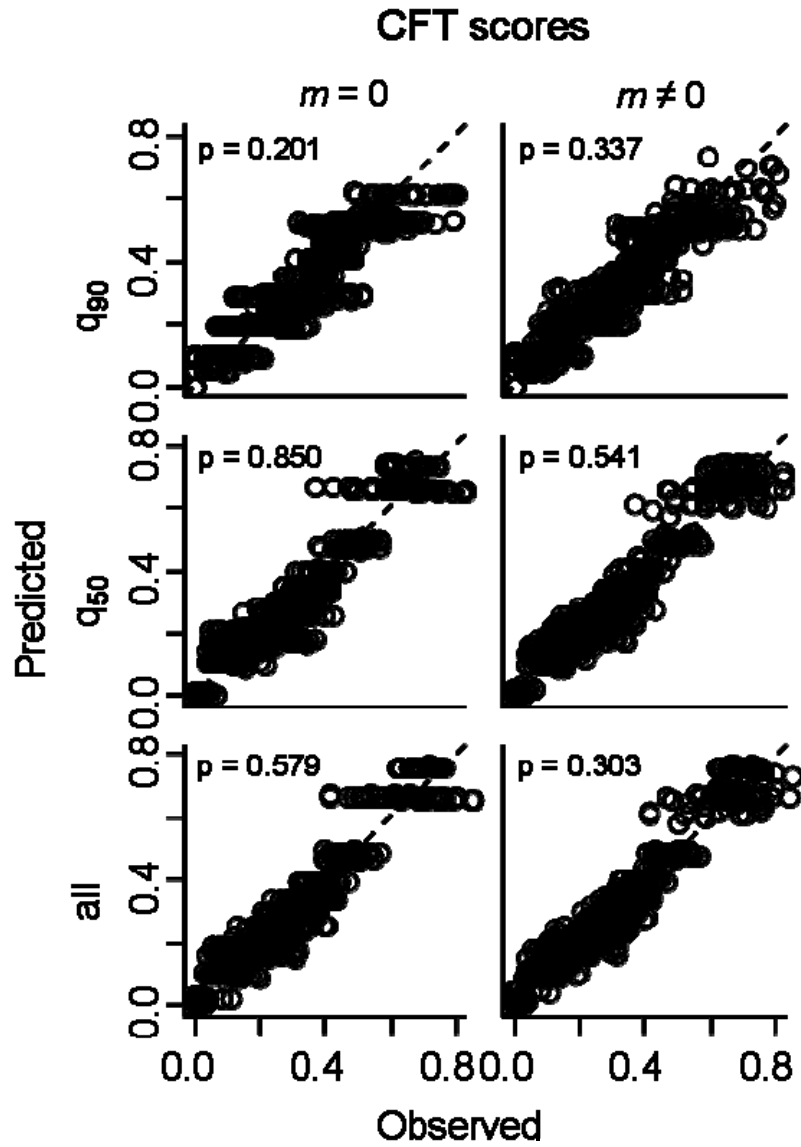


Figure D.2. Predicted CFT (community-aggregate functional trait) scores plotted against CFT scores calculated from observed data. See Figure 6 for label and p-value descriptions.

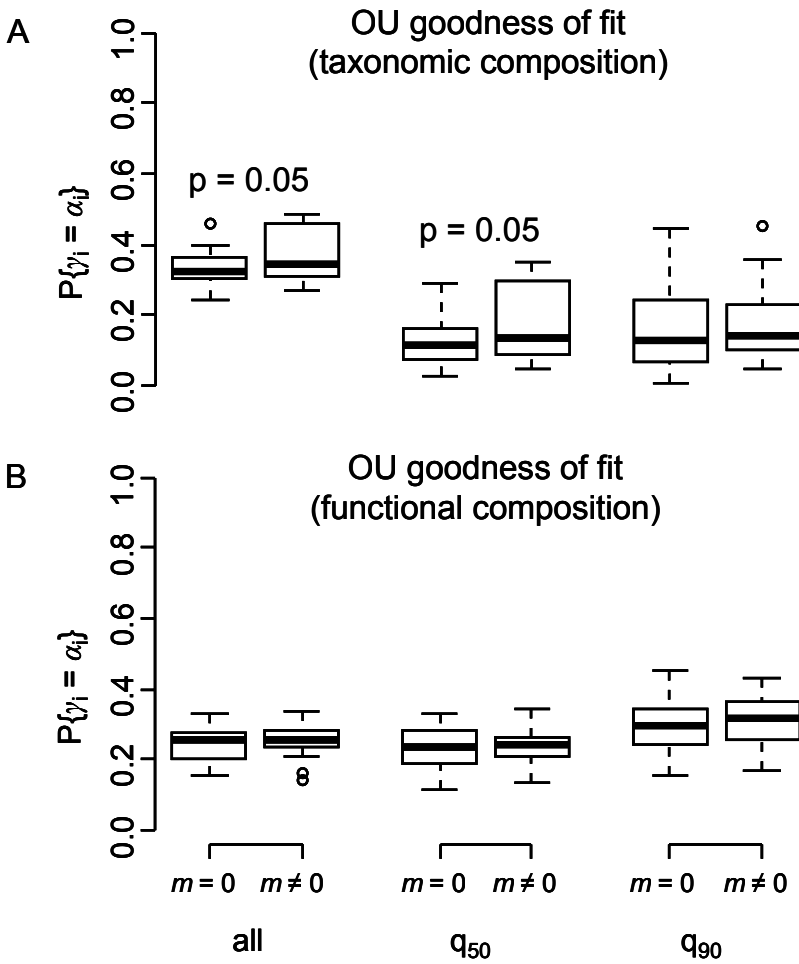


Figure D. 3. Distribution of OU goodness of fit values ($P\{\gamma_i = \alpha_i\}$) for (A) taxonomic composition and (B) functional composition predicted by $f(P_{\text{obs}}, D_{\text{geo}}, m = 0)$ and $f(P_{\text{obs}}, D_{\text{geo}}, m \neq 0)$ for all observed taxa (all), 50th percentile taxa (q_{50}), and 90th percentile taxa (q_{90}). Distributions of $P\{\gamma_i = \alpha_i\}$ values for $f(P_{\text{obs}}, D_{\text{geo}}, m = 0)$ and $f(P_{\text{obs}}, D_{\text{geo}}, m \neq 0)$ were compared with a t-test for each data subset, p-values ≤ 0.05 are listed.

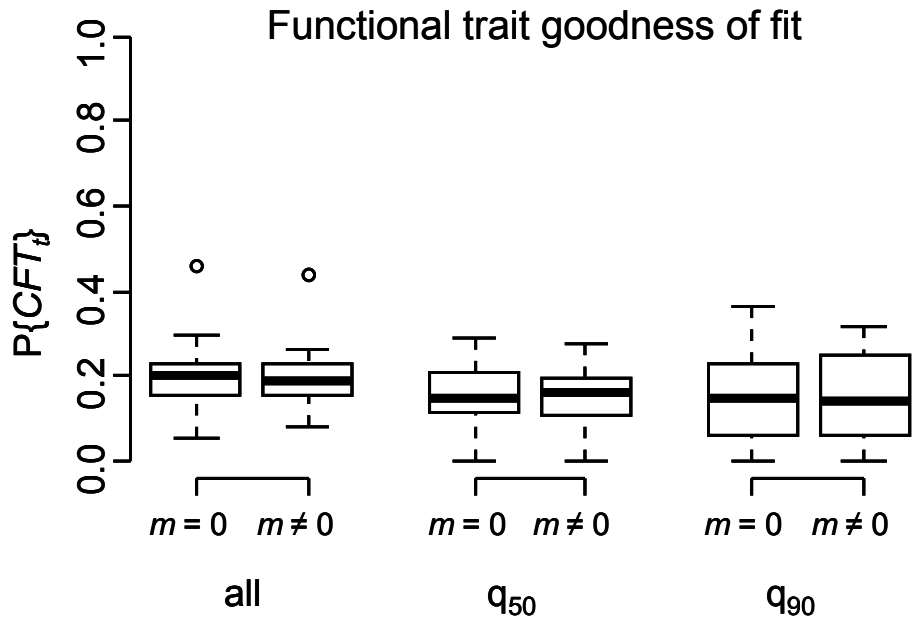


Figure D.4. Distribution of goodness of fit values ($P\{CFT_{ij}\}$) for traits predicted by $f(P_{\text{obs}}, D_{\text{geo}}, m = 0)$ and $f(P_{\text{obs}}, D_{\text{geo}}, m \neq 0)$ for all observed taxa (all), 50th percentile taxa (q_{50}), and 90th percentile taxa (q_{90}). Distributions of $P\{\gamma_i = \alpha_i\}$ values for $f(P_{\text{obs}}, D_{\text{geo}}, m \neq 0)$ and $f(P_{\text{obs}}, D_{\text{geo}}, m = 0)$ were compared with a t-test for each data subset, no comparisons resulted in p-values ≤ 0.05 .

Appendix E – Functional trait scores for Ray Branch sites

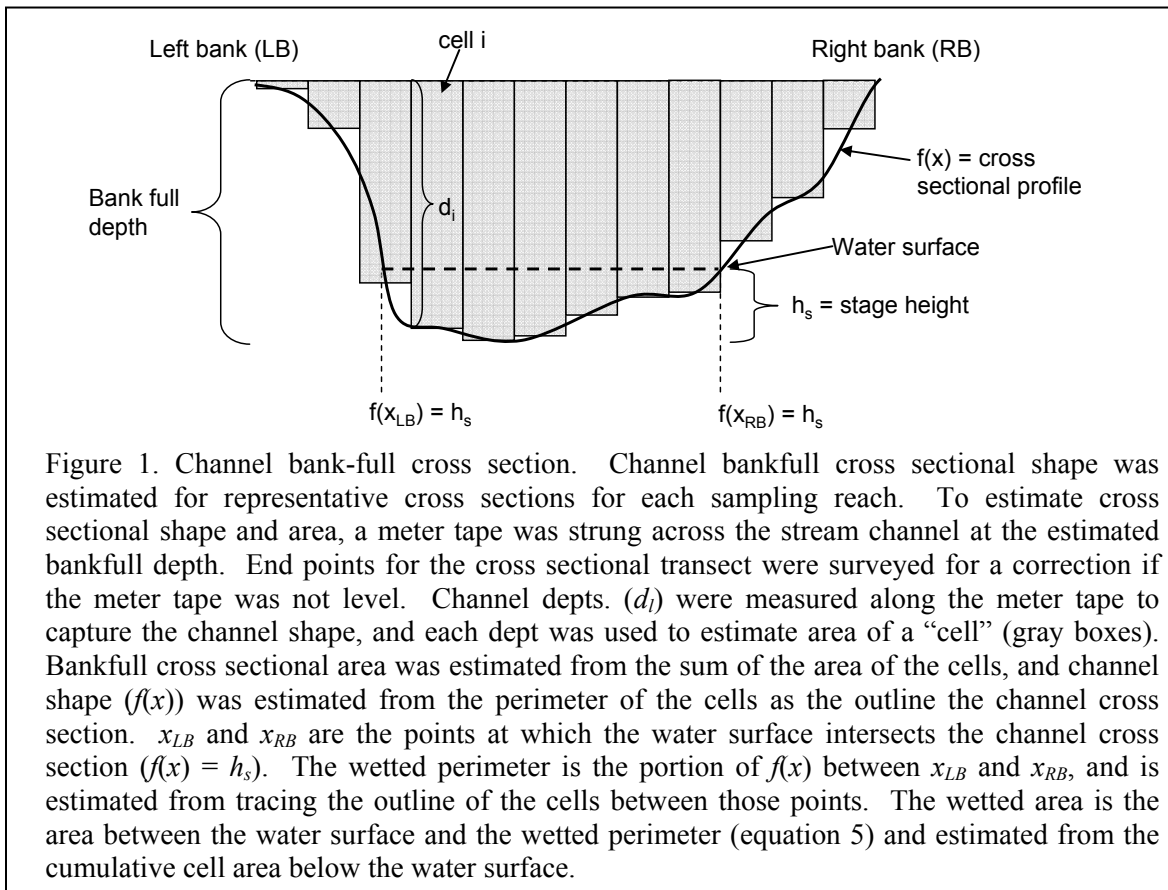
Table E.1. Functional trait scores for North American benthic macroinvertebrates, modified from Poff et al. (2006), used for analysis of Ray Branch sites. Scores were expanded for Tipulidae, as described in Chapter Three.

Order	Family	Genus	Volt	Devl	Sync	Life	Disp	Flgt	Exit	Drft	Crwl	Swim	Atch	Armr	Rho	Desi	Shpe	Size	Ther	Resp	FFG CG	FFG CF	FFG SC	FFG Pred	FFG SH	Hab Burrow	Hab Climb	Hab Sprawl	Hab Cling	Hab Swim	Hab Skate		
Coleoptera	Dryopidae	<i>Helichus</i>	0	0.5	0	1	0	0	0	0	0	0	0	1	1	0	1	0	0.5	1	0	0	1	0	0	0	0	0	1	0	0		
Coleoptera	Dryopidae	<i>Pelonomus</i>	0	1	0	1	0	0	0	0	0	0	0	1	0.5	0	1	0	0.5	1	0	0	1	0	0	0	1	0	0	0	0		
Coleoptera	Dytiscidae	<i>Agabus</i>	0	0.5	0	1	1	1	1	0	1	1	0	1	0.5	0	0	0.5	0.5	1	0	0	0	1	0	0	0	0	0	1	0		
Coleoptera	Dytiscidae	<i>Hydroporus</i>	0	0.5	0	1	1	1	1	0	1	1	0	1	0	0	0	0.5	0.5	1	0	0	0	1	0	0	0	0	0	1	0		
Coleoptera	Dytiscidae	<i>Oreodytes</i>	0	0.5	0	1	1	1	1	0	1	1	0	1	0	0	0	0.5	0.5	1	0	0	0	1	0	0	0	0	0	1	0		
Coleoptera	Elmidae		0	1	0	1	0	0	0	0.5	0.5	0	0	0.5	0.5	1	1	0	0.5	0	1	0	0	0	0	0	0	0	1	0	0		
Coleoptera	Halipidae	<i>Brychius</i>	0.5	0.5	1	1	0	1	1	0	0.5	0.5	0	1	1	0	1	0	0	0.5	0	0	0	1	0	0	0	0	0	1	0	0	
Coleoptera	Psephenidae	<i>Ectropia</i>	0	0.5	1	0.5	0	0	0	0	0	0	0.5	1	1	0	0	0.5	0.5	0.5	0	0	1	0	0	0	0	0	1	0	0		
Coleoptera	Psephenidae	<i>Psephenus</i>	0	0.5	1	0.5	0	0	0	0	0	0	0.5	0.5	1	0	0	0.5	0.5	0.5	0	0	1	0	0	0	0	0	1	0	0		
Diptera	Athericidae	<i>Atherix</i>	0.5	0.5	1	0	0	0	0	0	0.5	0	0	0.5	0.5	0	1	0.5	0.5	0	0	0	0	1	0	0	0	1	0	0	0		
Diptera	Blephariceridae	<i>Agathon</i>	0.5	0.5	1	0	0	0	0	0	0	0.5	1	0.5	0	0	0	0	0	0.5	0	0	1	0	0	0	0	0	1	0	0		
Diptera	Blephariceridae	<i>Bibiocephala</i>	0.5	0.5	1	0	0	0	0	0	0	0	0.5	1	1	0	0	0.5	0	0.5	0	0	1	0	0	0	0	0	1	0	0		
Diptera	Blephariceridae	<i>Blepharicera</i>	0.5	0.5	1	0	0	0	0	0	0	0	0.5	1	1	0	0	0	0	0.5	0	0	1	0	0	0	0	0	1	0	0		
Diptera	Blephariceridae	<i>Philorus</i>	0.5	0.5	1	0	0	0	0	0	0	0	0.5	1	1	0	0	0	0	0.5	0	0	1	0	0	0	0	0	1	0	0		
Diptera	Ceratopogonidae		0.5	0	0	0	0	0	0	0	0	0	0	0.5	0.5	0	1	0	0.5	0	0	0	1	0	0	0	0	1	0	0	0		
Diptera	Deuterophlebiidae	<i>Deuterophlebia</i>	0.5	0.5	1	0	0	0	0	0	0	0	0.5	1	1	0	0	0	0	0	0	0	1	0	0	0	0	0	1	0	0		
Diptera	Empididae		0.5	0.5	1	0	0	0	1	0	0.5	0	0	0	0.5	0	1	0.5	0.5	0	0	0	0	1	0	0	0	0	1	0	0	0	
Diptera	Psychodidae	<i>Maruina</i>	0.5	0	1	0	0	0	0	0	0	0	0.5	0.5	1	0	0	0	0	0	0	0	1	0	0	0	0	0	1	0	0	0	
Diptera	Psychodidae	<i>Pericoma</i>	0.5	0	0	0	0	0	0	0	0	0	0	0.5	0	0	1	0	0.5	0	0	1	0	0	0	0	1	0	0	0	0	0	
Diptera	Simuliidae		1	0	1	0	0	1	0	0.5	0.5	0	0.5	0	1	0	1	0	0.5	0	0	1	0	0	0	0	0	0	0	1	0	0	
Diptera	Tipulidae	<i>Antocha</i>	0.5	0.5	0	0.5	0	0	0	0	0.5	0	0	0	0.5	1	1	0.5	0.5	0.5	1	0	0	0	0	0	0	0	0	1	0	0	
Diptera	Tipulidae	<i>Dicranota</i>	0.5	0.5	0	0.5	0	0	0	0	0.5	0	0	0	0.5	1	1	0.5	0.5	0.5	0	0	0	1	0	0.5	0	0.5	0	0	0	0	
Diptera	Tipulidae	<i>Limnophila</i>	0.5	0.5	0	0.5	0	0	0	0	0.5	0	0	0	0.5	1	1	0.5	0.5	0.5	0	0	0	1	0	1	0	0	0	0	0	0	
Diptera	Tipulidae	<i>Hexatoma</i>	0.5	0.5	0	0.5	0	0	0	0	0.5	0	0	0	0.5	1	1	0.5	0.5	0.5	0	0	0	1	0	0.5	0	0.5	0	0	0	0	
Diptera	Tipulidae	<i>Tipula</i>	0.5	0.5	0	0.5	0	0	0	0	0.5	0	0	0	0.5	1	1	0.5	0.5	0.5	0	0	0	0	1	1	0	0	0	0	0	0	
Diptera	Tipulidae	<i>Molophilus</i>	0.5	0.5	0	0.5	0	0	0	0	0.5	0	0	0	0.5	1	1	0.5	0.5	0.5	0	0	0	0	1	1	0	0	0	0	0	0	
Diptera	Tipulidae	<i>Limonia</i>	0.5	0.5	0	0.5	0	0	0	0	0.5	0	0	0	0.5	1	1	0.5	0.5	0.5	0	0	0	0	1	1	0	0	0	0	0	0	
Diptera	Tipulidae	<i>Pseudolimnophila</i>	0.5	0.5	0	0.5	0	0	0	0	0.5	0	0	0	0.5	1	1	0.5	0.5	0.5	0	0	0	0	1	1	0	0	0	0	0	0	
Diptera	Tipulidae	<i>Rhabdomastix</i>	0.5	0.5	0	0.5	0	0	0	0	0.5	0	0	0	0.5	1	1	0.5	0.5	0.5	0	0	0	0	1	1	0	0	0	0	0	0	
Ephemeroptera	Acanthametropodidae	<i>Acanthametropus</i>	0.5	0.5	1	0.5	0	0	0	0	1	0.5	0	0	0	0	1	0	0	0.5	0	0	0	1	0	0	0	0	0	0	1	0	0
Ephemeroptera	Ameletidae	<i>Ameletus</i>	0.5	0	1	0.5	0	0	0	0	1	1	0	0	0.5	0	0	0	0	0.5	1	0	0	0	0	0	0	0	0	0	1	0	0
Ephemeroptera	Ametropodidae	<i>Ametropus</i>	0.5	0	1	0	0	0	0	0.5	0	0	0	0	0.5	0	0	0	0	0.5	0	0	1	0	0	0	1	0	0	0	0	0	0
Ephemeroptera	Baetidae	<i>Acentrella</i>	1	0	0	0	0	0	0	0.5	0	1	0	0	0.5	0	0	0	0.5	0.5	1	0	0	0	0	0	0	0	0	0	1	0	0
Ephemeroptera	Baetidae	<i>Acerpenna</i>	1	0	0	0	0	0	0	1	0	1	0	0	0.5	0	0	0	0.5	0.5	1	0	0	0	0	0	0	0	0	0	1	0	0
Ephemeroptera	Baetidae	<i>Apobaetis</i>	1	0	0	0	0	0	0	0	0	1	0	0	0.5	0	0	0	0.5	0.5	1	0	0	0	0	0	0	0	0	0	1	0	0
Ephemeroptera	Baetidae	<i>Baetis</i>	1	0	0	0	0	0	0	1	0	1	0	0	0.5	0	0	0	0.5	0.5	1	0	0	0	0	0	0	0	0	0	1	0	0
Ephemeroptera	Baetidae	<i>Callibaetis</i>	1	0	0	0	0	0	0	0	0.5	1	0	0	0	0	0	0	0.5	0.5	1	0	0	0	0	0	0	0	0	0	1	0	0
Ephemeroptera	Baetidae	<i>Camelobaetidius</i>	1	0	0	0	0	0	0	1	0.5	1	0	0	0	0	0	0	0.5	0.5	1	0	0	0	0	0	0	0	0	0	1	0	0
Ephemeroptera	Baetidae	<i>Centropilum/</i>																															
Ephemeroptera	Baetidae	<i>Procloeon</i>	1	0	0	0	0	0	0	0.5	1	0	0	0	0.5	0	0	0	0.5	0.5	1	0	0	0	0	0	0	0	0	0	1	0	0
Ephemeroptera	Baetidae	<i>Cloodes</i>	1	0	0	0	0	0	0	0.5	1	0	0	0	0.5	0	0	0	0.5	0.5	1	0	0	0	0	0	0	0	0	0	1	0	0
Ephemeroptera	Baetidae	<i>Dipheter</i>	1	0	0	0	0	0	0	0	0.5	1	0	0	0.5	0	0	0	0.5	0.5	1	0	0	0	0	0	0	0	0	0	1	0	0
Ephemeroptera	Baetidae	<i>Fallceon</i>	1	0	0	0	0	0	0	1	0.5	1	0	0	0.5	0	0	0	0.5	0.5	1	0	0	0	0	0	0	0	0	0	1	0	0
Ephemeroptera	Baetidae	<i>Heterocloeon</i>	1	0	0	0	0	0	0	0.5	1	0	0	1	0	0	0	0	0.5	0.5	0	0	1	0	0	0	0	0	0	0	1	0	0
Ephemeroptera	Baetidae	<i>Paracloeoedes</i>	1	0	0	0	0	0	0	0.5	1	0	0	0	0	0	0	0	1	0.5	0	0	1	0	0	0	0	0	0	0	1	0	0
Ephemeroptera	Baetidae	<i>Pseudocloeon</i>	1	0	0	0	0	0	1	0.5	0.5	0	0	0.5	0	0	0	0	0.5	0.5	1	0	0	0	0	0	0	0	0	0	1	0	0
Ephemeroptera	Baetiscidae	<i>Baetisca</i>	0.5	0	1	0	0	0	0	0	0	0	0.5	0	0	1	0.5	0.5	0.5	1	0	0	0	0	0	0	0	0	1	0	0	0	0
Ephemeroptera	Caenidae	<i>Amercaenis</i>	0.5	0	1	0	0	0	0	0	0.5	0.5	0	0	0	0	1	0	0.5	0.5	0	1	0	0	0	0	0	0	1	0	0	0	0
Ephemeroptera	Caenidae	<i>Brachycercus</i>	0.5	0.5	1	0	0	0	0	0	0.5	0.5	0	0	0	0	1	0	0.5	0.5	1	0	0	0	0	0	0	0	1	0	0	0	0
Ephemeroptera	Caenidae	<i>Caenis</i>	1	0.5	1	0	0	0	0	0	0.5	0.5	0	0	0	0	1	0	1	0.5	1	0	0	0	0	0	0	0	1	0	0	0	0
Ephemeroptera	Ephemerellidae	<i>Attenella</i>	0.5	0.5	1	0	0	0	0	0	0.5	0.5	0	0	1	0	1	0.5	0.5	0.5	1	0	0	0	0	0	0	0	0	1	0	0	0
Ephemeroptera	Ephemerellidae	<i>Caudatella</i>	0.5	0.5	1	0	0	0	0	0	0.5	0.5	0	0	0.5	0	1	0.5	0	0.5	1	0	0	0	0	0	0	0	0	1	0	0	0
Ephemeroptera	Ephemerellidae	<i>Caurinella</i>	0.5	0.5	1	0	0	0	0	0	0.5	0.5	0	0	0.5	0	1	0.5	0	0.5	1	0	0	0	0	0	0	0	0	1	0	0	0
Ephemeroptera	Ephemerellidae	<i>Drunella</i>	0.5	0.5	1	0	0	0	0	0	0.5	0.5	0																				

Plecoptera	Perlidae	<i>Eccoptura</i>	0.5	0.5	1	0.5	1	1	0	0	1	0.5	0	0.5	1	0	0	1	0	0.5	0	0	0	1	0	0	0	0	0	1	0	0	
Plecoptera	Perlidae	<i>Hansonoperla</i>	0.5	1	1	0.5	0	0	0	0	1	0.5	0	0.5	1	1	0	1	0	0.5	0	0	0	1	0	0	0	0	0	1	0	0	
Plecoptera	Perlidae	<i>Hesperoperla</i>	0	0.5	1	0.5	1	1	0	0	1	0.5	0	0.5	1	0	0	1	0	0.5	0	0	0	1	0	0	0	0	0	1	0	0	
Plecoptera	Perlidae	<i>Neoperla</i>	0.5	1	0	0.5	1	1	0	0	1	0.5	0	0.5	1	0	0	0.5	0	0.5	0	0	0	1	0	0	0	0	0	1	0	0	
Plecoptera	Perlidae	<i>Paragnetina</i>	0	0.5	0	0.5	1	1	0	0	1	0.5	0	0.5	1	1	0	0	0.5	0.5	0.5	0	0	0	1	0	0	0	0	1	0	0	
Plecoptera	Perlidae	<i>Perlesta</i>	0.5	0.5	0	0.5	1	1	0	0	1	0.5	0	0.5	0.5	0	0	1	0.5	0.5	0	0	0	1	0	0	0	0	0	1	0	0	
Plecoptera	Perlidae	<i>Perlinella</i>	0.5	0.5	1	0.5	1	1	0	0	1	0.5	0	0.5	0.5	1	0	1	0.5	0.5	0	0	0	1	0	0	0	0	0	1	0	0	
Plecoptera	Perlodidae	<i>Calliperla</i>	0.5	0.5	1	0.5	0	0	0	0	0.5	0.5	0	0.5	0.5	0	0	0	0.5	0.5	0	0	0	1	0	0	0	0	0	1	0	0	
Plecoptera	Perlodidae	<i>Cascadoperla</i>	0.5	0.5	1	0.5	0	0	0	0	0.5	0.5	0	0.5	1	0	0	0.5	0.5	0	0	0	0	1	0	0	0	0	0	1	0	0	
Plecoptera	Perlodidae	<i>Clioperla</i>	0.5	0.5	1	0.5	1	0	0	0	0.5	0.5	0	0.5	0.5	0	0	0	0.5	0	0	0	0	1	0	0	0	0	0	1	0	0	
Plecoptera	Perlodidae	<i>Culus</i>	0.5	0.5	1	0.5	0	0	0	0	1	0.5	0	0.5	1	0	0	0.5	0	0	0	0	0	1	0	0	0	0	0	1	0	0	
Plecoptera	Perlodidae	<i>Diploperla</i>	0.5	0.5	1	0.5	0	0	0	0	1	0.5	0	0.5	1	0	0	0.5	0	0	0	0	0	1	0	0	0	0	0	1	0	0	
Plecoptera	Perlodidae	<i>Diura</i>	0.5	0.5	1	0.5	0	0	0	0	1	0.5	0	0.5	1	0	0	0.5	0.5	0	0	0	1	0	0	0	0	0	0	1	0	0	
Plecoptera	Perlodidae	<i>Frisonia</i>	0.5	0.5	1	0.5	0	0	0	0	1	0.5	0	0.5	1	0	0	0.5	0	0	0	0	0	1	0	0	0	0	0	1	0	0	
Plecoptera	Perlodidae	<i>Helopicus</i>	0.5	0.5	1	0.5	1	0	0	0	1	0.5	0	0.5	1	0	0	1	0	0	0	0	0	1	0	0	0	0	0	1	0	0	
Plecoptera	Perlodidae	<i>Hydroperla</i>	0.5	0.5	1	0.5	1	0	0	0	1	0.5	0	0.5	0.5	0	0	1	0	0	0	0	0	1	0	0	0	0	0	1	0	0	
Plecoptera	Perlodidae	<i>Isogenoides</i>	0.5	0.5	1	0.5	1	0	0	0	1	0.5	0	0.5	0.5	0	0	1	0.5	0	0	0	0	1	0	0	0	0	0	1	0	0	
Plecoptera	Perlodidae	<i>Isoperla</i>	0.5	0.5	1	0	0	0	0	0.5	1	0.5	0	0.5	0.5	1	1	0.5	0.5	0	0	0	0	1	0	0	0	0	0	1	0	0	
Plecoptera	Perlodidae	<i>Kogotus</i>	0.5	0.5	1	0.5	0	0	0	0	1	0.5	0	0.5	1	0	0	0.5	0	0	0	0	0	1	0	0	0	0	0	1	0	0	
Plecoptera	Perlodidae	<i>Malirekus</i>	0.5	0.5	1	0.5	0	0	0	0	0.5	0.5	0	0.5	0.5	0	0	1	0	0	0	0	0	1	0	0	0	0	0	1	0	0	
Plecoptera	Perlodidae	<i>Megarctus</i>	0.5	0.5	1	0.5	0	0	0	0	0.5	0.5	0	0.5	1	0	0	1	0	0.5	0	0	0	1	0	0	0	0	0	1	0	0	
Plecoptera	Perlodidae	<i>Oroperla</i>	0.5	0.5	1	0.5	0	0	0	0	0.5	0.5	0	0.5	1	0	0	1	0	0.5	0	0	0	1	0	0	0	0	0	1	0	0	
Plecoptera	Perlodidae	<i>Osobenus</i>	0.5	0.5	1	0.5	0	0	0	0	0.5	0.5	0	0.5	1	0	0	0.5	0	0	0	0	0	1	0	0	0	0	0	1	0	0	
Plecoptera	Perlodidae	<i>Perlinodes</i>	0.5	0.5	1	0.5	0	0	0	0	0.5	0.5	0	0.5	1	0	0	1	0	0.5	0	0	0	1	0	0	0	0	0	1	0	0	
Plecoptera	Perlodidae	<i>Pictetiella</i>	0.5	0.5	1	0.5	0	0	0	0	0.5	0.5	0	0.5	1	0	0	1	0	0	0	0	0	1	0	0	0	0	0	1	0	0	
Plecoptera	Perlodidae	<i>Remenus</i>	0.5	0.5	1	0.5	0	0	0	0	0.5	0.5	0	0.5	0.5	0	0	0.5	0	0	0	0	0	1	0	0	0	0	0	1	0	0	
Plecoptera	Perlodidae	<i>Rickera</i>	0.5	0.5	1	0.5	0	0	0	0	0.5	0.5	0	0.5	0.5	1	1	0.5	0	0	0	0	0	1	0	0	0	0	0	1	0	0	
Plecoptera	Perlodidae	<i>Setvena</i>	0.5	0.5	1	0.5	0	0	0	0	0.5	0.5	0	0.5	0.5	0	0	1	0	0	0	0	0	1	0	0	0	0	0	1	0	0	
Plecoptera	Perlodidae	<i>Skwala</i>	0.5	0.5	1	0.5	0	0	0	0	0.5	0.5	0	0.5	1	0	0	1	0	0	0	0	0	1	0	0	0	0	0	1	0	0	
Plecoptera	Perlodidae	<i>Susulus</i>	0.5	0.5	1	0.5	0	0	0	0	0.5	0.5	0	0.5	0.5	0	0	1	0	0	0	0	0	1	0	0	0	0	0	1	0	0	
Plecoptera	Perlodidae	<i>Yugus</i>	0.5	0.5	1	0.5	0	0	0	0	0.5	0.5	0	0.5	0.5	0	0	1	0	0	0	0	0	1	0	0	0	0	0	1	0	0	
Plecoptera	Pteronarcyidae	<i>Pteronarcella</i>	0	0.5	1	0.5	0	0	0	0	0.5	0	0	0.5	0.5	0	1	0.5	0.5	0.5	0	0	0	1	0	0	0	0	0	1	0	0	
Plecoptera	Pteronarcyidae	<i>Pteronarcyus</i>	0	0.5	1	1	1	1	0	0.5	1	0	0	1	0.5	0	1	1	0	0.5	0	0	0	1	0	0	0	0	0	1	0	0	
Plecoptera	Taeniopterygidae	<i>Bolotoperla</i>	0.5	0	1	0	0	0	0	0	0	0.5	0	0	0.5	1	1	0.5	0.5	0	0	0	1	0	0	0	0	0	1	0	0	0	
Plecoptera	Taeniopterygidae	<i>Doddsia</i>	0.5	0	1	0	0	0	0	0	0.5	0.5	0	0	0.5	1	1	0.5	0	0	0	0	0	1	0	0	0	0	0	1	0	0	0
Plecoptera	Taeniopterygidae	<i>Oemopteryx</i>	0.5	0	1	0	0	0	0	0.5	0.5	0.5	0	0	0.5	1	1	0.5	0	0	0	0	0	1	0	0	0	0	0	1	0	0	0
Plecoptera	Taeniopterygidae	<i>Strophopteryx</i>	0.5	0	1	0	0	0	0	0.5	0.5	0.5	0	0	0.5	1	1	0.5	0	0	0	0	0	1	0	0	0	0	0	1	0	0	0
Plecoptera	Taeniopterygidae	<i>Taenionema</i>	0.5	0	1	0	0	0	0	0.5	0.5	0.5	0	0	0.5	1	1	0.5	0	0	0	0	0	1	0	0	0	0	0	1	0	0	0
Plecoptera	Taeniopterygidae	<i>Taeniopteryx</i>	0.5	0	1	0	0	0	0	0	0	0.5	0	0	0.5	1	1	0.5	0.5	0.5	0	0	0	1	0	0	0	0	0	1	0	0	0
Trichoptera	Apataniidae	<i>Allomyia</i>	0.5	0.5	1	0.5	0	0	0	0	0.5	0	0.5	1	1	0	1	0.5	0	0	0	0	1	0	0	0	0	0	0	1	0	0	0
Trichoptera	Apataniidae	<i>Moselyana</i>	0.5	0.5	1	0.5	0	0	0	0	0.5	0	0.5	1	1	0	1	0.5	0	0	1	0	0	0	0	0	0	0	1	0	0	0	0
Trichoptera	Apataniidae	<i>Pedomoecus</i>	0.5	0.5	1	0.5	0	0	0	0	0.5	0	0.5	1	1	0	1	0.5	0	0.5	0	0	1	0	0	0	0	0	0	1	0	0	0
Trichoptera	Brachycentridae	<i>Adicrophleps</i>	0.5	0.5	1	0.5	0	0	0	0	0	0	0	1	1	1	0	1	0.5	0	0	0	0	1	0	0	0	0	0	1	0	0	0
Trichoptera	Brachycentridae	<i>Amiocentrus</i>	0.5	0.5	1	0.5	0	0	0	0	0	0	0	1	1	1	0	1	0.5	0.5	0.5	1	0	0	0	0	0	0	0	1	0	0	0
Trichoptera	Brachycentridae	<i>Brachycentrus</i>	0.5	0.5	1	0.5	0	0	0	0	0	0	0	1	1	1	0	1	0.5	0.5	0.5	0	1	0	0	0	0	0	0	1	0	0	0
Trichoptera	Brachycentridae	<i>Micrasema</i>	0.5	0.5	1	0.5	0	0	0	0	0	0	0	1	1	1	0	1	0	0.5	0.5	0	0	1	0	0	0	0	0	1	0	0	0
Trichoptera	Calamoceratidae	<i>Heteroplectron</i>	0.5	0.5	1	0.5	0	0	0	0	0	0	0.5	1	0.5	0	1	0.5	0	0.5	0	0	0	1	0	0	0	0	1	0	0	0	0
Trichoptera	Calamoceratidae	<i>Phylloicus</i>	0.5	0.5	1	0.5	0	0	0	0	0	0	0.5	0.5	0.5	0	1	0.5	0	0.5	0	0	0	1	0	0	0	0	1	0	0	0	0
Trichoptera	Glossosomatidae	<i>Agapetus</i>	0.5	0.5	1	0.5	0	0	0	0	0.5	0	0	1	1	1	1	0	0	0	0	0	1	0	0	0	0	0	0	1	0	0	0
Trichoptera	Glossosomatidae	<i>Anagapetus</i>	0.5	0.5	1	0.5	0	0	0	0	0.5	0	0	1	1	0	1	0	0	0	0	0	0	1	0	0	0	0	0	1	0	0	0
Trichoptera	Glossosomatidae	<i>Culoptila</i>	0.5	0.5	1	0.5	0	0	0	0	0.5	0	0	1	1	0	1	0	0	0	0	0	0	1	0	0	0	0	0	1	0	0	0
Trichoptera	Glossosomatidae	<i>Glossosoma</i>	0.5	0.5	1	0.5	0	0	0	0	0.5	0	0	1	1	0	1	0	0.5	0	0	0	1	0	0	0	0	0	0	1	0	0	0
Trichoptera	Glossosomatidae	<i>Matrioptila</i>	0.5	0.5	1	0.5	0	0	0	0	0.5	0	0	1	1	0	1	0	0.5	0	0	0	1	0	0	0	0	0	0	1	0	0	0
Trichoptera	Glossosomatidae	<i>Protoptila</i>	0.5	0.5	1	0.5	0	0	0	0	0.5	0	0	1	1	0	1	0	0	0	0	0	0	1	0								

Appendix F – Estimating channel velocity

Stage levels were recorded in winter and spring 2006 using HOBO U20-001 water level loggers from the Onset Computer Corporation (correcting for changes in barometric pressure with a data logger recording air temperature) which were placed in vented wells near the 0m mark in each stream reach. Stream discharge (Q) estimates for the 0m site in each watershed were measured using the slug-injection method (Gordon et al. 1992). Estimates of Q were measured at various stage heights throughout the year and used to fit the parameters that established the relationship between d_i (recorded water level logger depth), Q , and V (mean channel velocity).



Channel cross sectional profiles (Figure 1) and the gradient of the stream bed (m elevation change / m of thalweg length) were measured for each sampling reach and were used in fitting the relationships between d_i , V , and Q as defined in Manning’s equation (Gordon et al. 1992), where

$$Q = \frac{1}{n} AR^{2/3} S^{1/2} \quad (1)$$

and

$$V = \frac{1}{n} R^{2/3} S^{1/2} \quad (2)$$

where A is the wetted cross sectional area, R is the hydraulic radius, n is *Manning's n*, S is channel slope (thalweg slope over a 10m reach). R is defined as A/P (Gordon et al. 1992), where P is the wetter perimeter, therefore

$$Q = \frac{A^{5/3} S^{1/2}}{nP^{2/3}} \quad (3)$$

and

$$V = \frac{A^{2/3} S^{1/2}}{nP^{2/3}} \quad (4)$$

In equations 3 and 4, n and S are independent of stage height, and constant over time; however, A and P are functions of stage height, which varies over time with the hydrograph. I used the relationships

$$A = \int_{x_{LB}}^{x_{RB}} (h_s - f(x)) dx \quad \text{while } h_s - f(x) > 0, \text{ and } x_{LB} \text{ and } x_{RB} \text{ are the points} \\ \text{at which } h_s - f(x) = 0 \text{ (the left and right wetted} \quad (5) \\ \text{bank)}$$

and

$$P = L(f(x)) \quad \text{for } x_{LB} < x < x_{RB} \quad (6)$$

where $f(x)$ is the function describing the curve of the channel profile, and $L(f(x))$ is an estimate of the length of the curve $f(x)$. The relationship between d_l and h_s was linear, but not 1:1, so I substituted $h_s = b_0 + b_1 d_l$ to determine the relationship between the recorded sensor depth and the actual stage height. Therefore, for a set of observations of d_l and Q (which vary with the hydrograph) and S (which is constant over time), I used *optim* (a parameter fitting function in the R software statistical package)(R Development Core Team 2007) to fit the parameters b_0 , b_1 , and n in

$$Q = \frac{\left(\int (b_0 + b_1 d_l - f(x)) dx \right)^{5/3} S^{1/2}}{n(L(f(x)))^{2/3}} \quad \text{while } b_0 + b_1 d_l - f(x) > 0 \quad (7)$$

by minimizing the residual sum of squared error between observed and predicted Q measurements. $f(x)$ is empirically estimated from the field measurements of each cross section and does not change with d_l . Once parameterized, equation 7 was used to calculate a hydrograph and a mean reach velocity (V) time series from the time series of d_l values provided by the water level logger.

There were no surface inputs, and I assumed no major ground water inputs between the -50m, 0m, and 25m sites, and assumed Q to be constant among those sampling reaches. Therefore equation 7 was parameterized with the same Q and d_l values for the -50m, 0m, and 25m sampling reaches in the same watershed, but channel shape and the fitted Manning's n varied among these sites.

There were tributaries between the three upstream sampling reaches and the 200m sampling reach in each watershed, therefore I measured discharge at the downstream sites using the slug injection technique. Due to a lack of data points for downstream sites, I fit a linear relationship between $\log(\text{upstream } Q)$ and $\log(\text{downstream } Q)$ to all observed pairs of upstream/downstream measurements of Q (Figure 2, $R^2 = 0.68$, $p < 0.05$). From this scaling relationship, I constructed a hydrograph and parameterized equation 7 for each 200m sampling reach.

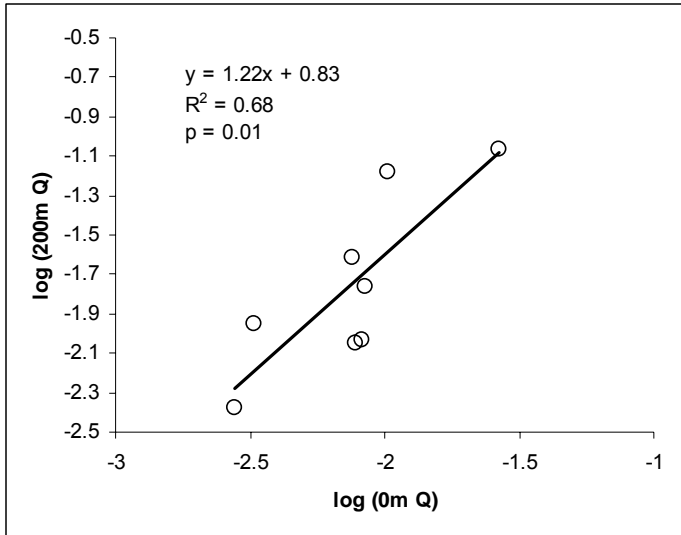


Figure 2. Regression of log(Q) at 200m reaches against log(Q) at 0m reaches.

Summary statistics (mean, range, standard deviation, and 0.05, 0.50, and 0.95 quantiles) were calculated from the time series data for each sampling reach. All of the summary statistics varied similarly among sites, so I only used overall median velocity (V_{med}) from these calculations as an environmental variable that describes the difference between high velocity and low mean reach velocity sites.

Appendix G – Path analysis of the habitat template

Figures illustrating the process for building path models to describe the relationship between the habitat template and community composition.

